DEVELOPMENT OF A MODEL REFERENCE ADAPTIVE SYSTEM WITH A FUZZY-PID REGULATOR FOR SPEED CONTROL OF A SINGLE-PHASE INDUCTION MOTOR

Faith Jepchirchir Kurui

A Thesis Submitted in Partial Fulfillment of the Requirements for the Degree of Master of Technology in Electrical and Electronics Engineering of Murang'a University of Technology

August, 2026

DECLARATION

Student Declaration

I hereby declare that this Thesis is my original work and to the best of my knowledge, has not been presented for a degree award in this or any other university. I understand what plagiarism is and I am aware of the University's policy in this regard. I understand that any false claim in respect of this work shall result in disciplinary action in accordance with the university Anti-Plagiarism Policy.

_____ _____

Faith Jepchirchir Kurui Date

EN400/5230/2018

Supervisors' Approval

The undesigned certify that they have read and hereby recommended for acceptance of Murang'a University of Technology a thesis entitled **"Development of a Model Reference Adaptive System with a Fuzzy-PID Regulator for Speed Control of a Single-Phase Induction Motor"**.

_____ _____

Prof. Christopher Muriithi Maina, Date

Department of Electrical and Electronics Engineering,

Murang'a University of Technology.

_____ _____

Dr. Nicholas Oyie Date

Department of Electrical and Electronics Engineering,

Murang'a University of Technology.

DEDICATION

This thesis is dedicated to the author's parents, who have been the cornerstone of all here accomplishments through their unwavering prayers, support, and encouragement. Their sacrifices and faith in her potential have been her greatest motivation. The thesis is further dedicated to the author's close friends, whose patience, care, and moral support sustained her through the highs and lows of this academic journey. Finally, it is dedicated to aspiring engineers, in the hope that this work will inspire them to keep pushing boundaries and believing in innovation.

ACKNOWLEDGEMENT

I am first and foremost grateful to God the Almighty for giving me the energy, wellness, and perseverance to carry out and complete this research successfully.

I extend my sincere appreciation to my supervisors Prof. Christopher Maina and Dr. Nicholas Oyie, for their invaluable advice, encouragement, and insightful feedback throughout this research. Your support has been instrumental in influencing the course of this thesis.

I am honestly thankful to the school and staff of the Department of Electrical and Electronic Engineering at Murang'a University of Technology for providing the academic foundation and resources required for the successful execution of this work.

Special thanks to my colleagues and classmates, whose constructive discussions, critiques, and togetherness made this research journey both enriching and enjoyable.

Lastly, the author is grateful to her family and friends for their unwavering support, patience, and understanding during the long hours and challenges of this research. Their belief in her made all the difference.

ABSTRACT

Accurate speed control of Single-Phase Induction Motors (SPIMs) is difficult to achieve without physical speed sensors, yet sensor-based schemes add cost, complexity, and vulnerability to noise and mechanical wear. Most sensorless control research has concentrated on three-phase machines, leaving SPIM sensorless control comparatively underexplored, and existing estimators such as the Model Reference Adaptive System (MRAS) lose accuracy under parameter variation and load disturbance while conventional PID regulation alone struggles to keep pace. This thesis addresses this gap by presenting the design, implementation, and validation of a sensorless speed control system for a SPIM that integrates MRAS speed estimator with a Fuzzy Logic-Proportional Integral Derivative (Fuzzy-PID) controller. Its novelty lies in combining MRAS's sensorless adaptability with a Fuzzy-PID regulator that dynamically retunes its gains from the estimated speed error, so that estimation and control adapt together rather than as separate stages. The control model was developed in MATLAB/Simulink and evaluated under varying load conditions. The MRAS estimated rotor speed by comparing reference and adjustable models, eliminating the need for physical sensors; the fuzzy logic controller handled system nonlinearities through linguistic rules and membership functions; and the PID controller continuously adapted its gains in response to the error signal. Simulation results showed that the integrated MRAS-Fuzzy-PID controller outperformed both MRAS-Fuzzy controller and a reference MRAS-only system on every metric tested. It achieved the fastest rise time, at 0.36 seconds, against 0.43 seconds for MRAS-Fuzzy and 0.45 seconds for the reference system; settling time was reduced to 1.3 seconds, a 50% improvement over the initial setup; and steady-state error was minimized to 0.03%, compared with 0.12% and 0.22% respectively. The final settled speed reached 1429 rpm, closely matching the reference and exceeding the accuracy of both comparative controllers. These results confirm the superior speed-tracking accuracy, faster dynamic response, and robust adaptability of the MRAS-Fuzzy-PID approach under load variation. By removing the physical speed sensor while retaining accurate, adaptive regulation, the proposed system offers strong potential for low-cost, energy-efficient, intelligent motor control in residential and industrial applications, contributing an integrated estimation-and-control framework for future sensorless single-phase drives.

TABLE OF CONTENTS

DECLARATION ..... **ii**
DEDICATION ..... **iii**
ACKNOWLEDGEMENT ..... **iv**
ABSTRACT ..... **v**
LIST OF TABLES ..... **ix**
LIST OF FIGURES ..... **x**
ACRONYMS AND ABBREVIATIONS ..... **xii**
CHAPTER ONE: INTRODUCTION **1**
1.1 Background of the Study 1
1.2 Problem Statement 3
1.3 Research Objectives 4
1.3.1 General Objective 4
1.3.2 Specific Objectives 4
1.4 Research Questions 4
1.5 Significance of the Study 5
1.6 Scope of the Study 5
1.7 Limitations of the Study 6
1.8 Contributions of the Thesis 6
1.9 Organization of the Thesis 7
CHAPTER TWO: LITERATURE REVIEW **8**
2.1 Introduction 8
2.2 Single-Phase Induction Motors (SPIMs) 8
2.2.1 Split-Phase Induction Motors 13
2.2.2 Capacitor-Start Induction Motors 13
2.2.3 Capacitor-Start Capacitor-Run Induction Motors 14
2.2.4 Shaded-Pole Induction Motors 14
2.3 SPIM Speed Control Techniques 15
2.3.1 Scalar Control 15
2.3.1.1 Voltage Control 16
2.3.1.2 Frequency Control 16
2.3.2 Vector Control 17
2.3.2.1 Direct Torque Control (DTC) 17
2.3.2.2 Indirect Field-Oriented Control (FOC) 17
2.3.3 Sensorless Vector Control 18
2.3.4 Variable Frequency Drives (VFD) 19
2.4 Speed Controllers of SPIM 20
2.4.1 PI Controllers 20

2.4.2 PID Controllers 20
2.4.3 Fuzzy Logic Controllers 22
2.5 Fuzzy Logic Control Techniques (FLCT) 22
2.6 Related Theories 23
2.6.1 Model Reference Adaptive System 23
2.6.2 Fuzzy-PID Regulator 24
2.6.3 Integration of MRAS and Fuzzy-PID Regulator 25
2.7 Research Gaps 28
2.8 Conceptual Framework 28
2.9 Summary 30
CHAPTER THREE: RESEARCH METHODOLOGY 32
3.1 Introduction 32
3.2 Single-Phase Induction Motor Model and its Speed-Torque Characteristic 33
3.2.1 Existing model of a Single-Phase Induction Motor 33
3.2.2 Simulation of Single-Phase Induction Motor 34
3.2.3 Simulation Procedure 39
3.2.4 Sensor-Less Vector Control Model of SPIM 43
3.3 MRAS for a SPIM Sensorless Speed Control Design 44
3.3.1 Designing MRAS 45
3.3.2 Simulation of MRAS Model 47
3.4 Designing Fuzzy-PID Regulator 50
3.4.1 Fuzzy Logic Controller 51
3.4.2 Simulation of Fuzzy Logic Controller 53
3.4.3 Designing of PID Controller Model 57
3.4.4 Simulation of PID Controller 60
3.5 Comparative Performance Analysis and Evaluation 61
3.6 Summary 62
CHAPTER FOUR: RESULTS AND DISCUSSION 63
4.1 Introduction 63
4.2 Single Phase Induction Motor (SPIM) Results 63
4.2.1 Input Voltage Response 63
4.2.2 Rotor d–q Flux Estimation Accuracy 65
4.2.3 Stator and Rotor d–q Axis Flux Responses 66
4.2.4 Stator and Rotor d–q Axis Current Responses 67
4.2.5 Electromagnetic Torque and Rotor Speed Response under Load Variations 68
4.2.6 Slip Response under Varying Load Conditions 70
4.2.7 Electromagnetic Torque and Speed Relationship 72
4.2.8 Electromagnetic Torque Variation with Slip 73

4.2.9 Analysis of the SPIM 74
4.3 Model Reference Adaptive System (MRAS) Results 75
4.4 Fuzzy Logic Controller and Proportional Integral Derivative (PID) Results 77
4.4.1 Fuzzy Logic Controller Simulation 77
4.4.2 PID Controller Simulation 79
4.4.3 Fuzzy-PID Controller Simulation Results 80
4.5 Performance Evaluation of the MRAS-Fuzzy-PID Controller 84
4.6 Summary 86
CHAPTER FIVE: CONCLUSION AND RECOMMENDATIONS 87
5.1 Conclusion 87
5.2 Recommendations 88
5.3 Future Work 89
REFERENCES 90
APPENDICES 95

LIST OF TABLES

Table 2.1: Summary matrix of key related literature on SPIM/induction-motor speed control 27
Table 3.1: SPIM Initialized parameters 39
Table 3.2: Fuzzy logic controller rule base 1 52
Table 3.3: Fuzzy logic controller rule base 2 53
Table 3.4: Relation of increase in Kp, Ki, and Kp gains 59
Table 3.5: Parameter analysis of P, PI, and PID controllers 60
Table 4.1: SPIM Speed Analysis 85

LIST OF FIGURES

Figure 1.1: Overall block diagram of proposed sensorless MRAS-Fuzzy-PID speed control system for the single-phase induction motor 3
Figure 2.1: Torque-Slip relationship [17] 10
Figure 2.2: Split-Phase Single-Phase Induction Motor [16] 11
Figure 2.3: Phasor diagram of the Split-Phase Single-Phase Induction Motor 11
Figure 2.4: Torque-Speed relationship [18] 12
Figure 2.5: Schematic circuit diagram of a capacitor-start induction motor 13
Figure 2.6: A scalar-controlled induction motor's block diagram [27] 15
Figure 2.7: Indirect field-oriented control 18
Figure 2.8: Drive for a single-phase induction motor (SPIM) [34] 19
Figure 2.9: PID block diagram [44] 21
Figure 2.10: Conceptual framework of the study 30
Figure 3.1: Flow chart of the research methodology followed in this thesis 33
Figure 3.2: Equivalent circuits of SPIM [8] 34
Figure 3.3: q-axis (Main winding) 35
Figure 3.4: d-axis (Auxiliary winding) 36
Figure 3.5: Phase to d-q axis calculation as per equation 3.14 40
Figure 3.6: Conversion of ωm to ωr as per equation 3.14 41
Figure 3.7: Slip calculation as per equation 2.1 and 3.11 and disconnection speed calculation 42
Figure 3.8: Block Diagram Sensorless Vector Control 44
Figure 3.9: MRAS speed scheme estimator 45
Figure 3.10: Reference model calculation simulation as per equation 3.15 and equation 3.16 48
Figure 3.11: Adaptive System calculation as per equation 3.17 and equation 3.18 49
Figure 3.12: Model Reference Adaptive System Block diagram simulation and calculation of equation 3.19. 50
Figure 3.13: Regulator for fuzzy PID Block diagram 51
Figure 3.14: Fuzzy logic Controller block diagram 52
Figure 3.15: Fuzzy Logic Controller error setting diagram 54
Figure 3.16: Fuzzy Logic Controller change in error setting diagram 55
Figure 3.17: Fuzzy Logic Controller control output signal setting diagram 56
Figure 3.18: Fuzzy Logic Controller Mamdani rules setting diagram 57
Figure 3.19: PID controller block diagram 58
Figure 3.20: Fuzzy Logic controller integrated with a PID controller diagram 60
Figure 3.21: Overall SPIM speed control simulation overview 61
Figure 4.1: Input Voltage (V_m) 64

Figure 4.2: Reference rotor d-q fluxes (φ_{rqd}) (a) and Rotor d-q fluxes (φ_{rqd}') (b) comparison graphs 65
Figure 4.3: Stator d-q fluxes (Phisqd) (a) and Rotor d-q fluxes (Phirqdbar) (b) graphs 66
Figure 4.4: Stator d-q currents (Isqd) (a) and rotor d-q currents (Iqdrbar) (b) graphs 68
Figure 4.5: Speed (a) and Torque (b) graphs 69
Figure 4.6: Speed, time and torque graphs 70
Figure 4.7: Slip graphs (a) and (b) 71
Figure 4.8: Electromagnetic Torque vs Speed graph 72
Figure 4.9: Electromagnetic Torque vs Slip graph 73
Figure 4.10: Model Reference Adaptive System graph 75
Figure 4.11: Error vs Load Torque graph 76
Figure 4.12: Error vs Rotor Speed graph 77
Figure 4.13: Graphical interface of FLC 78
Figure 4.14: Simulated speed at which the SPIM using PID controller only 80
Figure 4.15: MRAS output (ew + change in error), MRAS+FLC output (Fuzzy Logic Controller output) and MRAS+FLC+PID controller (PID results) results over maximum loading only 81
Figure 4.16: MRAS output (ew + change in error), MRAS+FLC output (Fuzzy Logic Controller output) and MRAS+FLC+PID controller (PID results) results over varying load 83
Figure 4.17: SPIM speed response under PID and Fuzzy-PID controller 84
Figure 4.18: SPIM speed response analysis 84

ACRONYMS AND ABBREVIATIONS

Abbreviation	Definition
AC	Alternating Current
ANFIS	Adaptive Neuro-Fuzzy Inference System
DC	Direct Current
DTC	Direct Torque Control
FLC	Fuzzy Logic Controller
FLCT	Fuzzy Logic Control Techniques
FOC	Field Oriented Control
IM	Induction Motor
MATLAB	Matrix Laboratory
MRAS	Model Reference Adaptive System
NB	Negative Big
NS	Negative Small
PB	Positive Big
PI	Proportional Integral
PID	Proportional Integral Derivative
PS	Positive Small
PWM	Pulse Width Modulation
SPIM	Single Phase Induction Motor
SVC	Sensorless Vector Control
VFD	Variable Frequency Drives

CHAPTER ONE
INTRODUCTION

1.1 Background of the Study

Single-phase induction motors are commonly employed in both household and industrial applications because they are cost-effective, long-lasting, and require little maintenance [1], but have the disadvantage of requiring an auxiliary winding for starting. Speed and torque parameters were controlled in this motor to achieve effective performance, with the torque output optimized by controlling speed to achieve induction-motor drive [2]. Setting the induction motor speed has been a problem, leading to an error when it is operated on [3].

Sensorless speed control has garnered significant interest in recent years, as it eliminates the need for physical speed sensors, thereby lowering costs and improving reliability. This study explores the integration of a Model Reference Adaptive System (MRAS) and Fuzzy-PID regulator as an advanced approach for sensorless speed regulation in single-phase induction motors, offering promising avenues for enhanced efficiency and accuracy in speed control. The MRAS scheme has been used for real-time estimation of rotor resistance and speed [4]. Due to stator voltages and currents, concurrent evaluation of rotor speed and resistance in Induction Motors (IM) is possible by utilising an adjustable model in a fixed stator reference frame and a reference model [5]. MRAS is known for its adaptability to varying operating conditions, making it an attractive choice for dynamic systems such as induction motors. Incorporating MRAS into the control scheme, the system can continuously adapt to changes in motor parameters, ensuring robust and reliable speed control.

A Fuzzy-PID regulator enhances transient response and maintains stable speed regulation across different voltages, by facilitating fast and accurate speed estimation [6]. Refining traditional PID control with fuzzy logic, this approach improve adaptability and compensates nonlinearities challenges in motor behavior. Changing the speed of induction motors requires variation of the voltage and frequency magnitudes, which can be implemented using Voltage/Frequency (V/F) control [7], this control can be implemented with a small number of components [8]. However, the Fuzzy-PID control method struggles with high dynamic performance and extremely low-speed operations, as well as applications necessitating direct control of

motor torque rather than frequency [9]. Incorporating a fuzzy logic model would address these challenges by enabling intelligent decision-making based on error signals and the rate of change of error. Appliances have used fuzzy controllers because they provide a fast time response without unwanted overshoot and low steady-state error, which helps prevent rare oscillations [3], even when controlling a nonlinear, unsettled system without a mathematical model. Complex systems require many rules for their implementation, which can make them overwhelming and tedious [10]. Fuzzy-PI control of induction motors runs at specific speed errors, maximizing their advantages. The motor's speed is regulated by a Fuzzy logic controller that operates according to predetermined rules governing its inputs and outputs [11], where two input signals are fed into the fuzzy controller: the instantaneous error signal and its rate of change. Fuzzy-PID controllers use fuzzy logic to refine traditional PID parameters, employing predefined rules to optimize them.

Integration of a Fuzzy-PID regulator introduced a level of intelligent decision-making to the control system. Fuzzy logic enables the integration of human-like reasoning into controllers, allowing them to handle uncertainties and accommodate the non-linearities inherent in the motor's behavior. The combination of MRAS and Fuzzy-PID created a synergistic effect, with adaptability and intelligent control mechanisms working in concert to improve the sensorless speed control system's overall performance, aiming to construct a precise, reliable, and economical control system that significantly advances speed control stabilization in induction motors. This study focused on integrating MRAS and Fuzzy-PID control for speed regulation in single-phase induction motors without physical sensors, with an emphasis on evaluating their combined effect on system stability, accuracy, and efficiency. It addresses the challenges associated with sensorless control. The study advances motor control technology, opening way for more reliable and cost-effective solutions in industrial settings [12] [13].

Figure 1.1 illustrates the overall block diagram of the proposed sensorless MRAS-Fuzzy-PID speed control system for the single-phase induction motor developed in this study

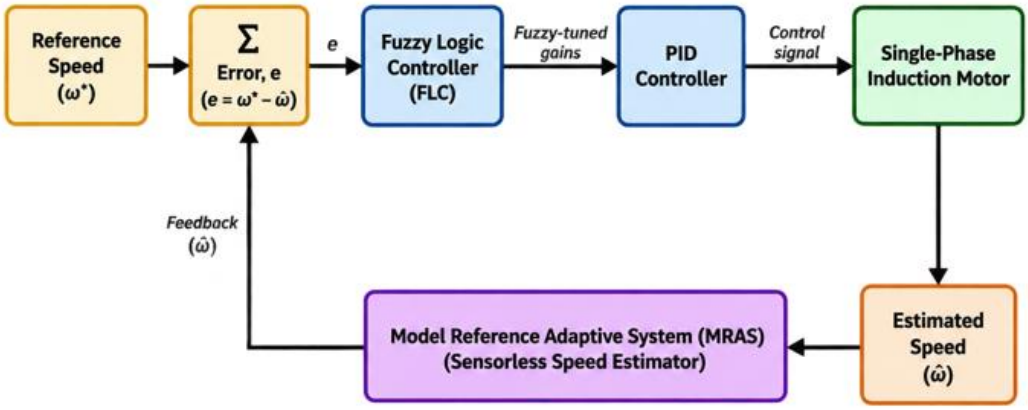


Figure 1.1: Overall block diagram of proposed sensorless MRAS-Fuzzy-PID speed control system for the single-phase induction motor

1.2 Problem Statement

The control of speed in single-phase induction motors (SPIMs) remains a significant challenge in electric drive systems, particularly due to the inherent limitations of conventional control methods. Scalar control, though widely used for its simplicity, suffers from a pronounced torque drop at low speeds. Vector control techniques, on the other hand, offer improved dynamic performance but face limitations when applied to SPIMs operating at low speeds. Furthermore, traditional vector control methods depend on physical speed sensors, which introduce several drawbacks, including increased system cost, greater complexity, and vulnerability to signal noise, environmental interference, and mechanical wear. These issues ultimately affect the accuracy, robustness, and long-term reliability of the motor control system.

Given the drawbacks of sensor-based control, there is growing interest in sensorless control techniques that deliver accurate, stable performance without the need for physical sensors.

Sensorless vector control methods are particularly promising for SPIMs, as they can estimate essential motor parameters, such as voltage and current magnitudes and their respective phase angles, thereby enhancing low-speed and torque control. Additionally, eliminating sensors reduces system costs and power consumption, making the approach highly suitable for applications where affordability, energy efficiency, and reliability are essential.

Considering these factors, the research addressed single-phase induction motors sensorless speed-control system design for dependability, affordability, and adaptability. The suggested method combined a fuzzy-PID controller that dynamically adjusted control parameters based on the system's response with a Model Reference Adaptive System (MRAS) for real-time motor parameter estimation. The combination of MRAS adaptability and the robustness of fuzzy logic and PID regulation provides a comprehensive solution that maintains precise speed control under varying operating conditions. This integrated control strategy addressed the limitations of existing methods and advanced intelligent, sensorless motor control systems.

1.3 Research Objectives

1.3.1 General Objective

The main objective of this study was to develop a Model Reference Adaptive System (MRAS) integrated with a Fuzzy-PID regulator for sensorless speed control of a single-phase induction motor, so as to achieve reduced speed-tracking error, faster dynamic response, and improved robustness to load variation relative to a conventional MRAS-only reference system.

1.3.2 Specific Objectives

To achieve the main objective the following specific objectives were accomplished:

i. Design and validate a sensorless speed-controller mathematical model of a single-phase induction motor.
ii. Design and simulate a MRAS for accurate speed estimation of a single-phase induction motor.
iii. Integrate a Fuzzy-PID regulator with the MRAS to optimize speed control performance of a single-phase induction motor.
iv. Evaluate the performance of the proposed single-phase induction motor speed control system against other control techniques under defined load and speed test conditions.

1.4 Research Questions

i. Could a sensorless speed-controller mathematical model be designed for a single-phase induction motor using the existing single-phase induction motor model?

ii. Could a MRAS be designed and simulated to accurately estimate the speed of a sensorless single-phase induction motor?
iii. Could a Fuzzy-PID regulator be integrated with the MRAS to improve the speed control of a sensorless single-phase induction motor?
iv. How did the performance of the proposed single-phase induction motor speed control system compare against other control techniques?

1.5 Significance of the Study

Existing sensorless speed-control techniques for single-phase induction motors (SPIMs) often struggle to accurately estimate motor speed and adapt to varying operational conditions, limiting efficiency, dynamic response, and reliability under fluctuating loads. This study was justified by the need for an advanced, adaptive control strategy to address these limitations: integrating a Model Reference Adaptive System (MRAS) with a Fuzzy-PID controller, where the MRAS compensated for parameter uncertainties while the Fuzzy-PID controller enabled real-time adjustment of control parameters for stable, accurate speed regulation.

The significance of this study lies in demonstrating a sensor-free speed-control strategy that removes the cost, wiring complexity, and failure points associated with physical speed sensors, while matching or exceeding sensor-based accuracy. For manufacturers and operators of SPIM-driven equipment such as pumps, fans, and compressors, the MRAS-Fuzzy-PID approach offers a pathway to lower-cost, more reliable drives. For the research community, the study extends MRAS-based sensorless estimation, previously studied mainly for three-phase machines, into the comparatively underexplored single-phase domain, providing a basis for further work on adaptive, intelligent control of single-phase drives.

1.6 Scope of the Study

This research was confined to developing a SPIM sensorless speed-control model by integrating a Fuzzy-PID regulator with a MRAS estimator in MATLAB/Simulink; no physical prototype or hardware-in-the-loop implementation was undertaken. The study used MATLAB to model and simulate motor parameter estimation, leveraging the MRAS to adapt to variations and uncertainties in motor characteristics. The model further explored the dynamic adjustment of control parameters by the Fuzzy-PID regulator, employing fuzzy logic rules to fine-tune the PID parameters in response to

the estimated speed error. Model performance was evaluated under a range of simulated load, speed, and disturbance conditions chosen to represent typical residential and light-industrial operating scenarios, rather than under field deployment. Throughout, the integrated MRAS-Fuzzy-PID controller was benchmarked against a MRAS-only reference system and a MRAS-Fuzzy controller to isolate the contribution of each stage of integration.

1.7 Limitations of the Study

Despite the successful outcomes, this research had the following limitations:

- The study was conducted entirely through MATLAB/Simulink simulations, without hardware implementation.
- The motor model used was limited to a single-phase split-phase induction motor; results may not generalize across all motor types.
- The fuzzy rule base and membership functions were kept relatively simple to avoid computational complexity, potentially limiting fine-grained adaptation under extreme disturbances.

Torque ripple and speed fluctuations were observed under certain load conditions, which may affect efficiency and mechanical stability in practical setups.

1.8 Contributions of the Thesis

This study contributes a validated sensorless speed-control model for single-phase induction motors (SPIMs) that integrates a Model Reference Adaptive System (MRAS) with a Fuzzy-PID regulator: extending MRAS-based sensorless estimation, previously studied mainly for three-phase machines, into the underexplored single-phase domain. By benchmarking the integrated MRAS-Fuzzy-PID controller against a MRAS-only reference and a MRAS-Fuzzy controller under identical simulated load, speed, and disturbance conditions, the study isolates and quantifies the improvement contributed by each stage of integration, offering a cost-effective, reliable alternative to sensor-based speed control for SPIM-driven equipment such as pumps, fans, and compressors. The resulting MATLAB/Simulink model, together with its fuzzy rule base and adaptive-system formulation, also provides a foundation for future hardware implementation and extension to other single-phase motor types.

1.9 Organization of the Thesis

This thesis details the development of model for integrating Model Reference Adaptive System (MRAS) and Fuzzy-PID model for improving the control for speed pertaining to a single-phase induction motor without sensors, and was arranged in the following manner:

Chapter 1 serves as the background for the study and includes an overview of a single-phase induction motor speed control, motor parameters controlled, together with a summary of the methodologies used to address similar issues. The chapter also covers the research problem, justification, objectives, significance, and scope of the study.

Chapter 2 provides an overview of the literature regarding various approaches used in single phase induction motors. The chapter covers the types of single-phase induction motor control techniques affecting the speed of a motor, the different types of speed controllers used to address challenges such as accuracy of motor parameter estimation, compensating for variations and uncertainties and dynamically adjusting control parameters based on real-time operating conditions of the motor how these SPIM have been applied in various applications.

Chapter 3 outlines the parameters used to create sensorless single phase induction motor control model for speed control. The chapter provides a comprehensive description of the methodology used to develop the speed control technique that employs sensorless vector control, MRAS, Fuzzy control and PID control for speed regulation.

Chapter 4 presents the results of the simulation of the proposed speed control integration in MATLAB/SIMULINK. The chapter evaluates the single-phase induction motor classification performance using results from various speed controllers obtained through integration of MRAS and Fuzzy-PID controller. It also discusses the results of error produced by the controller in improving accuracy performance.

Chapter 5 summarizes the key conclusions and contributions of the thesis and provides suggestions for future work.

CHAPTER TWO
LITERATURE REVIEW

2.1 Introduction

This chapter provides a comprehensive review of literature on Single-Phase Induction Motors (SPIMs), Model Reference Adaptive System (MRAS), Fuzzy Logic Controller (FLC) and Proportional Integral Derivative (PID) in speed control [14]. This lays a foundation for the proposed study, highlighting the work of earlier scholars in the field and establishing the fundamental ideas. The chapter also offers a critical evaluation of the relevant literature to find gaps and opportunities for further research.

2.2 Single-Phase Induction Motors (SPIMs)

SPIMs are applied in various industrial or residential applications, such as pumps, fans, compressors, and drilling machines, due to their low cost, simple construction, and robustness. However, controlling their speed is challenging due to the absence of a rotating magnetic field: driven by a single winding alone, a SPIM produces a pulsating rather than a rotating field, which develops zero net starting torque at standstill and only begins to produce net torque once the rotor is set in motion, with the magnitude of that torque varying with the motor's operating speed, or equivalently its slip, as explained by the double-field revolving theory below. This is why an auxiliary winding or other starting mechanism is required, and SPIMs are accordingly classified according to their methods of starting: split-phase, capacitor-start, capacitor-start capacitor-run, and shaded-pole [15].

In SPIMs, the double-field revolving theory explains that a sinusoidal signal has two oppositely-rotating flux vectors with each having half the magnitude [16]. Each flux rotates synchronously in opposite directions at Ns as shown in equation 2.1:

$$N_S = \frac{120f}{p} rad/\text{s} \qquad (2.1)$$

Where: N_s = Synchronous speed, f = frequency and p = number of pole pairs

The resultant flux, ϕ after the two have rotated through the angle range of $+\theta$ and $-\theta$ as shown in equation 2.2:

$$\phi = 2 \times \frac{\Phi_m}{2} \times \cos\left(\frac{2\theta}{2}\right) = \Phi_m \cos\theta \tag{2.2}$$

Where: ϕ_m = maximum alternating flux

The rotor's slip with respect to the backward rotating flux is $(2 - s)$ if its slip with respect to the forward rotating flux is *s*. While rotating around the stator, each of the two component fluxes cuts the rotor, creates an e.m.f., and generates its own torque. The net resultant torques are equal to the difference between the forward and backward torques since they are directed in opposite directions. In other words,

Power developed by a rotor is as shown in equation 2.3:

$$P_g = \left(\frac{1-s}{s}\right) I_2^2 R_2 \tag{2.3}$$

Where: R_2 = Rotor Resistance and I_2 = Rotor current

The rotor speed, N in revolutions per second (r.p.s.) is provided by equation 2.4:

$$N = N_s(1-s) \tag{2.4}$$

and the torque, T_g is given by equation 2.5:

$$-T_g = \frac{P_g}{\omega} = \frac{1}{2\pi N}\left(\frac{1-s}{s}\right) I_2^2 R_2 \tag{2.5}$$

Therefore equation 2.4 becomes equation 2.6:

$$-T_g = \frac{1}{2\pi N_s} . \frac{I_2^2 R_2}{s} = k . \frac{I_2^2 R_2}{s} \tag{2.6}$$

Hence, the forward torque,T_f and backward torque,T_b are identified by equation 2.7:

$$T_f = k . \frac{I_2^2 R_2}{s} \text{ and } T_b = -k . \frac{I_2^2 R_2}{1-s} \tag{2.7}$$

Thus, the total torque is given by equation 2.8:

$$-T = T_f + T_b \tag{2.8}$$

Since T_f and T_b have the same numerical value but are directed in different directions, no torque is produced. This indicates that an SPIM lacks starting torque.

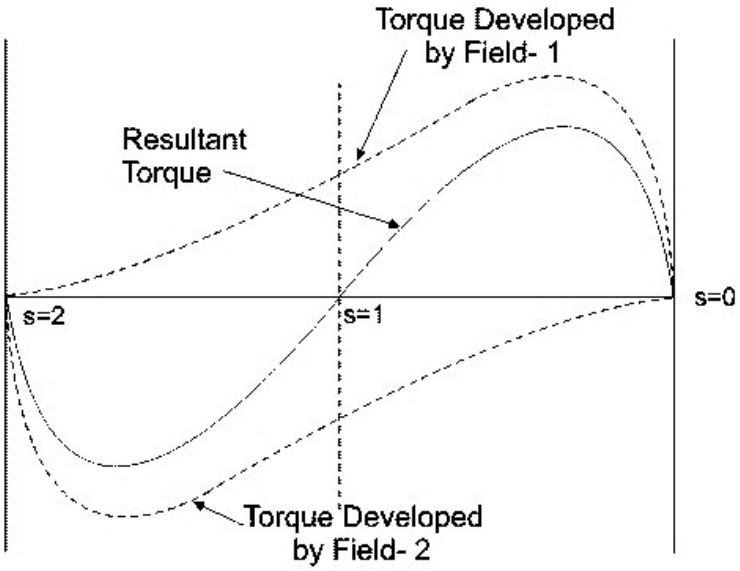


Figure 2.1: Torque-Slip relationship [17]

From Figure 2.1 above, as for the red dotted curve, we note that between s = 2 and s = 0, the side below the reference line represents a backward torque relation to slip and is developed by field 2. Between s =2 and s = 0, the side above the reference line represents the forward torque relation to slip and is developed by field 1. The blue line represents the resultant curve after the combination of the forward and backward torques. At s = 1, the torque is zero, making the SPIM non-self-starting.

The motor is momentarily switched to a two-phase motor during the starting phase in order to get over this disadvantage of not self-starting [16]. To do this, a single-phase motor's stator should be equipped with an additional winding, referred to as the beginning or auxiliary winding, in addition to the main or running winding (see Figure 2.2).

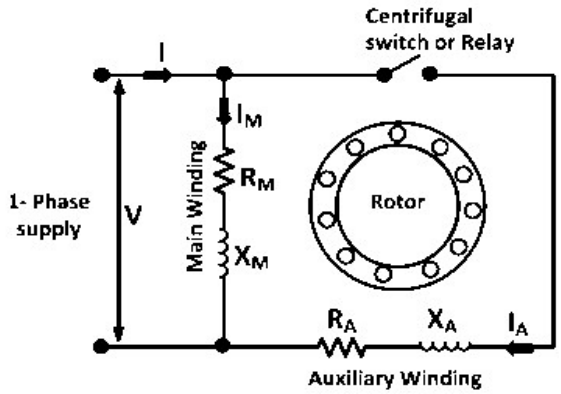


Figure 2.2: Split-Phase Single-Phase Induction Motor [16]

The two windings are linked in parallel across the single-phase supply and are electrically separated by 90 degrees. As can be seen in Figure 2.3, the motor acts as a two-phase motor because of the extremely large phase-difference between the currents in the two stator windings (ideal value being 90º) [6].

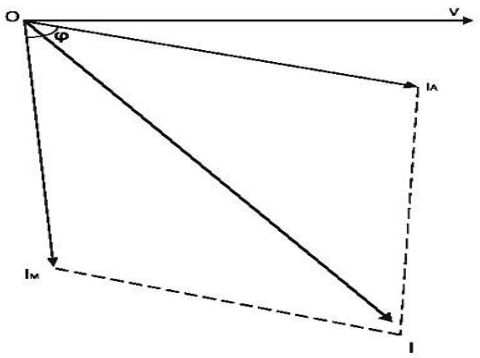


Figure 2.3*:* Phasor diagram of the Split-Phase Single-Phase Induction Motor

In split-phase single-phase induction motors (SPIMs), a revolving magnetic field is generated by two stator currents intentionally phase-shifted, enabling the motor to self-start. This project specifically concentrates on the characteristics and operation of split-phase SPIMs. Typically, the main winding of such motors is designed with low resistance and high reactance, whereas the starting or auxiliary winding exhibits high resistance and low reactance [6].

Due to these electrical properties, the current through the auxiliary winding lags the applied voltage by a relatively small angle, while the current in the main winding lags by a significantly larger angle. This intentional phase displacement between the two currents is crucial, as the starting torque of a split-phase motor is directly proportional

to the sine of the phase angle (α) between them [18]. To ensure efficient transition to steady-state operation, a centrifugal switch or an electromagnetic relay is connected in series with the auxiliary winding. Positioned within the motor housing, this device automatically disconnects the auxiliary winding from the power supply once the motor attains approximately 70% to 80% of its rated full-load speed, as illustrated in Figure 2.4.

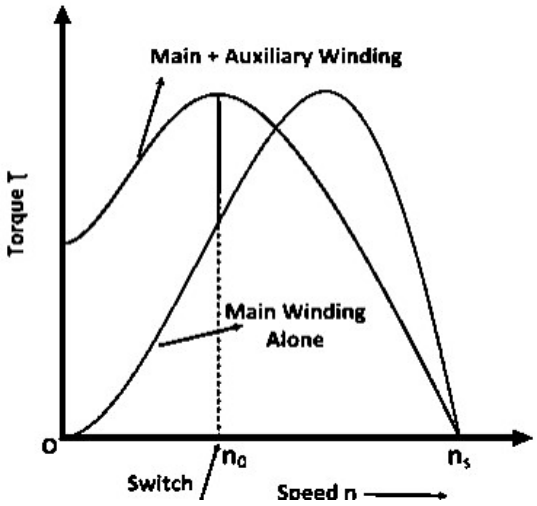


Figure 2.4: Torque-Speed relationship [18]

The direction of rotation of a single-phase induction motor can be reversed by interchanging the connections of one of the two stator windings typically the auxiliary (starting) winding while keeping the main winding connections unchanged.

At no load, the SPIM operates at synchronous speed, N_s, and thus $N_s = N_r$ .Thus the slip at no load is zero. As the SPIM is loaded, the N_r (rotor speed) reduces and thus the slip increases as seen in equation 2.4. The maximum loading is arrived at the breakdown or pullout torque beyond which the speed reduces rapidly. The motor operates in the stable region between the starting and breakdown torque [19]. The speed-torque characteristics are influences by supply voltage, winding configuration (split-phase, capacitor-start, capacitor-run, capacitor-start-and-run) and motor size and power ratings.

Classification of SPIMs

2.2.1 Split-Phase Induction Motors

The primary and auxiliary stator windings, as well as a squirrel cage rotor, make up split-phase induction motors. Usually, only during startup does the auxiliary winding become active. In low-power applications, however, the auxiliary winding can be turned on while the system is operating to enhance performance [20]. When the motor reaches about 70 to 80 percent of its synchronous speed, a centrifugal switch disconnects the auxiliary winding, leaving only the main winding to sustain motor operation. When both windings are revitalized the difference in their impedance triggers a phase shift between the currents flowing in them, creating a revolving magnetic field that generates the initial torque required to start the motor.

2.2.2 Capacitor-Start Induction Motors

Capacitor-start induction motors improve upon split-phase motors by coupling a capacitor in series with an auxiliary winding, capacitor-start induction motors beat split-phase motors. The starting torque is improved by the capacitor's improvement caused by the difference in phase between the primary and secondary windings. Disconnecting a centrifugal switch the auxiliary winding and capacitor once the motor attains a high sufficiently speed. These motors tend to appear in appliances as air compressors, refrigerators, and machine tools requiring a strong starting torque [19]. Using a capacitor connected in series with the auxiliary winding, the currents in the two windings to create greater a phase shift in capacitor-start induction motors. The schematic circuit configuration of a capacitor-start induction motor is presented in Figure 2.5.

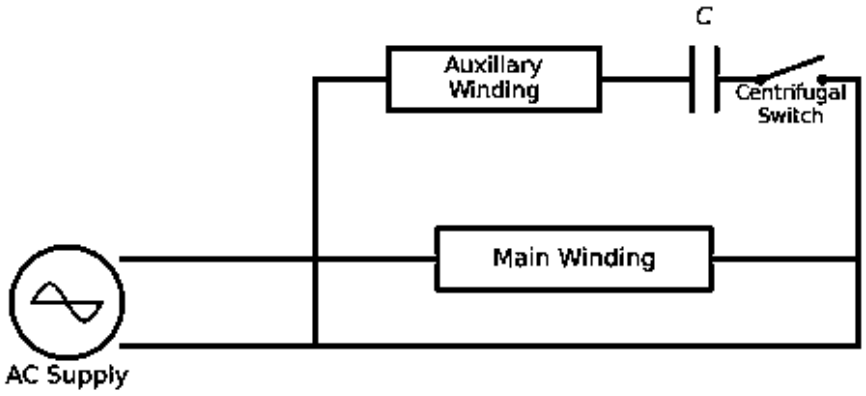


Figure 2.5*:* Schematic circuit diagram of a capacitor-start induction motor

A stronger initial torque is an outcome from a greater phase difference. Both the primary winding and the auxiliary winding (with capacitor) are activated when the motor is switched on. Approximately 2.5 to 4.5 times the torque at full load is the beginning torque, which is greatly increased by the capacitor. Upon reaching around 75–80% of synchronous speed, a centrifugal switch cuts off the auxiliary winding and capacitor, enabling the motor to continue operating exclusively on the primary winding [21].

2.2.3 Capacitor-Start Capacitor-Run Induction Motors

In order to further improve motor performance, capacitor-start capacitor-run motors use two capacitors: one for starting and another for continuous running. During startup capacitor-start is used; the running capacitor remains in the circuit to optimize power factor and efficiency. [22]. Induction at Capacitor Start, the motor employs a capacitor to give strong beginning torque, upon reaching approximately 70–80% of its rated speed, it only uses the main winding and the capacitor is removed from the circuit [21] The capacitor in a Capacitor-Run Induction Motor, on the other hand, stays in the circuit during both startup and operation, improving running efficiency and power factor and resulting in smoother operation. It is more efficient during steady-state operation, [23]. Due to significantly better starting torque, smoother operation, and improved efficiency, these motors are suitable for demanding applications like industrial machinery, pumps, and refrigeration systems.

2.2.4 Shaded-Pole Induction Motors

In SPIMs, shaded-pole motors are among the most fundamental and least priced. A short-circuited copper ring, usually referred to as a shading coil, is placed around a section of the stator pole and is accompanied by a single main winding. A postponed magnetic flux generated by the shade coil results in a weak rotating field that is sufficient for self-starting. These motors are limited to use in small devices such as fans, hair dryers, and small ventilation systems due to their extremely low starting torque, low efficiency, and limited power output [24].

2.3 SPIM Speed Control Techniques

SPIMs have nonlinear characteristics and are sensitive to load disruptions and parameter changes. Therefore, controlling accurately the speed of SPIMs is essential for their efficient operation. The following techniques try to achieve speed control.

2.3.1 Scalar Control

A motor's speed can be adjusted by changing its voltage and frequency. For the voltage-to-frequency (V/F) ratio to remain constant, the voltage and frequency are adjusted proportionately to each other. This is important as the motor's magnetic flux is proportionately directly to the voltage applied, whereas the frequency is proportional to the motor's speed [25]. To guarantee motor performance and effective torque generation, it is crucial to keep the V/F ratio unchanged. In order to avoid overheating and maintain steady performance, this method enables the motor to run at a steady flux level.

The scalar control technique, involves the two main techniques of voltage control and frequency control, which are frequently employed to regulate motor speed. In voltage control, the motor's voltage is modified to preserve the intended working conditions. In frequency control, the desired motor speed is attained by varying the frequency. A well-controlled V/F ratio is necessary for both techniques to function effectively without going above the motor's operating limits [26]. Figure 2.6 presents the block diagram of a scalar-controlled induction motor.

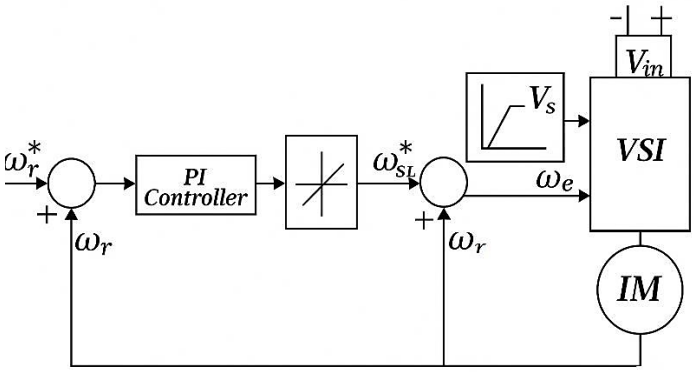


Figure 2.6: A scalar-controlled induction motor's block diagram [27]

2.3.1.1 Voltage Control

The motor is powered with a voltage that is varied using a variable autotransformer or a series of tapped autotransformers, while the supply frequency and the voltage-to-frequency (V/F) ratio are correspondingly adjusted to prevent the motor from being over- or under-fluxed. This technique was simple and economical, since it only requires mechanically adjusting the position of a moveable tap or wiper on the autotransformer's secondary winding relative to its primary winding to raise or lower the voltage supplied to the motor, without requiring power-electronic switching components. Because the electromagnetic torque developed by an induction motor was approximately proportional to the square of the applied voltage at a given slip, reducing the supply voltage reduced the torque available at every operating speed; to supply the same load torque, the motor must then run at a higher slip, and therefore a lower speed, than it would at rated voltage. This relationship limited voltage control to a comparatively narrow useful speed range close to the motor's rated speed, since a large voltage reduction was needed to achieve even a modest speed reduction, and it increased rotor losses, and therefore heating, at low speed because more slip power was dissipated in the rotor circuit for the same load. Voltage control was consequently not ideal for high-performance tasks requiring a wide, precisely controlled speed range, but it remained a practical choice for low-cost applications with a limited speed-adjustment range, such as small fans and pumps [28].

2.3.1.2 Frequency Control

The voltage applied to the motor at this frequency is varied by using a variable frequency drive

(VFD). The voltage is proportionally adjusted alongside the frequency to uphold the V/f ratio. This technique provides better control over the motor's speed and is appropriate for high performance uses.

Scalar control has some limitations, such as reduced efficiency at lower speeds and difficulties in starting the motor at full load. Therefore, it is mostly used suitable for uses where great performance or precision are not necessary. Scalar control is a simple and cost-effective technique to regulate the speed of induction motors that run in single phase. It entails adjusting the motor's voltage and frequency in relation to preserving

a steady V/f ratio. The particular application requirements determine whether to use frequency or voltage control [27].

2.3.2 Vector Control

It is referred to as field-oriented management, this method represents a more complex approach for regulating the torque and speed of induction motors that run in single phase. It enables precise management of motor performance by manipulating the magnetic field generated by the motor. In vector control, the stator currents and voltages are converted to a two-phase system (d-q reference frame) from the three-phase system that aligns with the motor's magnetic field [29]. This conversion facilitates the separation of the components of torque and flux of the current, permitting for independent control. There are two main vector control techniques typically applied to SPIMs: Indirect field-oriented control (FOC) and direct torque control (DTC).

2.3.2.1 Direct Torque Control (DTC)

It is possible to directly alter the torque of the motor by changing the voltage and frequency supplied to it. This is accomplished by maintaining the desired values by altering the voltage and frequency after comparing the measured motor speed and torque with the desired values [30]. Although DTC offers precise and quick torque control, there is a risk of significant torque ripple.

2.3.2.2 Indirect Field-Oriented Control (FOC)

The torque and flux of the motor are regulated independently by adjusting the components of the stator current. This is done by first estimating the rotor flux and position and then controlling the torque and flux components by converting currents from the stator into the reference frame d-q [31]. FOC provides smoother torque control and reduced torque ripple, but it requires more complex calculations and control algorithms [32]. The structure of an indirect field-oriented control scheme is shown in Figure 2.7.

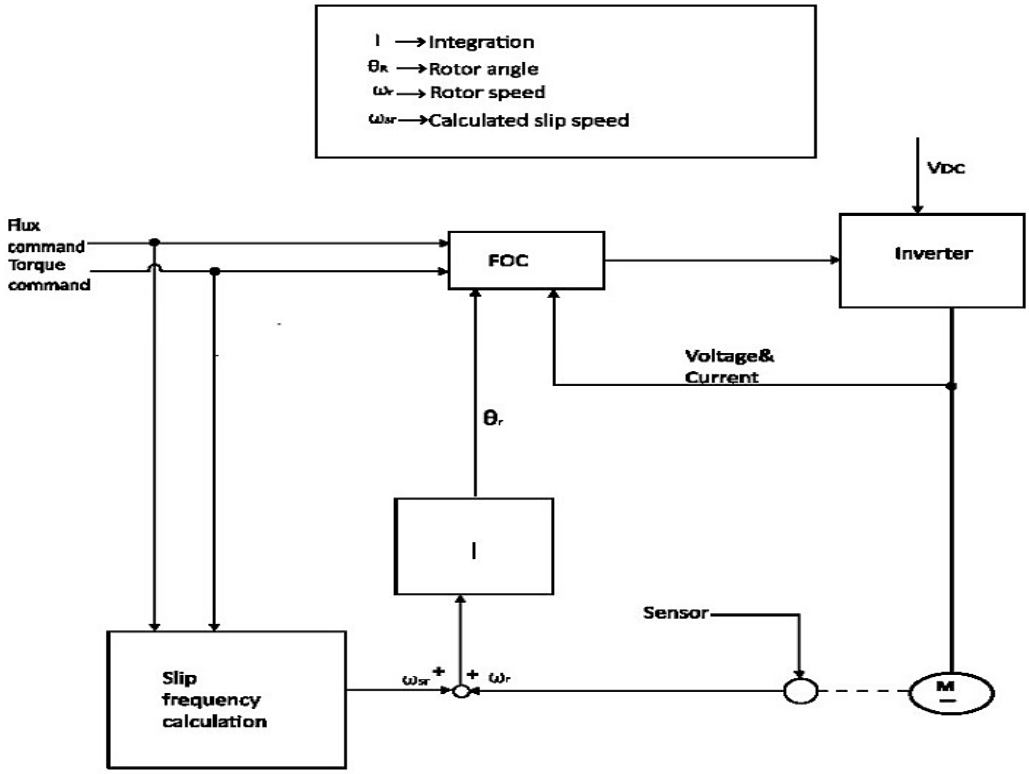


Figure 2.7: Indirect field-oriented control

Vector control provides high precision and dynamic performance for SPIMs, making it appropriate for high-performance uses including electric cars, robots, and industrial drives.

2.3.3 Sensorless Vector Control

Sensorless vector control (SVC) has become an approach that is widely used to regulate SPIM speed [24]. SVC of SPIMs involves the use of advanced signal processing techniques to estimate the motor speed and position. These techniques include high-frequency signal injection, it measures the motor position with the introduction of a high-frequency pulse into the motor windings, and model-based estimation, which calculates the position and speed of the motor using a mathematical model [33].

Once the speed and position of SPIM are estimated, the motor speed and torque can be controlled by the control system using a vector control method. The vector control algorithm involves the use of two orthogonal components of the motor current, known as the direct and quadrature components, to regulate torque and speed of the motor. By adjusting the amplitude and phase of these components, the control system can

regulate single-phase induction motors (SPIMs) speed and torque without sensors, known as sensorless vector control, represents a dependable and economical approach for low-power applications. However, it requires sophisticated signal processing algorithms and motor models, and its performance may be affected by motor parameter variations and other factors [34].

Sensorless vector control techniques have gained significant attention in single-phase induction motor control in the recent years due to their advantages such as cost-effectiveness, reliability, and ease of implementation [35]. Fuzzy-PID regulators have been widely used to enhance sensorless performance vector control techniques for single-phase induction motors [36] while MRAS plays a pivotal role in sensorless control systems by providing a mechanism to adapt and estimate parameters of the motor in real-time [37]. Figure 2.8 illustrates a typical sensorless vector control drive configuration for a single-phase induction motor.

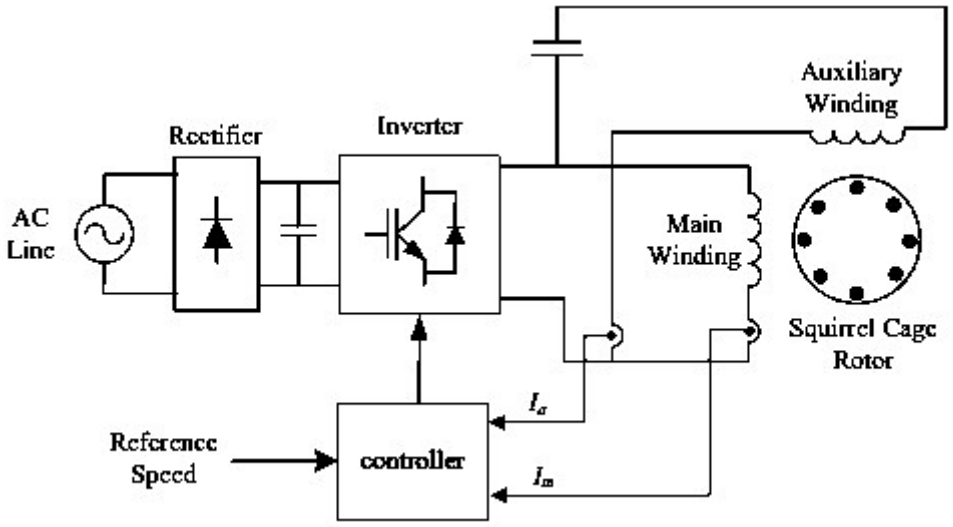


Figure 2.8: Drive for a single-phase induction motor (SPIM) [34]

2.3.4 Variable Frequency Drives (VFD)

Single-phase induction motor that uses pulse width modulation (PWM) techniques to vary the power supply's frequency, typically consist of a rectifier, DC link, inverter, and control circuitry [38]. VFDs can provide accurate speed control, high efficiency, and improved power factor, but they can also generate harmonic distortion and require careful filtering and grounding. a reference signal is compared to a modulating signal, such as a sine wave or a sawtooth wave. The resulting waveform is a series of pulses

that vary in width according to the modulating signal. The frequency of the pulses, also known as the switching frequency, is typically in the range of tens of kilohertz to several megahertz. PWM signal is used in order to regulate the switching of transistors that are connected to the motor windings, which can change the frequency and voltage of the power supply [39].

2.4 Speed Controllers of SPIM

SPIMs have various types of controllers that have been used to improve motor speed for it to achieve desired stabilities.

2.4.1 PI Controllers

A PI controller where the discrepancy between the intended and calculated values of a process variable (such as motor speed) is measured and used to adjust the control signal that drives the motor [40]. The PI controller lowers steady-state error and increases system stability by combining proportional and integral control actions which adjust frequency drive used to control the speed of the motor [41]. The PI controller alters the frequency of the power supply supplied to the motor based on input from a speed sensor. The proportional term of the PI controller adjusts the frequency of the power supply in proportion to the error between the motor's intended and actual speeds, while the integral term adjusts the frequency to eliminate any steady-state error [42]. PI control equation is illustrated i equation (2.9).

$$u(t) = K_p e(t) + K_i i \int_0^t e(\tau)\, d(\tau) \tag{2.9}$$

Where:

- $u(t)$: control signal (output of the PI controller)
- $e(t)$: error (difference between reference and actual speed)
- K_p: proportional gain
- K_i: integral gain

2.4.2 PID Controllers

PID controllers are simple and well-established controllers that can provide good control performance for linear systems and are commonly used in SPIM drives to

achieve speed control and improve dynamic response. The PID controller calculates an error signal that symbolizes the distinction between the desired speed as well as the true speed of the motor and then modifies the motor voltage or frequency accordingly to minimize this error signal [43]. The basic structure of a PID controller is illustrated in Figure 2.9.

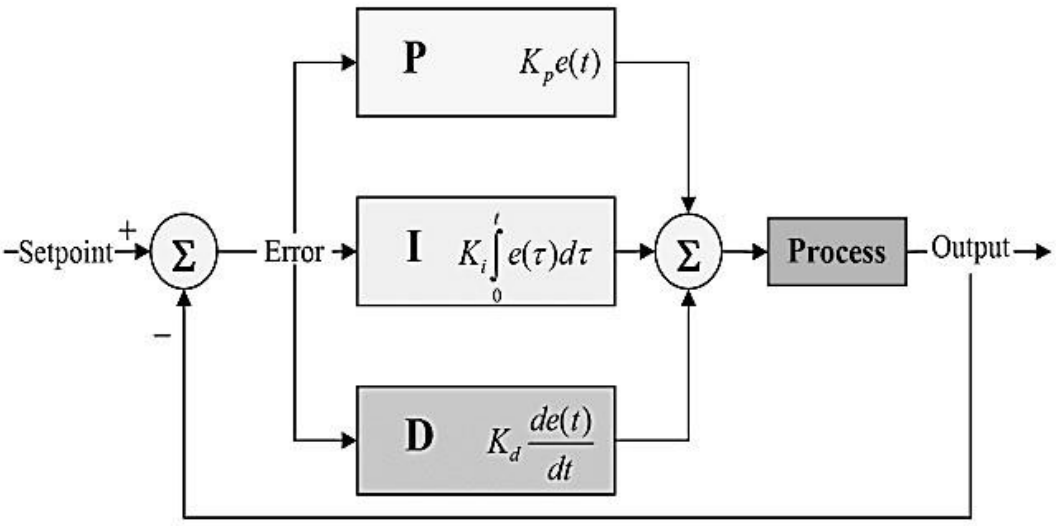


Figure 2.9: PID block diagram [44]

The gains of each component of the PID controller may be adjusted or tuned to achieve the desired reaction of the system. Generally, the P component is used to achieve fast response, the I component is employed to get rid of steady-state mistakes, and the D component is utilized to lessen overrun and oscillations. The equation illustrated in the block are as follows;

$$u(t) = K_p e(t) + K_i \int_0^t e(\tau)\, d(\tau) + K_d \frac{d\, e(t)}{dt} \tag{2.10}$$

Where:

- $u(t)$: controller output
- $e(t)$: error between reference
- K_p: proportional gain
- K_i: integral gain
- K_d: derivative gain

The application of a PID controller to an induction motor operating in single phase can be done using analog or digital circuits, or through software in a microcontroller. Creating and utilising a PID controller for an induction motor that runs on a single phase necessitates a comprehensive comprehension feature of the motor, the various load conditions it encounters, and the specific control objectives targeted [45].

2.4.3 Fuzzy Logic Controllers

Fuzzy logic controllers (FLCs) are widely applied in motor control applications due to their ability to handle nonlinearities and uncertainties. Fuzzy rules are used in a fuzzy logic controller (FLC) to map inputs to outputs. Linguistic variables are utilised to indicate the controller's inputs and outputs [46]. The inputs are usually the error and its rate of change, and the output is the control signal, which can be the voltage or frequency of the motor. The expert knowledge or experimental data and can be modified to optimize performance because of the fuzzy rules derived. Several approaches to designing and implementing FLCs for SPIM drives, such as Mamdani-type FLCs, Sugeno-type FLCs, and Takagi-Sugeno-Kang-type FLCs. The approach selected is determined by the particular needs and limitations of the application, the performance of FLCs depends on the choice of membership functions, fuzzy rules, and tuning parameters, which can be time-consuming and may require trade-offs between conflicting performance criteria. The design and implementation of FLCs can be complex, and their performance depends on the choice of membership functions, fuzzy rules, and tuning parameters [47].

2.5 Fuzzy Logic Control Techniques (FLCT)

In situations where creating a mathematical model of a system is challenging, FLCT is especially helpful, or when the system is too complex for traditional control methods. In FLCT, the control system inputs and outputs are described using fuzzy sets, which are a generalization of crisp sets that allow for degrees of membership between 0 and 1. The rules of the control system are specified using fuzzy if-then rules, which define how the input variables should be combined to produce the output [2].

Fuzzification

Fuzzification is a process in fuzzy logic that converts crisp (non-fuzzy) input values into fuzzy values, which are represented as membership functions [9]. In a fuzzy set,

membership functions give each input value a degree of membership, demonstrating the degree to which the input value is a member of that set. It represents a critical stage in the fuzzy logic process, empowering the system to effectively manage imprecise or uncertain input values in a more flexible way than traditional logic systems. By representing input values as fuzzy sets with membership functions, the system can reason about the input values in a more human-like way, using degrees of certainty rather than binary true/false values.

Numerous methods, including triangular, trapezoidal, and Gaussian membership functions, could be utilized for fuzzification. The characteristics of the fuzzy logic system and the input values determine which membership function should be used [47].

2.6 Related Theories

2.6.1 Model Reference Adaptive System

Model Reference Adaptive System (MRAS) main goal is to lessen the discrepancy between estimated and actual values. It is used to determine the induction motor's rotational velocity by relying just on the stator current and voltage information. MRAS play a pivotal role in sensorless control systems by providing a mechanism to adapt and estimate the parameters of the motor in real-time. These adaptive systems contribute to accurate speed and position estimation, compensating for variations and uncertainties in motor characteristics. The fundamental principle involves comparing the output of a reference model, often representing an idealized motor, with the actual system output, and adjusting parameters to minimize the difference [48].

The adaptation mechanism typically involves an adaptive law that updates the parameters according to the discrepancy between the output of the reference model and the real output. Rotor flux is one of the widely used MRAS structures for estimating speed in induction motors.

The MRAS speed estimation equation is often formulated as follows:

$$\varpi MRAS = \frac{1}{P} \frac{d\overline{\theta} MRAS}{dt} \omega \tag{2.11}$$

Where:

- $\bar{\omega}MRAS$ is the rotor speed estimated,
- $\bar{\theta}MRAS$ *is the rotor's predicted position,*
- P *is t*he quantity of pole pairs.

The parameters of the MRAS are modified in order to reduce the speed estimation error. The success of MRAS lies in its ability to adapt to varying conditions, making it particularly suitable for sensorless control where accurate parameter estimation is crucial [49].

2.6.2 Fuzzy-PID Regulator

Fuzzy-PID-based speed controller is an effective strategy for controlling the speed of SPIMs using SMVC. When managing nonlinearities and uncertainties, the controller performs well in terms of controlling speed and transient responsiveness. The recommended controller exceeds the performance of the traditional PID controller, according to data from experiments and simulations [10]. The fuzzy-PID controller combined the advantages of the PID and FLC controllers, resulting in a controller that could handle nonlinearities and uncertainties while providing good control performance [50].

A based speed controller designed for a sensorless vector-controlled SPIM has been implemented and the proposed controller was designed to enhance the functionality of the motor in relation to speed regulation and transient response. Simulation findings indicated that the suggested controller provided improved efficiency compared to the traditional PID controller [44]. The controller for fuzzy-PID was devised to regulate a single-phase induction motor's velocity, rotor position estimation applying an adaptive neuro-fuzzy inference system (ANFIS).

The Fuzzy-PID system evaluates linguistic variables, indicating that the inputs and outputs should be categorised as Z, NB, NM, NS, PS, PM, and PB. These variables include error (e), error change (e_c), and control signal [51]. Fuzzy rules govern the interaction of these linguistic variables to determine the adjustments required for the gains of the PID controller. The linguistic rules typically manifest as "if-then" statements, reflecting the expert understanding of the system. Here are the two inputs and three outputs of the fuzzy PID controller that is adaptive. The inputs of the fuzzy

control are the error of the speed (e) and the change in speed error (e_c), while the outputs fuzzy were determined by $\overline{\Delta K_p}$, $\overline{\Delta K_\iota}$, and $\overline{\Delta K_d}$ as shown in Equation 2.12.

$$\begin{aligned} \Delta K_p &= K_p \times \Delta K_p^* \\ \Delta K_i &= K_i \times \Delta K_i^* \\ \Delta K_d &= K_d \times \Delta K_d^* \end{aligned} \tag{2.12}$$

Fuzzy inference system output guides the adjustments to the PID parameters. The fuzzy output is then combined with the traditional PID output to form the overall control signal [52]. The blending of fuzzy logic with PID control allows for a more flexible and adaptive response to varying and nonlinear system dynamics.

Mathematically, the Fuzzy-PID controller output $u(t)$, is often expressed as in equation (2.13):

$$u(t) = Fuzzy\ Output + K_p.e(t) + K_i.\int_0^t e(\tau)\,d(\tau) + K_d\ .\ \frac{d\,e(t)}{dt} \tag{2.13}$$

Where:

- $u(t)$ is the control signal,
- $e(t)$ is the error signal,
- Kp, Ki, and Kd are the proportional, integral, and derivative gains, respectively.

All things considered, these investigations show how well fuzzy-PID-based speed control works with SVC for single-phase induction motors. It has been noted that the fuzzy-PID controller outperforms the speed regulation, transient response, and resilience to parameter changes and load disturbances than other fuzzy-based controllers and traditional PID controllers. Fuzzy-PID-based induction motors with single-phase speed control can be optimized using intelligent control algorithms to achieve enhanced robustness, energy economy, and speed control performance figures.

2.6.3 Integration of MRAS and Fuzzy-PID Regulator

The integration of the Model Reference Adaptive System (MRAS) with a Fuzzy-PID controller is a strategic approach aimed at enhancing the robustness, adaptability, and

overall performance of sensorless control of speed systems for single-phase induction motors (SPIMs). This combined control scheme leverages the strengths of both MRAS and fuzzy logic-based PID regulation to overcome the limitations of conventional controllers [53].

The MRAS component is responsible for accurate real-time estimation of motor parameters, particularly the rotor speed, by continuously comparing the outputs of a reference model and an adaptive model. It compensates for variations and uncertainties in system dynamics without the requirement for physical sensors, which lowers expenses and system difficulty. The adaptive nature of MRAS ensures that parameter estimation evolves in response to operational changes, thus maintaining consistent control accuracy.

Fuzzy-PID controller dynamically tunes the proportional, integral, and derivative gains using a rule-based fuzzy inference system. These fuzzy rules are derived from expert knowledge and designed to manage nonlinearities, uncertainties, and external disturbances more effectively than traditional fixed-gain controllers. The controller uses error and change in error as inputs to adjust the PID gains in real time, resulting in a more responsive and stable system. The integration process involves a coherent interaction between the two systems. The accurate parameter estimates generated by MRAS inform and adjust the fuzzy logic rules or membership functions of the Fuzzy-PID controller [54]. This ensures that the controller's decision-making process is based on real-time motor behavior, thereby improving the precision and stability of speed control. Such synergy allows the system to maintain excellent performance in a range of load and environmental circumstances, making it especially suitable for applications in industry where dependability and effectiveness are paramount.

Mathematically, the integrated output could be expressed as:

$$u(t) = FuzzyPID\,Output + MRAS\,Output \tag{2.14}$$

Where:

- u(t) is the overall control signal,
- Fuzzy PID Output is the output of the Fuzzy-PID controller,

- MRAS Output is the output of the MRAS system.

In summary, the integration of MRAS and Fuzzy-PID regulation offers a hybrid control strategy that combines model-based adaptation with intelligent rule-based tuning. This results in a sensorless control solution capable of achieving faster response times, minimal steady state error, and increased reliability, thus addressing the key challenges in SPIM speed regulation.

Table 2.1: Summary matrix of key related literature on SPIM/induction-motor speed control

Reference	Approach	Strengths	Gap Identified
[1] , [8] Hussain & Mugheri (2021)	Fuzzy Logic-based PI controller with V/f control	Improved dynamic response over conventional PI	Sensor-based; not applied to single-phase machines
[3] Irianto et al. (2021)	Comparison of PI, PID and Fuzzy Logic controllers for SPIM speed stability	Direct SPIM comparison of three controller types	No sensorless estimation; controllers evaluated independently, not integrated
[5] Zorgani et al. (2023)	MRAS scheme for sensorless induction motor drive	Removes physical speed sensor; adaptive estimation	Not SPIM-specific; no fuzzy adaptation of the controller
[6] Hamdi et al. (2023)	MRAS with a deadbeat regulator for sensorless speed control	Fast regulator response paired with MRAS estimation	Deadbeat regulator lacks nonlinear adaptability of fuzzy control; not SPIM-specific
[7] Mohamed & El-Sehiemy (2019)	Fuzzy-based PID controller for a split-phase induction motor	Demonstrates Fuzzy-PID benefit for a single-phase-type machine	Physical-sensor feedback scheme; no MRAS-based

Reference	Approach	Strengths	Gap Identified
			sensorless estimation
[13] Soni et al. (2022)	Adaptive-neuro fuzzy technique integrated with MRAS module	Combines MRAS with an intelligent (ANFIS) estimator	Adds computational complexity; not evaluated on a single-phase machine
[15] Vennapusa et al. (2021)	Hybrid controller for SPIM speed control	Targets SPIM directly with a hybrid control strategy	Does not integrate MRAS sensorless estimator with the hybrid controller

As Table 2.1 shows, MRAS-based sensorless estimation and Fuzzy-PID control have each been studied, and occasionally combined, for three-phase and split-phase machines, but no reviewed study integrates a MRAS sensorless estimator with a Fuzzy-PID regulator specifically for single-phase induction motors; this is the gap addressed in this thesis.

2.7 Research Gaps

Reviewed studies on scalar and vector control, PI/PID regulation, and fuzzy logic control have largely targeted three-phase induction machines; sensorless speed control of single-phase induction motors remains comparatively underexplored, and few studies have combined a MRAS estimator with a Fuzzy-PID regulator in which the fuzzy stage retunes the PID gains from the MRAS-estimated speed error in real time. This gap, correlating directly with the problem stated in Section 1.2, motivates the MRAS-Fuzzy-PID integration developed in Chapter 3 of this thesis.

2.8 Conceptual Framework

The conceptual framework of this study illustrates the relationship between the independent, intervening, and dependent variables underlying the proposed sensorless

speed-control system for the single-phase induction motor (SPIM), as depicted in the figure 2.10.

The independent variables, comprising input voltage and frequency, load torque, motor parameters (stator and rotor resistance and inductance), and the reference speed setpoint, represent the operating conditions and system inputs that the controller must respond to.

These inputs pass through an intervening process consisting of three stages. First, the MRAS estimator computes the rotor speed by comparing the outputs of a reference model and an adjustable model, generating an adaptive error signal without requiring a physical speed sensor. Second, this error and its rate of change are fed into the fuzzy logic tuner, which applies linguistic rules to determine appropriate adjustments to the controller gains. Third, the PID controller uses these fuzzy-tuned gains (Kp, Ki, Kd) to compute the final control signal applied to the motor. The estimated speed is fed back into the MRAS stage, forming a closed adaptive loop.

The dependent variables, namely speed-tracking error, dynamic (transient) response, and robustness to load variation, represent the performance outcomes used in Chapter 4 to evaluate the proposed MRAS-Fuzzy-PID controller against the MRAS-only and MRAS-Fuzzy benchmark systems.

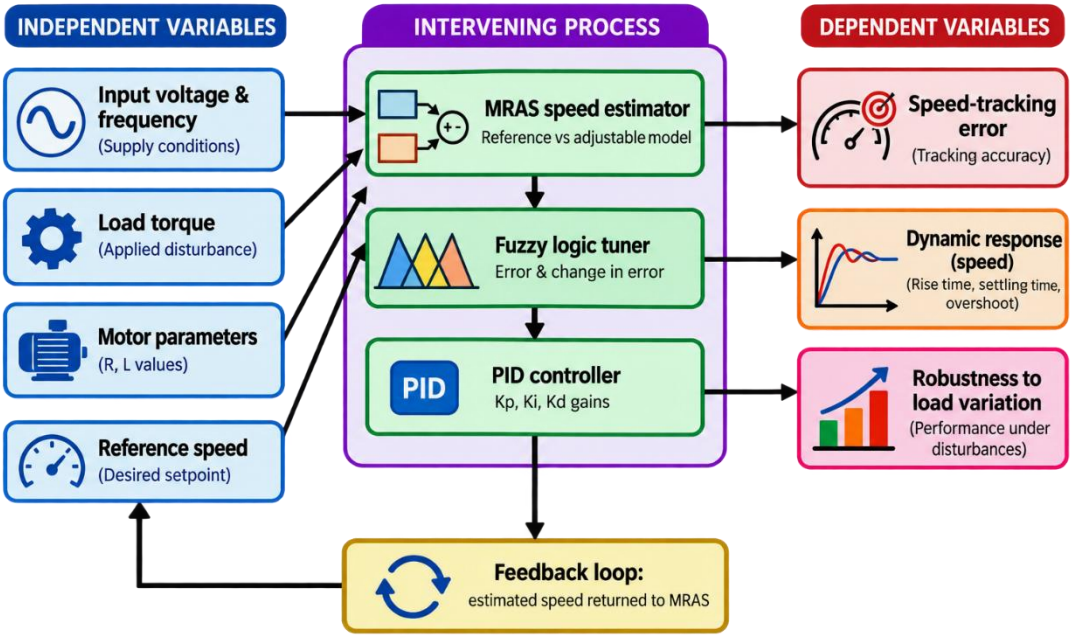


Figure 2.10: Conceptual framework of the study

2.9 Summary

This chapter has provided a comprehensive evaluation of the theoretical and technical foundations underpinning the control of single-phase induction motors (SPIM), with particular emphasis on sensorless speed control strategies. The limitations of conventional techniques for control, including vector and scalar control, were discussed, highlighting the challenges associated with torque reduction, low-speed instability, and the reliance on physical sensors.

To address these challenges, the chapter examined the Model Reference Adaptive System (MRAS) as a robust framework for estimating motor parameters in real time without physical sensors. Additionally, the Fuzzy-PID controller was explored as an intelligent control strategy capable of dynamically tuning control parameters based on system behavior. The integration of MRAS and Fuzzy-PID was introduced as a hybrid control solution that leverages the adaptive estimation capability of MRAS and the nonlinear decision-making strength of fuzzy logic to achieve enhanced speed regulation performance.

This integrated approach provides a promising direction for sensorless SPIM control, offering improved accuracy, robustness, and adaptability under varying load and environmental conditions. The concepts and findings discussed in this chapter form the theoretical basis for the system modeling, design, and implementation addressed in the subsequent chapters of this thesis.

CHAPTER THREE
RESEARCH METHODOLOGY

3.1 Introduction

This chapter presents the design stages, control architecture, modeling equations, parameter definitions, and implementation steps undertaken to achieve the research objectives, describing the design and implementation of the technique used to achieve accurate and stable speed control of a single-phase induction motor (SPIM) through a hybrid control system that integrates a Model Reference Adaptive System (MRAS) with a Fuzzy-PID controller. The objective of this work was to enhance the dynamic performance of the SPIM by improving speed estimation and reducing control error under varying load conditions.

The methodology began with the modeling of the SPIM using fundamental electrical and mechanical equations, where key parameters such as stator and rotor resistances and inductances, supply frequency, input voltage, motor inertia, number of poles, and frictional losses were defined. These parameters were essential for constructing a simulation model that accurately represents the motor's real-world behavior.

To estimate the rotor speed without direct measurement, a MRAS observer was designed. The MRAS consisted of a reference model and an adjustable model, with the difference between their outputs forming an adaptive error signal. This estimated error was then fed into a fuzzy logic system, which made intelligent decisions based on linguistic rules and membership functions to handle nonlinearities and uncertainties.

The fuzzy output was used to adjust the gains of a traditional PID controller, which computes the final control signal to regulate the motor speed. This combined Fuzzy-PID approach ensured both adaptability and precision in response to system disruptions and changes in parameters.

The complete system was implemented and tested in a simulation environment, where various load torque conditions were utilized to assess how successful the suggested control strategy. The simulation results were analyzed based on performance indicators such steady-state error, overshoot, and settling time, and torque response.

The overall research methodology followed in this study was summarized in the flow chart presented in Figure 3.1.:

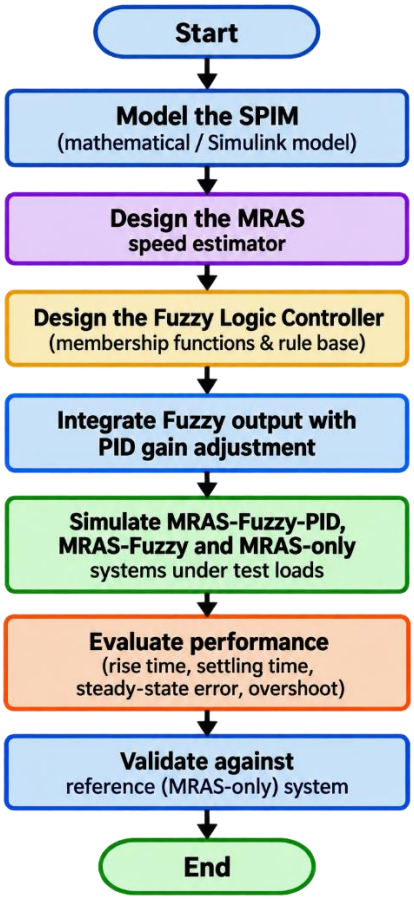


Figure 3.1: Flow chart of the research methodology followed in this thesis

3.2 Single-Phase Induction Motor Model and its Speed-Torque Characteristic

The mathematical representation of a sensorless speed control system for a single-phase induction motor (SPIM) forms the foundation for developing an efficient control strategy. The approach involved utilizing existing SPIM model to implement a sensorless vector speed control scheme. A detailed understanding of the electrical and mechanical behavior of the SPIM was essential to accurately estimate speed and torque without using physical sensors.

3.2.1 Existing Model of a Single-Phase Induction Motor

Figure 3.2 illustrates the conventional comparable circuit model of a single-phase induction motor. This model includes key components necessary for deriving the fundamental voltage equations of both the stator and rotor. These formulae for voltage,

together with the flux linkage and electromagnetic torque expressions, form the basis of the SPIM's dynamic behaviour. The motor was typically modeled with a main winding (β)and an auxiliary winding (α), where the auxiliary winding generally possesses fewer turns than the main winding. The interaction between these windings was crucial for initiating and sustaining the rotating magnetic field needed for motor operation.

The equivalent circuit model also served as the foundation for developing the mathematical framework of a sensorless vector control strategy. Specifically, it guided the derivation of state space equations, which were later employed in the implementation of the Model Reference Adaptive System (MRAS) and the Fuzzy-PID controller.

This modeling approach enables real-time estimation of rotor speed and electromagnetic torque, which were essential for controlling closed-loop speed and provided a necessary starting point for the design of the sensorless control system explored in this thesis.

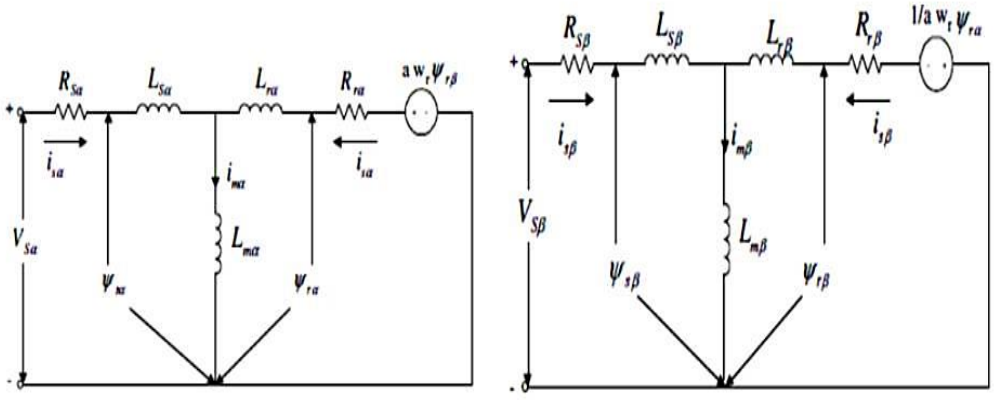


Figure 3.2: Equivalent circuits of SPIM [8]

3.2.2 Simulation of Single-Phase Induction Motor

The mathematical model of a single-phase induction motor (SPIM) was essential in the design and implementation of a sensorless speed control system, as it captured both the electrical and mechanical dynamics of the motor through a set of differential equations. This model enabled accurate representation of motor behavior under various operating conditions, which was critical for control system development.

The SPIM consists of a stator with two windings primary (main) and secondary (auxiliary) as well as a rotor squirrel-cage. The windings of the stator are placed ninety (90) electrical degrees apart to establish a quasi-rotating magnetic field. Typically, only after startup does the auxiliary winding become engaged in order to generate the necessary phase shift for rotation. However, in low-power applications, the auxiliary winding may remain energized during operation to improve performance and efficiency [16]

The simulation model incorporated the fundamental voltage formulas for the rotor and stator, in addition relating to the flux linkage and electromagnetic torque expressions. These equations were derived in the stationary reference frame using the d-q axis transformation, which simplified the analysis and control of the AC machine.

Figures 3.3 and 3.4 illustrated the corresponding circuits for the main and auxiliary windings on the d-axis and q-axis, respectively. These circuits formed the basis of the simulated model used in this study, serving as a platform for implementing the sensorless control strategy predicated on the Model Reference Adaptive System (MRAS) and Fuzzy-PID controller. The simulation provided critical insights into motor performance, enabling validation of the proposed control techniques under various loading and speed conditions.

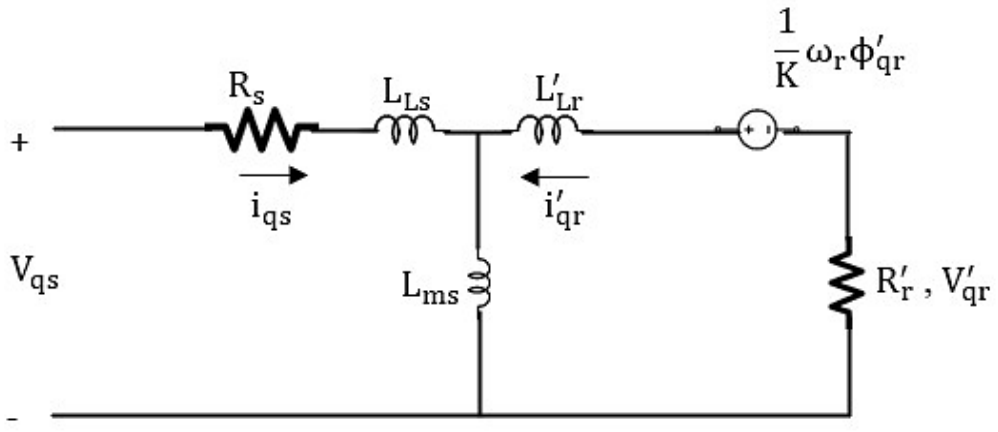


Figure 3.3: q-axis (Main winding)

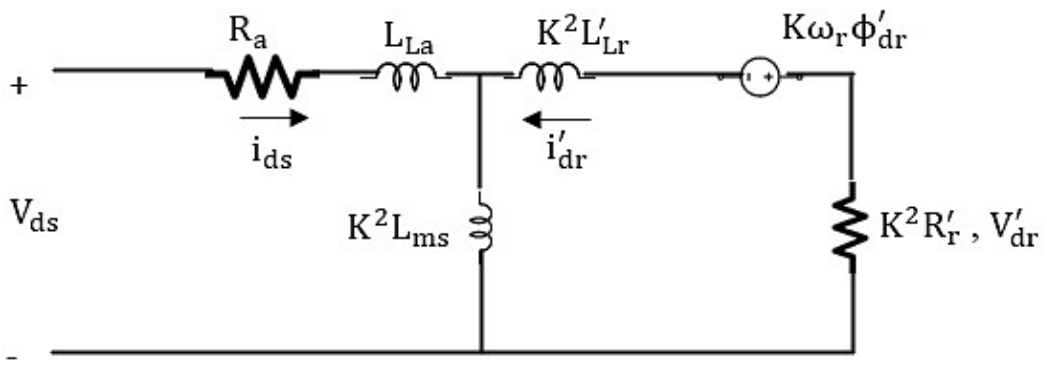


Figure 3.4*:* d-axis (Auxiliary winding)

To develop an accurate mathematical model of the single-phase induction motor (SPIM), it was essential to derive the fundamental formulae for the stator and rotor voltages, as well as the equations governing electromagnetic torque and magnetic flux. These equations provided the foundation for examining the changing behaviour of the motor under varying conditions. The voltage equations for the SPIM are formulated using Kirchhoff's Voltage Law (KVL), which accounts regarding the resistive and inductive components of the windings of the stator and rotor. The modeling approach adopts the d–q axis transformation to represent the motor's equations in the stationary reference frame, thereby simplifying the analysis of the time-varying electrical quantities. The derived equations were presented by equations (3.1 to 3.4) as applied by [47]:

$$V_{qs} = R_s i_{qs} + \frac{d\phi_{qs}}{dt} \tag{3.1}$$

$$V_{ds} = R_a i_{ds} + \frac{d\phi_{ds}}{dt} \tag{3.2}$$

$$V_{qr} = 0 = R'_r i'_{qr} + \frac{d\phi'_{qr}}{dt} - \frac{1}{K}\omega_r \phi'_{qr} \tag{3.3}$$

$$V_{dr} = 0 = K^2 R'_r i'_{dr} + \frac{d\phi'_{dr}}{dt} + K\omega_r \phi'_{dr} \tag{3.4}$$

The equations provide dynamic behavior of the SPIM which were instrumental in constructing simulation models that formed the basis for sensorless speed control.

Then the flux linkage equations of the single-phase induction motor (SPIM) were essential in modeling of electromagnetic interactions between the stator and rotor windings. These equations described relationship between flux linkages and the corresponding winding currents. They were derived from the magnetic circuit and mutual coupling relationships within the motor. The following expressions define the flux connections for the stator and rotor windings on the d and q axes:

$$\phi_{qs} = (L_{ls} + L_{ms})i_{qs} + L_{ms}i'_{qr} \tag{3.5}$$

$$\phi_{ds} = (L_{la} + K^2 L_{ms})i_{ds} + K^2 L_{ms}i'_{dr} \tag{3.6}$$

$$\phi'_{qr} = (L'_{lr} + L_{ms})i'_{qr} + L_{ms}i_{qs} \tag{3.7}$$

$$\phi'_{dr} = K^2(L'_{lr} + L_m s)i'_{dr} + K^2 L_{ms}i_{ds} \tag{3.8}$$

The flux equations, were then combined with voltage equations to form the basis of the SPIM's dynamic model which were key for accurate simulation and control.

The electromagnetic torque which was expressed, T_e was acquired by use of virtual displacement principle [55] which related mechanical output torque to the way magnetic fields of the rotor and stator interacted.

$$T_e = p(K\phi'_{qr}i'_{dr} - \frac{1}{K}\phi'_{dr}i'_{qr}) \tag{3.9}$$

p being the pole pairs.

This expression defined torque as a function of the relationship between components of the rotor current and the rotor flux in the quadrature and direct axes.

To clearly explain the induction's dynamic behavior motor, the mechanical equation of motion was also incorporated. It represented Newton’s second law as applied to rotational system:

$$J\frac{d\omega_m}{dt} = T_e - T_L - B_m\omega_m \tag{3.10}$$

Where:

J = rotor inertia

ω_m = Rotor mechanical angular velocity

B_m = Friction coefficient

T_L = Load Torque

Slip is a pivotal factor in induction motor operation, representing the distinction between rotor speed and synchronous speed. It was calculated using equation (2.1) and (3.11):

$$S = \frac{N_S - N_r}{N_S} \tag{3.11}$$

Where:

N_s = synchronous speed

N_r = Rotational speed

The winding turns ratio parameter was considered in the motor design, particularly when auxiliary windings were used. The turns ratio was computed using equation 3.12:

$$\text{Winding turns ratio, } K = \frac{N_a}{N_m} \tag{3.12}$$

Where:

N_a = number of auxiliary stator winding

N_m = number of main stator winding

To maintain control and analysis, single-phase induction motor stator voltages were transformed into a two-axis reference frame representing auxiliary and main windings.

The conversion formed the single-phase quantities can be represented in relation to the d-q reference frame by:

$$\begin{bmatrix} V_q \\ V_d \\ V_o \end{bmatrix} = \begin{bmatrix} \frac{2}{3} & -\frac{1}{3} & -\frac{1}{3} \\ 0 & -\frac{1}{\sqrt{3}} & \frac{1}{\sqrt{3}} \\ \frac{1}{3} & \frac{1}{3} & \frac{1}{3} \end{bmatrix} \times \begin{bmatrix} V_a \\ V_b \\ V_c \end{bmatrix} \tag{3.13}$$

The interaction between rotor mechanical angular velocity and rotor electrical angular velocity were formulated as presented by model 3.14:

$$\omega_m \times pole\ pair = \omega_r \tag{3.14}$$

Where:

ω_m Mechanical angular velocity of a rotor

ω_r Electrical angular velocity of the rotor

Equations 3.1 to 3.14 were applied to illustrate how single-phase induction motor respond mathematically.

3.2.3 Simulation Procedure

Following the formulation of the mathematical model, the simulation was conducted by defining the initial parameters as listed in Table 3.1. These parameters served as the basis for initializing the motor model and provide the necessary inputs to accurately replicate the motor's dynamic behavior under varied operating conditions.

Table 3.2: SPIM Initialized parameters

Parameter	Value
Frequency	50Hz
R_S	2.02Ω
R_a	7.14Ω
R′r	4.12Ω

Parameter	Value
L_{ls}	$7.4 * 10^{-3}$H
L_{la}	$8.5 * 10^{-3}$H
L_{ms}	0.1772H
L′lr	$5.6 * 10^{-3}$H
Input Voltage	230V
K	1.18
Stator: rotor turns ratio	1
J	0.0146kg. m^2
T_L	Vary
B_m	0.0001N. m. s
P	2 pole pairs
Disconnection speed	98% synchronous speed

The input voltage was converted into the d-q axis components employing the transformation described by Equation (3.14). The corresponding waveform or simulation outcome is presented in Figure 3.5.

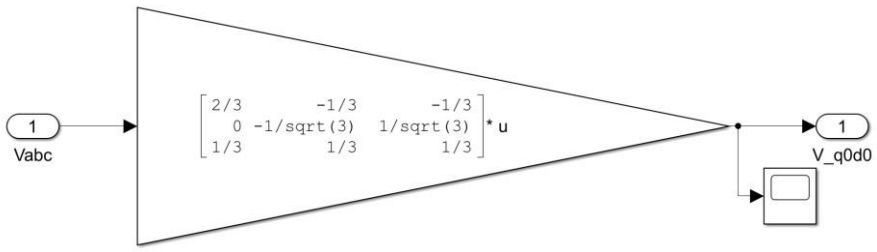


Figure 3.5: Phase to d-q axis calculation as per equation 3.14

The fluxes of the stator as well as rotor were computed using equation 3.1 to 3.4, with the rotor electrical angular velocity ω_r calculated according to equation (3.14) and was presented in figure 3.6.

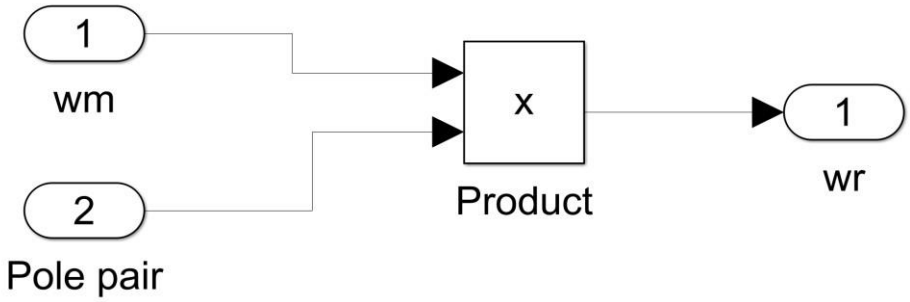


Figure 3.6: Conversion of ω_m to ω_r as per equation 3.14

In the direct and quadrature d-q axis, the stator and rotor currents were computed using the dynamic equations found in equations (3.5) to (3.8). These equations form the current model of the motor, where the d-axis typically represents the magnetizing an element of the current, and the q-axis corresponds to the torque-producing component. Accurate computation of these currents is essential for analyzing the electromagnetic performance of the motor, as they directly influenced torque generation and flux dynamics. The resulting current calculations were presented in appendix 1.5, which clearly depicts the time-domain behavior of both stator and rotor d–q axis currents under the defined operating conditions.

The speed of the rotor and electromagnetic torque were subsequently calculated using equations (3.9) and (3.10), respectively. These equations describe the mechanical dynamics of the motor and the interaction between the electrical and mechanical subsystems. The electromagnetic torque reflects the energy conversion within the motor, while the rotor speed indicates the resulting mechanical output. The simulation results illustrating the time response of both torque and speed are shown in appendix 1.6.

Finally, the slip of the motor was calculated using equations (2.1) and (3.11), which defined the relationship between the rotational speed and the synchronous speed. Slip is a key performance parameter in induction motor analysis, as it shows how much the synchronous speed is outpaced by the rotor, directly affecting torque production and efficiency. The calculated slip profile was presented in Figure 3.7, demonstrating its variation under the simulated operating conditions.

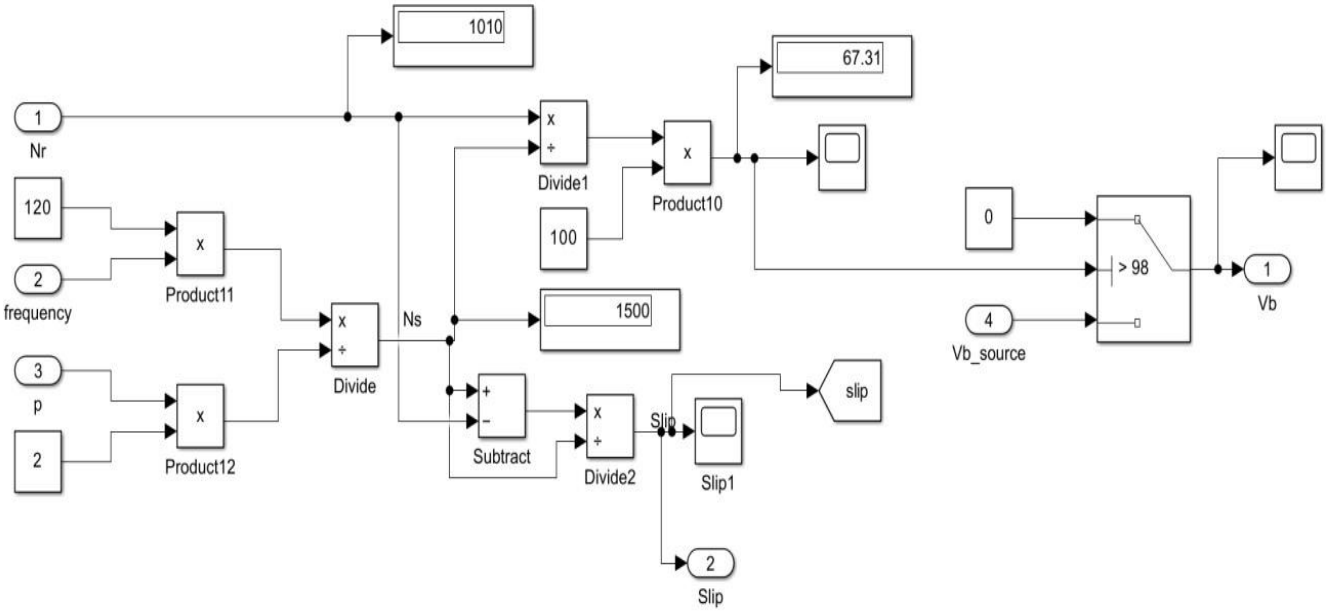


Figure 3.7: Slip calculation as per equation 2.1 and 3.11 and disconnection speed calculation

The complete model developed for the sensorless single-phase induction motor (SPIM), according to the mathematical equations outlined in this chapter, is illustrated in appendix A.7. This model integrates the electrical and mechanical dynamics, coordinate transformations, and slip estimation necessary for sensorless control implementation. It serves as the foundation for subsequent simulation and controller design in this study.

The load torque was then varied incrementally between circumstances of no load and full load in order to evaluate the dynamic response of the motor model under varying mechanical demands. The resulting system behavior was observed and recorded through simulation. Following this, the Model Reference Adaptive System (MRAS) was developed and integrated into the control framework to enable sensorless estimation of rotor speed and to enhance system performance and robustness.

3.2.4 Sensor-Less Vector Control Model of SPIM

Sensorless Vector Control functions as a frequency-based control strategy in which slip compensation is employed to keep the actual rotor speed close to the reference speed, even under varying load conditions. This approach eliminated the need for a physical speed sensor by estimating rotor speed through adaptive algorithms.

To facilitate effective torque production, a torque current estimator is integrated entering the loop of control. As illustrated in figure 3.8, the torque current estimator calculates the part of the stator current that coincides with the stator voltage in phase. This estimation provides an approximate value of the torque-producing current.

Using this information, the slip value was computed, which in turn allows for accurate estimation of rotor speed. This mechanism enhances the motor’s ability to maintain desired performance under dynamic loading conditions, ensuring improved speed regulation and system efficiency.

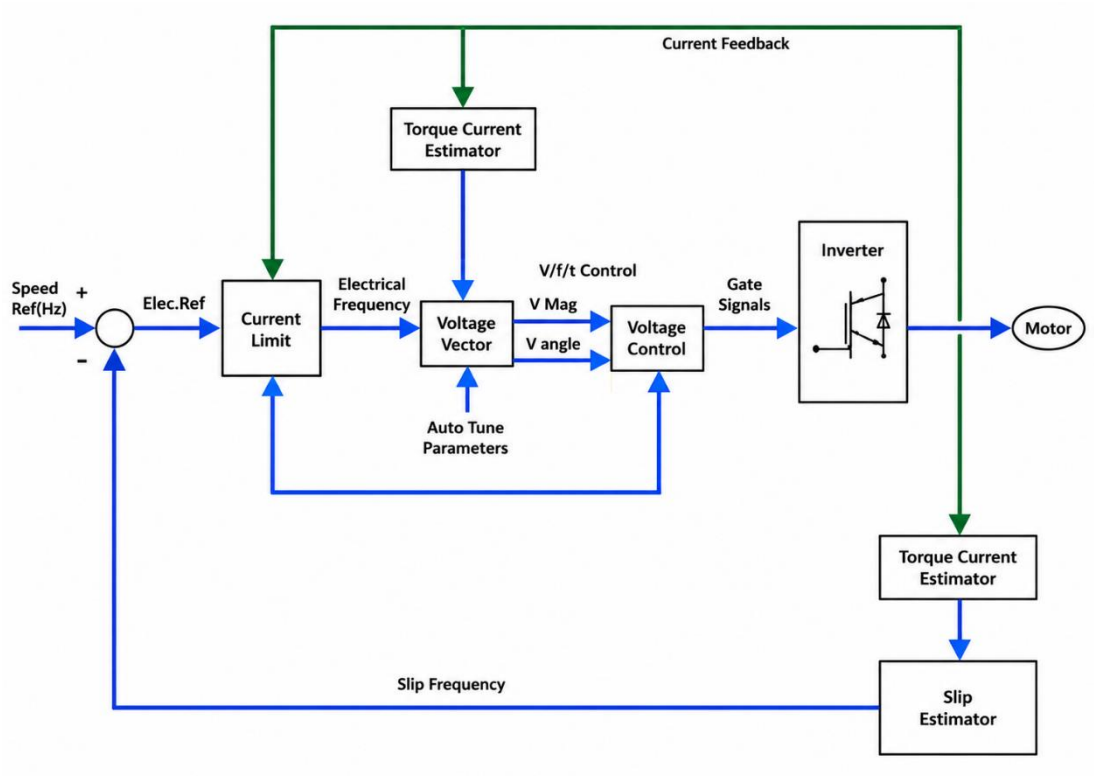


Figure 3.8: Block Diagram Sensorless Vector Control

The sensorless vector control approach provides and phase angle and its magnitude between the current and voltage of the stator, thereby enhancing the performance of the traditional V/Hz control method. While conventional V/Hz drives regulate only the voltage magnitude in proportion to frequency, they do not account for the vector angle between current and voltage. In contrast, the vector control strategy enabled by the Torque Current Estimator controls the phase angle and its magnitude of the stator current.

This allows the system to regulate the entire motor current based on the desired torque and flux components, significantly improving dynamic response. By adjusting the vector angle, the control system enables more precise torque management and superior low-speed performance when compared to conventional scalar (V/Hz) control methods. This makes sensorless vector control particularly effective for applications requiring high efficiency and smooth operation across a wide range of speeds.

3.3 MRAS for a SPIM Sensorless Speed Control Design

To enable accurate and reliable speed estimation without the use of physical sensors, a Model Reference Adaptive System (MRAS) was developed and integrated with a

Fuzzy-PID regulator. These two components were initially modeled independently and later combined to form a complete control system for sensorless speed estimation and regulation of the single-phase induction motor (SPIM).

3.3.1 Designing MRAS

The MRAS was designed using MATLAB Simulink, with the objective of minimizing the error between the actual and estimated motor states. Its primary function is to estimate the rotor speed based on stator voltage and current measurements, thereby eliminating the need for a shaft-mounted speed sensor.

The MRAS strategy relies on two machine model structures: A reference model and a model that can be adjusted. Each model was designed to compute the same motor state variables (typically stator currents or fluxes), but the model with Adjustment incorporates the approximated rotor speed as a variable. As illustrated in figure 3.8, the core principle involves comparing the outputs of the two models. The discrepancy or error between them was fed into an adaption mechanism that modifies the rotor speed estimation to minimize this error over time.

By continuously adapting to changes in the motor's operating conditions, the MRAS structure enhances robustness and provides accurate real-time speed estimation for effective implementation of sensorless vector control.

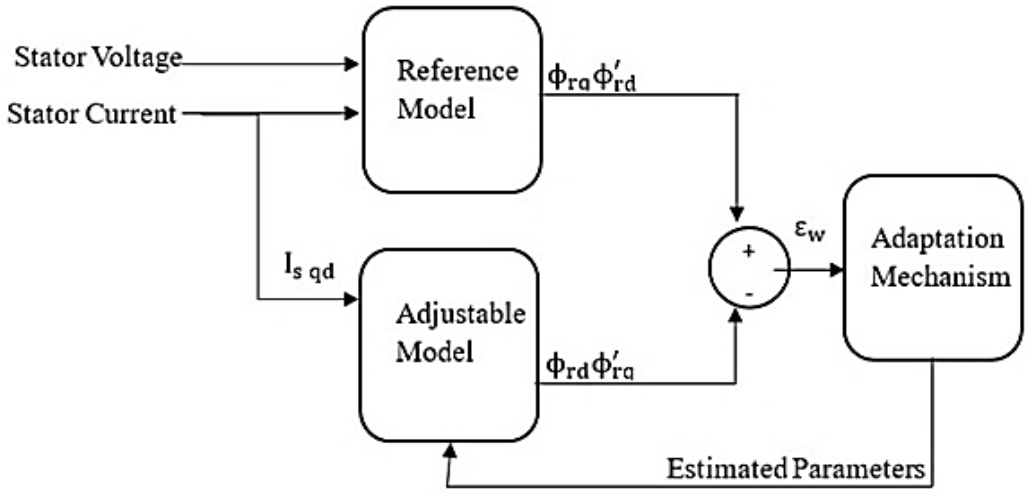


Figure 3.9: MRAS speed scheme estimator

The output variable for both the Reference Model and Adjustable Model is the rotor flux, which serves as the key state variable to be estimated. The Reference Model utilizes voltage and current calculations for the stator to compute the rotational flux, providing a baseline flux value. Simultaneously, the Adjustable Model incorporates the rotor flux equations where the electrical rotor speed is treated as an adjustable parameter. By comparing the rotor flux estimates from both models, the MRAS adaptation mechanism updates the rotor speed estimate to minimize the difference, thus ensuring accurate sensorless speed estimation.

The Reference mechanism

From Figure 3.9, the inputs to the MRAS are the stator voltage and current signals, which serve as inputs to the Reference Model. The Reference Model computes the rotor flux components using the stator voltage and current inputs, as described by equations (3.15) and (3.16):

$$\frac{d\phi_{rd}}{dt} = \frac{L_r}{L_{ms}}\left(V_{sd} - R_s i_{sd} - \sigma L_s \frac{\partial i_{sd}}{\partial t} \right) \tag{3.15}$$

$$\frac{d\phi_{rq}}{dt} = \frac{L_r}{L_{ms}}\left(V_{sq} - R_s i_{sq} - \sigma L_s \frac{\partial i_{sq}}{\partial t} \right) \tag{3.16}$$

Simultaneously, the Adjustable Model used the stator current inputs which was defined by the following equations (3.17) and (3.18):

$$\frac{d\phi'_{rd}}{dt} = \frac{L_{ms}}{T_r} i_{sd} - \frac{\phi'_{rd}}{T_r} - \omega'_r \phi'_{rq} \tag{3.17}$$

$$\frac{d\phi'_{rq}}{dt} = \frac{L_{ms}}{T_r} i_{sq} - \frac{\phi'_{rq}}{T_r} + \omega'_r \phi'_{rd} \tag{3.18}$$

The results of the Adjustable Model and Reference Model, which are the rotor flux components, were combined to produce an error signal as defined by Equation (3.19):

$$\varepsilon_w = \phi_{rq}\phi'_{rd} - \phi_{rd}\phi'_{rq} \tag{3.19}$$

This error ε_w represented the cross-product difference between the rotor flux vectors estimated by the two models and serves as the input to the adaptation mechanism.

As depicted in figure 3.8, the error ε_w is fed into the adaptation mechanism, which comprises a Fuzzy Logic Controller (FLC) integrated with a PID controller. The combined FLC-PID controller processes this error to adjust the estimated rotor speed, thereby minimizing the discrepancy between the Reference and Adjustable Models and ensuring accurate sensorless speed estimation.

3.3.2 Simulation of MRAS Model

The stator voltage and stator current of the single-phase induction motor (SPIM) were used as inputs to the MRAS. Utilizing equations (3.15) and (3.16), As seen in figure 3.10, the Reference Model was created to estimate the rotational flux. The simulation involved running this model to observe the behavior of the estimation of rotor flux and to evaluate the precision of the speed estimation process under varying operating conditions.

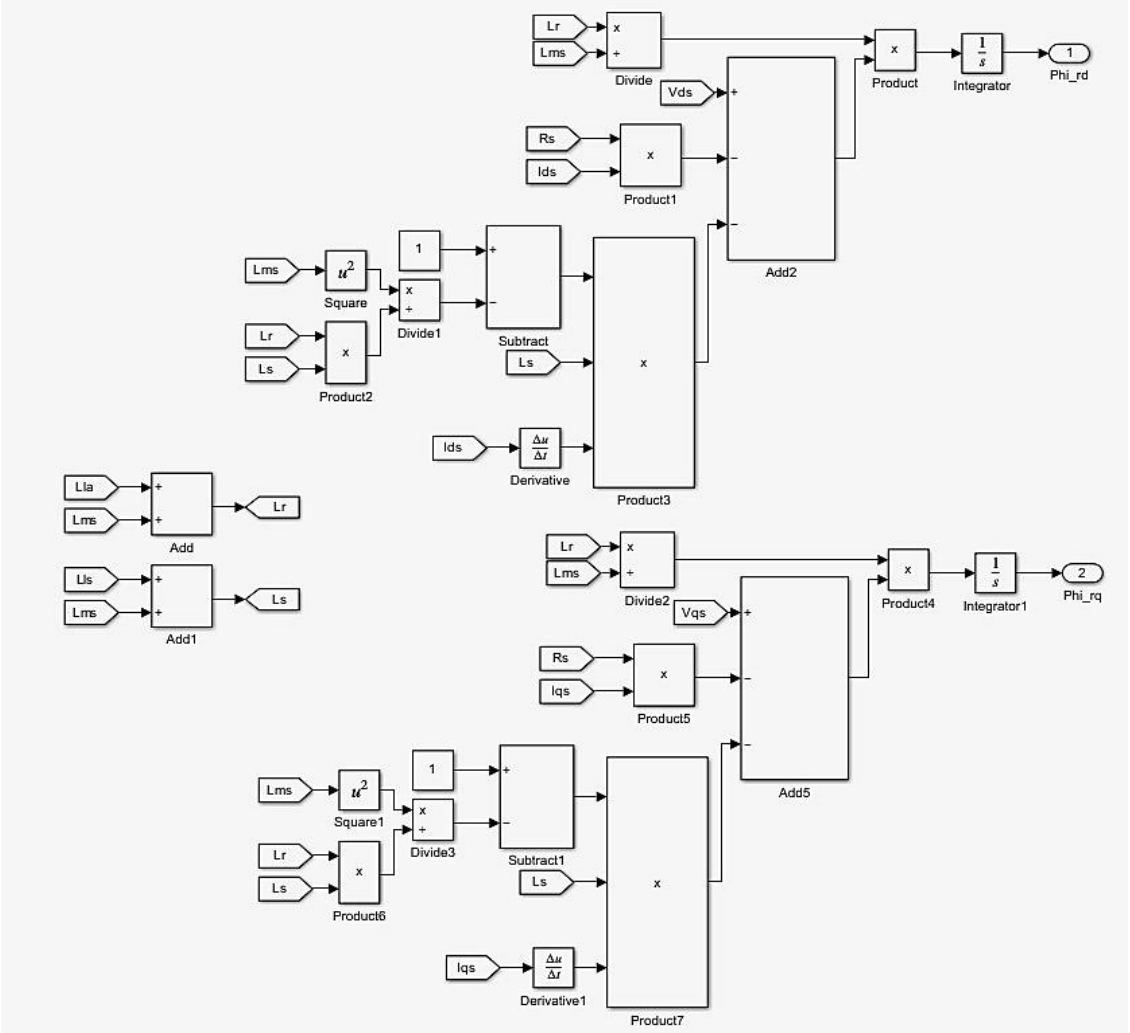


Figure 3.10: Reference model calculation simulation as per equation 3.15 and equation 3.16

Equations (3.17) and (3.18) were implemented to simulate the Adjustable Model within the MRAS framework. The results of this simulation were illustrated in figure 3.11, demonstrating the model's response and its role in estimating the rotor flux with the adjustable rotor speed parameter.

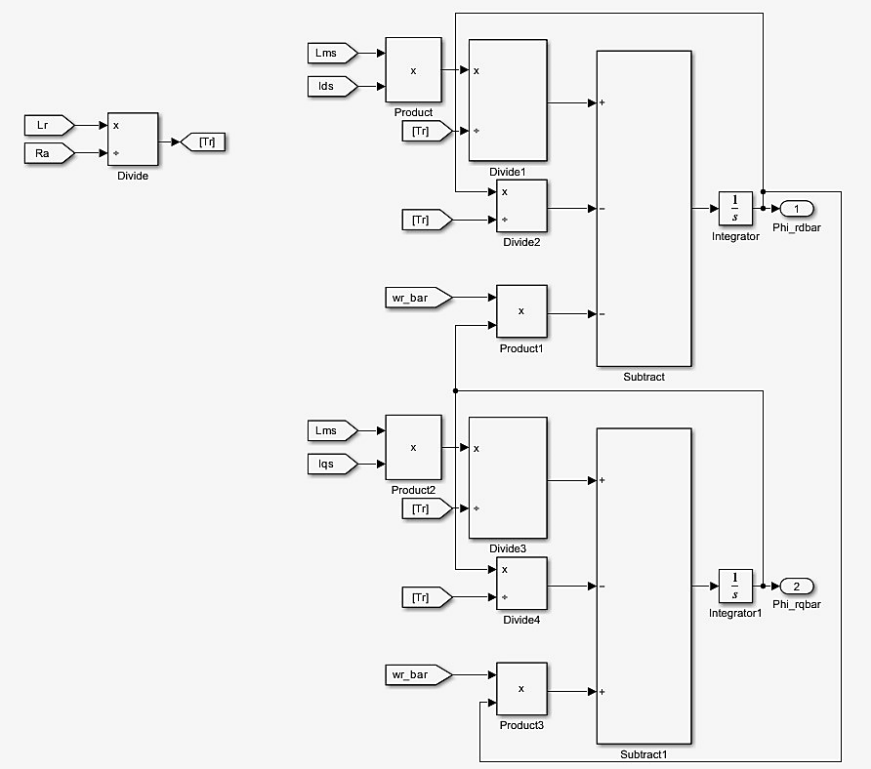


Figure 3.11: Adaptive System calculation as per equation 3.17 and equation 3.18

The Reference and Adjustable Models were then combined using equation (3.19) to generate the error signal ε_w. This error, illustrated in figure 3.12, serves as a critical component of the Fuzzy Logic Controller (FLC) model, enabling adaptive adjustment of the rotor speed estimate to minimize discrepancies between the two models.

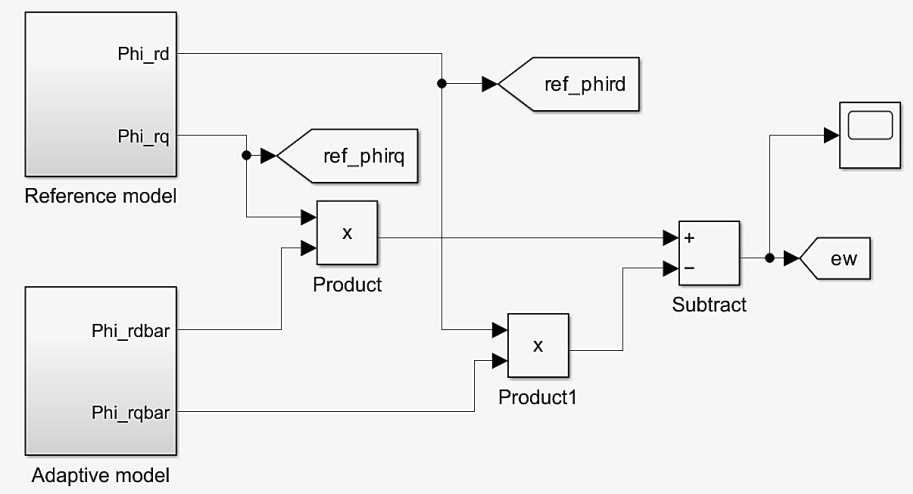


Figure 3.12: Model Reference Adaptive System Block diagram simulation and calculation of equation 3.19.

This error signal formed the basis for developing the Fuzzy-PID controller, which combined the adaptive capabilities of fuzzy logic coupled with the precision of PID regulation to improve the precision and robustness of the rotor speed estimation in the MRAS framework.

3.4 Designing Fuzzy-PID Regulator

The Fuzzy-PID regulator integrated the strengths of both the conventional PID controller and fuzzy logic control, providing adaptability throughout a broad spectrum of dynamic circumstances and input variations. This hybrid controller was particularly effective for systems characterized by nonlinearities or uncertainties, such as single-phase induction motors (SPIMs).

The primary objective of the Fuzzy-PID controller was to optimize system performance for both dynamic and steady-state and by reducing overshoot, improving rise and settling times, and minimizing inaccuracy in the steady state. The fuzzy logic component tasked by adjusting the PID parameters (K_p, K_i, and K_d) in real period depending on the fault and its evolution, thus enabling adaptive tuning to maintain desired response characteristics.

In this design, the conventional PID controller generated the base control signal through its proportional, integral, and derivative actions. The fuzzy logic controller then fine-tuned these parameters to respond to variations in system behavior. Each

component was individually implemented and simulated in MATLAB/Simulink before being integrated into a unified Fuzzy-PID regulator, as illustrated in figure 3.13. This regulator was subsequently integrated with the MRAS speed estimation model, providing a robust and adaptive speed control mechanism for the sensorless SPIM drive.

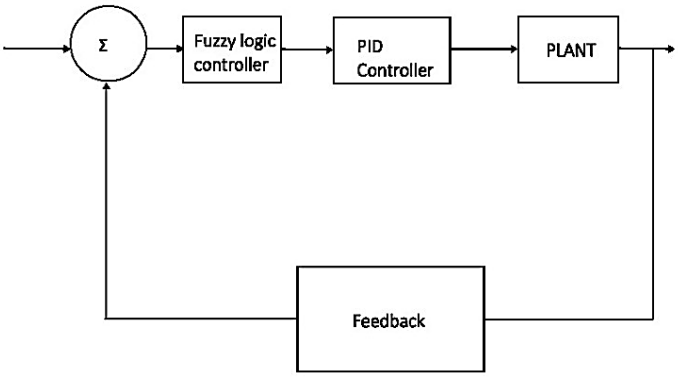


Figure 3.13: Regulator for fuzzy PID Block diagram

3.4.1 Fuzzy Logic Controller

Two input variables and one output variable constituted the design of the fuzzy logic controller

(FLC) in this system. The input was the error (e) represented by the distinction between the reference and estimated speed, and the rate of change of error ($d\varepsilon_w$) which represented the time derivative for the error signal. These two variables capture both the current deviation and its trend, enabling the controller to react effectively to dynamic changes in the system. The fuzzy logic controller's output serves as a control signal for adjusting the PID parameters, which ultimately regulate the rotor speed of the SPIM.

Figure 3.14 illustrated how the fuzzy logic controller utilized linguistic variables for each input and the output. These variables were defined using fuzzy sets such as Negative (N), Zero (Z), and Positive (P). The fuzzification process converted crisp input values into these linguistic categories. The rule base then mapped the input conditions to the output using IF–THEN rules, and defuzzification, which turned the fuzzy output into clear values.

This integration allowed the system to dynamically adapt to varying conditions, providing enhanced control precision and responsiveness compared to fixed-gain PID controllers.

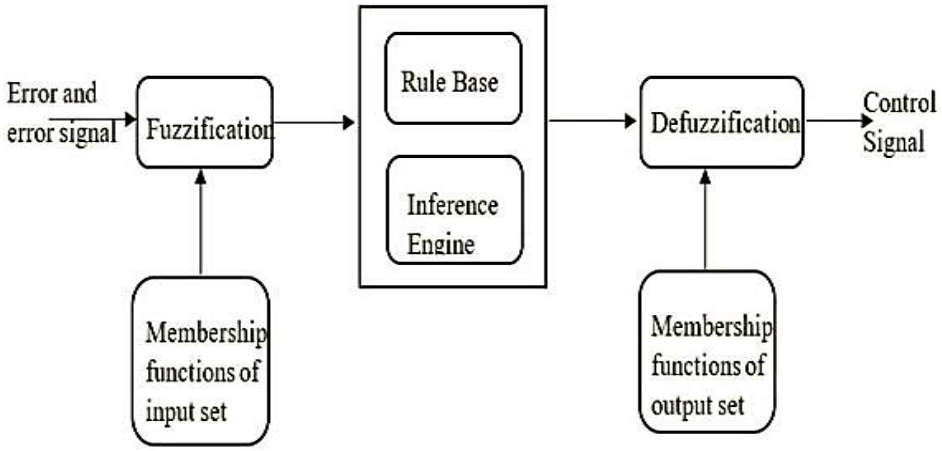


Figure 3.14: Fuzzy logic Controller block diagram

The linguistic variables as well as corresponding fuzzy rules were defined and implemented in the controller, as summarized in Table 3.2. The usefulness of the fuzzy logic control largely depends on selection of membership function shapes, types, and the structure of the rule base. In this work, triangular and trapezoidal membership functions were utilized to symbolize the terminologies used in language: Negative (N), Zero (Z), and Positive (P) for both inputs and output.

The Fuzzy Logic Controller was developed in MATLAB/Simulink using the Mamdani fuzzy inference system, which is well-suited for control applications involving expert knowledge and heuristic rule formulation. Each rule within the rule base defines a specific control action depending on how input error and error change are combined, allowing the controller to adaptively tune the PID gains in real time.

Table 3.3: Fuzzy logic controller rule base 1

Error/change in error	Negative	Zero	Positive
Negative	Negative	Negative	Zero
Zero	Negative	Zero	Positive
Positive	Zero	Positive	Positive Big

The linguistic variables and corresponding fuzzy rules were also defined and applied to the controller, as listed in Table 3.3. These guidelines comprise the core of the decision-making process within the fuzzy inference system, mapping input conditions: error and change in error, to appropriate output actions for dynamic PID gain adjustment.

Table 3.4: Fuzzy logic controller rule base 2

Error/change in error	Negative	Positive	Zero
Negative	Increase	Increase	No change
Positive	Increase	Decrease	No change
Zero	Increase	Decrease	No change

3.4.2 Simulation of Fuzzy Logic Controller

In the Fuzzy Logic Controller (FLC) simulation, the input variables are error (e) and error change ($d\varepsilon_{\omega}$) as well as the output control signal, were analyzed within a fuzzy logic framework. The linguistic states considered for each variable were categorized as Negative, Zero, and Positive, representing the fundamental fuzzy subsets of the control plane.

The universe of discourse for each variable was defined and partitioned into corresponding fuzzy subsets. For the input error, the range was set between –1 and 1, with each fuzzy subset mapped to a linguistic label. This partitioning was essential for the fuzzification process, allowing crisp input values to be translated into degrees of membership across the defined linguistic states.

The membership functions assigned to these fuzzy subsets were illustrated shown in figure 3.15, which illustrated the fuzzy partitioning for the input error variable. Similar membership functions were constructed for the change in error and output control signal. These membership functions play a critical role in defining the rule base's behavior and the overall responsiveness of the fuzzy controller.

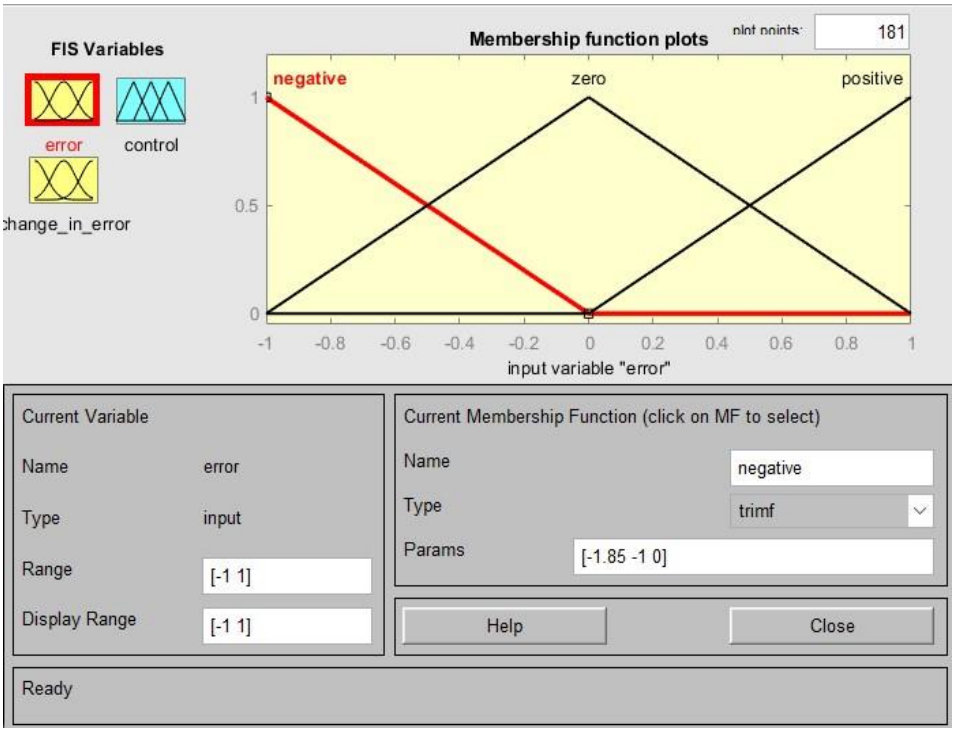


Figure 3.15: Fuzzy Logic Controller error setting diagram

For the input variable representing the change in error ($d\varepsilon_{\omega}$), the universe of discourse was defined over the range –100 to 100, as illustrated in figure 3.16. This wider range reflected the rapid dynamic variations that may occur in the system, particularly under transient conditions.

Similar to the error input, this range was divided up into three fuzzy subsets; Negative, Zero, and Positive, each associated with its own membership function. These functions demonstrated that the controller interpreted the trend of the error and respond accordingly. The profile and overlap of these membership functions directly influence the control smoothness and adaptability of the system.

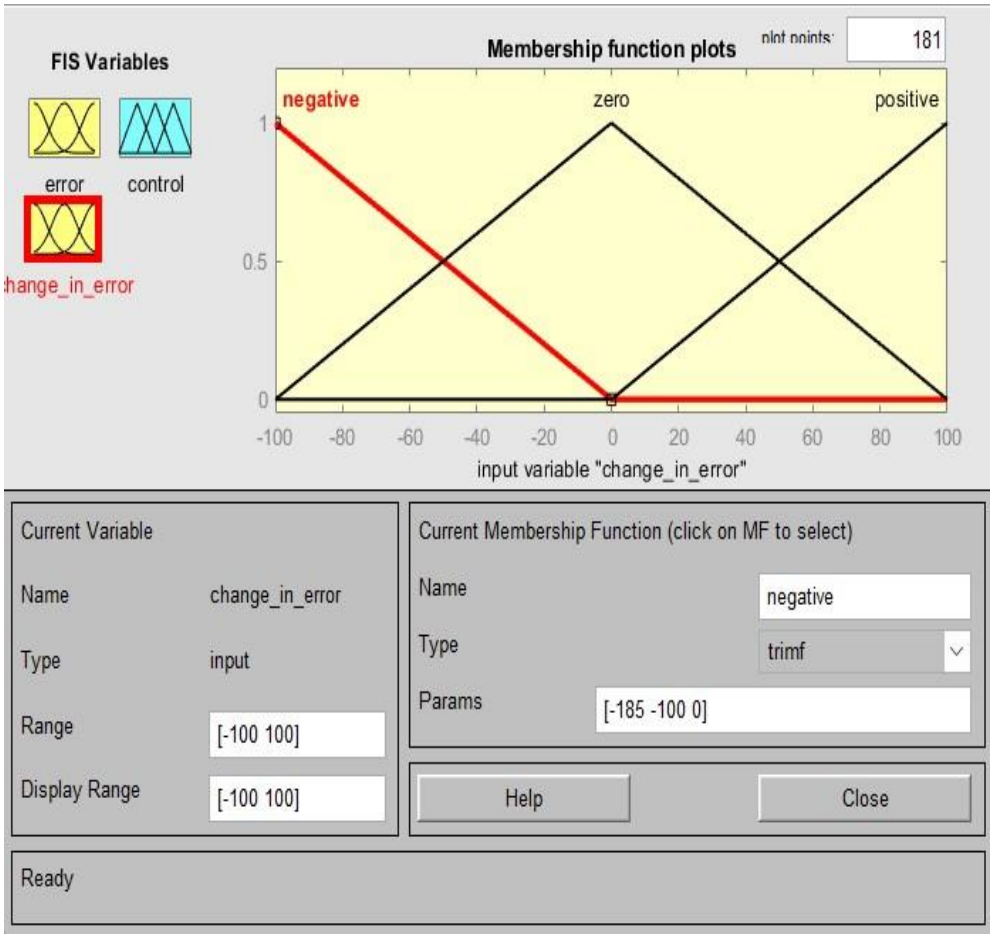


Figure 3.16: Fuzzy Logic Controller change in error setting diagram

For the output control signal, the universe of discourse was also defined over the range –100 to 100, as depicted in figure 3.17. This range was selected to accommodate the full span of corrective actions that the controller might issue in response to varying system conditions.

The output was similarly divided into three fuzzy subsets; Negative, Zero, and Positive, each represented by its own membership function. These output membership functions govern how the fuzzy inference system generates the control action based on the rule base. The design ensures smooth transitions and avoids abrupt changes in control output, thereby enhancing the closed-loop system's performance and stability.

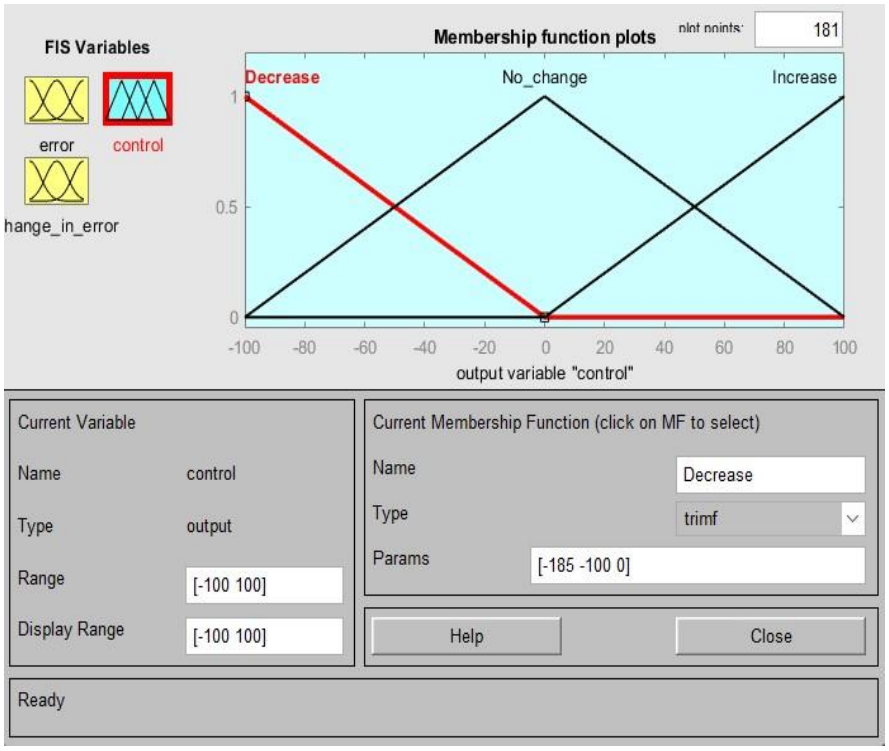


Figure 3.17: Fuzzy Logic Controller control output signal setting diagram

The defined fuzzy subsets collectively cover the entire universe of discourse for each variable, ensuring complete representation of all possible system states. Membership functions were formulated for each subset, enabling the transformation of crisp input values into degrees of membership. Subsequently, fuzzy relationships were established between the input subsets (error and error change) and the subgroups of output (control signal), thereby constructing the rule base.

This rule base encapsulates the fuzzy logic controller's control approach, dictating control output corresponding to each possible input condition. The complete rule mapping is visually represented in figure 3.18, which illustrates how linguistic combinations of inputs lead to specific fuzzy control actions.

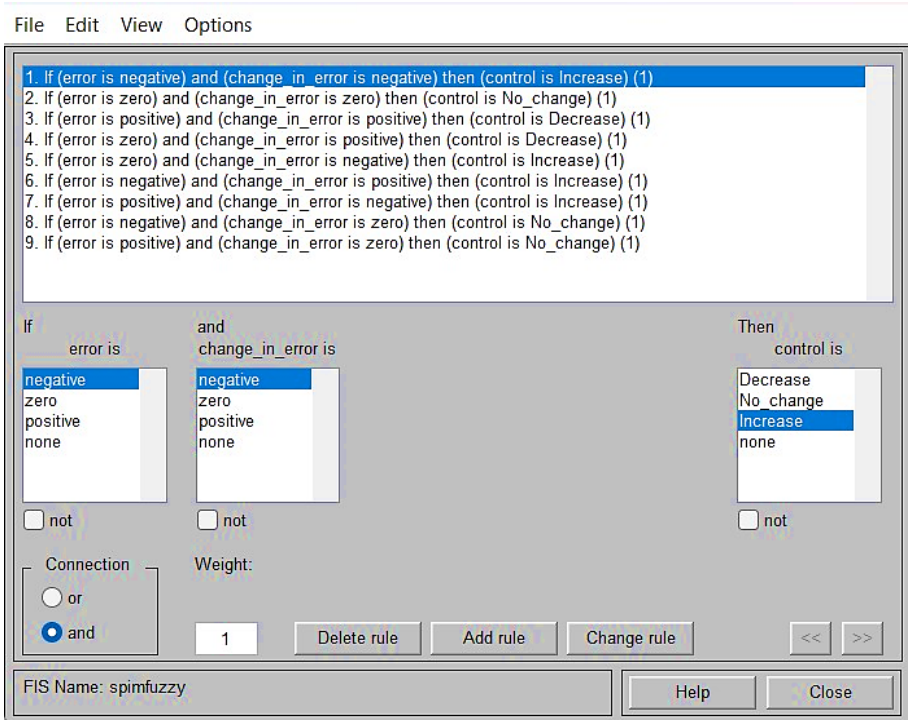


Figure 3.18: Fuzzy Logic Controller Mamdani rules setting diagram

Following the establishment of the rule base, the fuzzification process was executed to convert crisp input values into corresponding fuzzy values based on the defined membership functions. Each activated rule contributed a fuzzy output through fuzzy approximate reasoning, which interprets the strength and relevance of each rule based on the degree of membership of the input variables.

The individual fuzzy outputs from all active rules were then aggregated to form a composite fuzzy output set. This combined fuzzy result was subsequently subjected to the defuzzification process, typically using the centroid method, to generate a crisp control signal. This crisp output served as the control input to the PID controller, thereby enabling dynamic and adaptive regulation of the motor speed.

3.4.3 Designing of PID Controller Model

The PID controller was designed to provide precise and stable control by dynamically modifying three key parameters: the gain in (K_p), integral gain (K_i), and derivative gain (K_d). The main objective of this controller was to enhance the system's transient and steady-state performance while reducing the error between the reference speed and the estimated motor speed. The PID controller's generated control signal is mathematically expressed by equation 3.20:

$$\omega'_r = K_p \varepsilon_w + K_i \int \varepsilon_w .dt + K_d \frac{d\varepsilon_w}{dt} \tag{3.20}$$

The Proportional Gain (K_p) was primarily used in order to decrease the system's rising time response, enabling motor speed to reach desired value more quickly. The Derivative Gain (K_d) served to decrease overshoot and improve settling time by anticipating the future trend of the error and damping oscillations. Meanwhile, the Integral Gain (K_i) was responsible for eliminating steady-state error, ensuring accurate tracking of the reference speed over time.

These gain values were dynamically adjusted during the controller design process using MATLAB, allowing fine-tuning to achieve optimal system performance across different operating conditions.

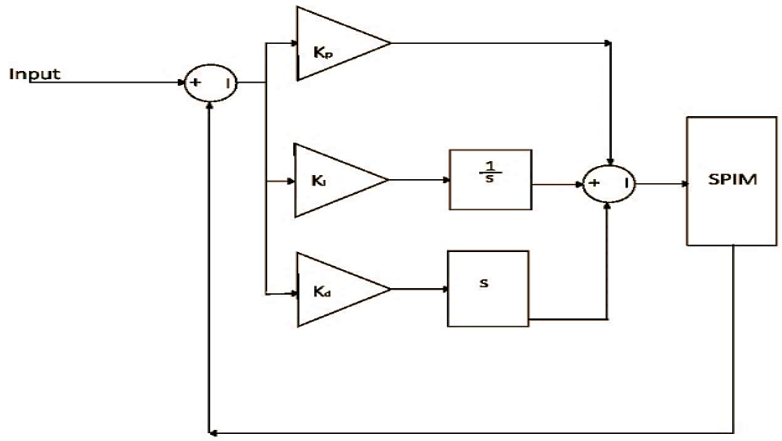


Figure 3.19: PID controller block diagram

According to figure 3.19, the input signal was processed sequentially through the proportional, integral, and derivative gain blocks. Using equation 3.21, these gains were combined to compute the final estimated speed error used for control. The specific values and relationships among the Gains that are proportionate, integral, and derived applied during the controller design are summarized in Table 3.4.

Table 3.5: Relation of increase in K_p, K_i, and K_p gains

Gain	Response Speed	Stability	Accuracy
Increase in kp	Increase	Deteriorates	Improves
Increase in ki	Decrease	Deteriorates	Improves
Increase in kd	Increase	Improves	No impact

The proportional control component produces a control signal by multiplying the error signal by the proportional gain K_p. While this reduces the amount of inaccuracy and shortens system's rise time, it does not completely eliminate the steady-state error.
The integral control action generates a control signal proportional to the error's time integral, scaled by integral gain K_i. The primary objective of integral term is to reduce the steady-state error to zero by accumulating past errors. However, practical limitations in physical systems often prevent perfect elimination of error, affecting overall accuracy.

The derivative control anticipates the error signal's future behavior by responding to its rate of change. The derivative of the error determines the proportion of the control signal, multiplied by gain from derivatives K_d. This predictive action improves system stability, reduces overshoot, and enhances transient response. Nevertheless, derivative control alone cannot maintain control effectively, as its impact is limited to transient periods and it is sensitive to noise in the error signal.

The PID controller significantly improves the control loop by speeding up the response, reducing overshoot, and enhancing system stability. Due to its versatility and effectiveness, it is one of the most commonly employed control strategies in practice. As shown in Table 3.5, the integrated action of the proportional, integral, and derivative terms combines their individual advantages: steady-state error is completely eliminated, while settling time, overshoot time, and rising time are all minimized. This comprehensive approach enables the PID controller to outperform both the proportional-only (P) and proportional-integral (PI) controllers in achieving more precise and stable control.

Table 3.6: Parameter analysis of P, PI, and PID controllers

Parameter	P Controller	PI Controller	PID Controller
Rise time	Decrease	Decrease	Minor Decrease
Overshoot	Increase	Increase	Minor Decrease
Settling time	Small change	Increase	Minor Decrease
Steady-state error	Decrease	Significant change	No change
Stability	Worse	Worse	If Kd Small Better

3.4.4 Simulation of PID Controller

The components corresponding to equation 3.21 were implemented as individual blocks in MATLAB Simulink and interconnected to form the complete PID controller model, as demonstrated in figure 3.20.

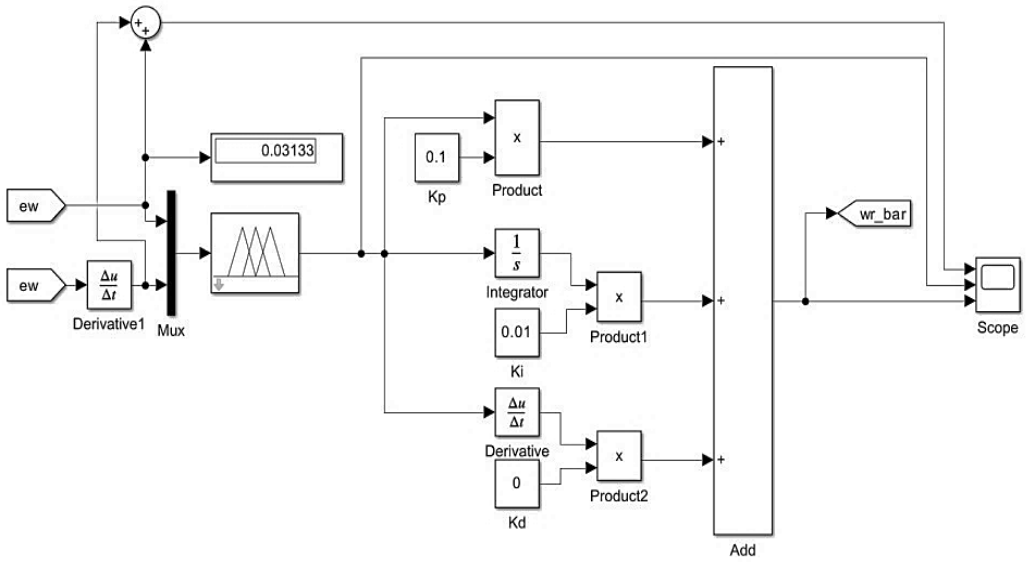


Figure 3.20: Fuzzy Logic controller integrated with a PID controller diagram

The values of gains K_p, K_i, and K_p were then adjusted accordingly to ensure minimize the speed error and optimize the control performance. The resulting control signal, representing the corrected error, was then summed with the SPIM speed feedback to produce the final controlled speed output as shown in figure 3.21.

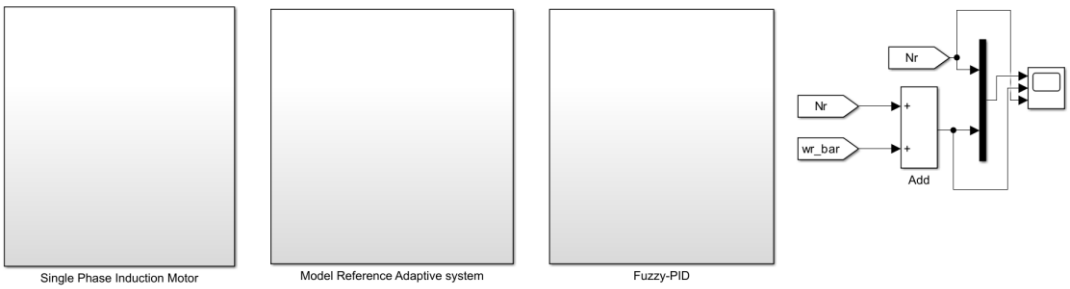


Figure 3.21: Overall SPIM speed control simulation overview

3.5 Comparative Performance Analysis and Evaluation

This section sets out the framework used to compare the proposed sensorless SPIM speed control system against alternative techniques, covering:

(i) integration of the MRAS estimator with the Fuzzy-PID control (Figure 3.20), including the expected benefits of adaptability, intelligent control, and robustness that this integration targets;
(ii) the simulation setup and test scenarios used;
(iii) the performance evaluation criteria and metrics applied; a validation of the simulation results against the reference (MRAS-only) system.

The speed regulation model of the Single-Phase Induction Motor (SPIM), as developed in figure 3.21, was implemented in MATLAB/Simulink. This model integrated both a Fuzzy Logic Controller (FLC) and a PID controller to form a Fuzzy-PID hybrid regulator. The purpose of this integration was to harness the self-adaptive characteristics of fuzzy logic with the precise tuning capabilities of PID control, thereby improving system reactions in both the steady-state and transient states, with the goal of reduced overshoot, minimized steady-state error, and improved robustness under varying load, as quantified in Chapter 4.

The discrepancy between the reference speed and the actual rotor speed is known as the error signal (e), was continuously monitored and minimized through combined action of the fuzzy system and PID terms (K_p, K_i, and K_p). The fuzzy logic controller adjusted the PID gains dynamically in real time, ensuring that the control system responded adaptively to any changes in load or disturbances.

In order to consider the effectiveness regarding the suggested speed control technique, output of the controller was contrasted to the simulated rotor speed of the SPIM. The

goal was to verify that the actual motor speed closely tracked the reference input. This close match would demonstrate the controller's capability to observe the desired speed accurately, thus achieving the core objective of speed regulation in a sensorless vector control system.

In contrast to traditional methods of control such as fixed-gain PID or basic V/f (voltage/frequency) control, the Fuzzy-PID controller exhibited superior performance. It was more responsive to disturbances, showed reduced overshoot and settling time, and maintained low steady-state error. This enhanced performance is critical in applications where precise speed tracking, quick recovery from load changes, and improved robustness are required.

The simulation results validate the controller's robustness and effectiveness under different loading conditions, confirming its advantage over traditional control methods. These findings are further discussed and quantified in Chapter 4, which presents the simulation plots, comparative performance metrics, and time-domain analysis of the controlled SPIM system.

3.6 Summary

This chapter presented the methodology used to design and develop the sensorless MRAS-Fuzzy-PID speed control system for the single-phase induction motor (SPIM). It described the mathematical modelling of the SPIM and its speed-torque characteristics, the design of the MRAS estimator for sensorless speed estimation, and the development of the Fuzzy-PID regulator, before outlining the framework used to compare the proposed system against the MRAS-only reference. Together, these methods established the simulation model in MATLAB/Simulink used to generate the results presented and discussed in Chapter 4.

CHAPTER FOUR
RESULTS AND DISCUSSION

4.1 Introduction

The principal aim of this study was to establish an integrated control system that combines a Model Reference Adaptive System (MRAS) with a Fuzzy-PID controller for robust and accurate speed control of a Single-Phase Induction Motor (SPIM). This integrated approach aimed to eliminate the need for physical speed sensors by estimating rotor speed through MRAS, while enhancing dynamic response and steady-state performance using adaptive fuzzy logic tuned PID control.

The developed model ensured precise tracking of reference speed and resilient performance under varying load and speed conditions. The MRAS estimator provided real-time rotor speed information based on stator voltage and current inputs, which fed into the fuzzy-PID controller for appropriate corrective action. The controller dynamically altered PID parameters according to the instantaneous speed error and its rate of change, thereby maintaining system stability and minimizing overshoot and settling time.

In this chapter, a thorough investigation of the simulation results alongside analysis, highlighted how the integrated MRAS and Fuzzy-PID system to achieve superior speed regulation performance. The outcomes clearly demonstrate the system's ability to accurately follow reference speed commands, even during load disturbances and speed transitions, confirming that the suggested control approach was effective.

4.2 Single Phase Induction Motor (SPIM) Results

After the Single-Phase Induction Motor (SPIM) was successfully modelled mathematically utilizing equations (3.1) to (3.15), the simulation was carried out in MATLAB/Simulink to observe the motor's dynamic behavior under sensorless control. The system was tested under defined initial conditions and excitation parameters. The key results are presented and analyzed in the sub-sections:

4.2.1 Input Voltage Response

The first observed output from the simulation was the input voltage (V_m) waveform applied to the SPIM stator windings. This voltage, denoted as (V_m), represented the

fundamental excitation signal that initiated motor operation and forms the basis for subsequent calculations such as stator flux, d–q transformation, and electromagnetic torque.

Figure 4.1 represents the waveform of the input voltage (V_m), which serves as the primary excitation parameter in the SPIM model:

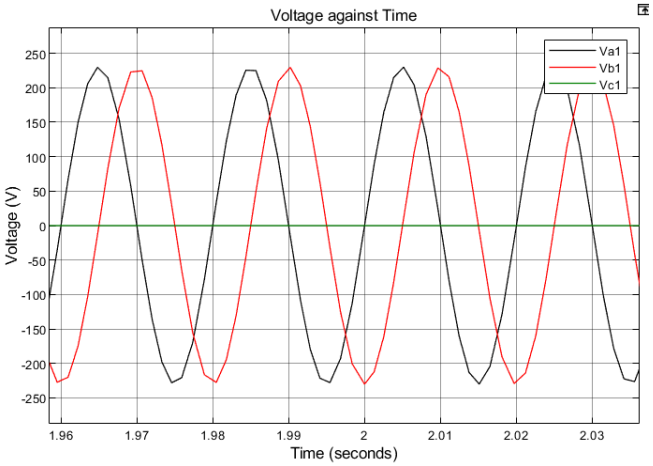


Figure 4.1: Input Voltage (V_m)

From figure 4.1, the simulated input voltage applied to the SPIM is consistent with the motor specifications. The waveform includes two distinct components:

- Va1: Voltage applied to the main winding
- Vb1: applied voltage to the auxiliary winding

The simulation confirmed that the input voltage (V_m) was 230V for both windings, which matched the motor's rated supplied voltage. Notably, the auxiliary winding voltage (V_{b1}) was observed to lag the main winding voltage (V_{a1}) by 90 degrees, as expected in single-phase induction motor design. This 90-degree phase shift was essential for creating rotating magnetic field that initiated torque production, effectively emulating a two-phase operation.

This phase displacement, along with equal magnitude, ensured proper torque generation and balanced magnetic flux within the motor. It also laid the foundation for accurate flux estimation and speed control in the MRAS-based vector control strategy implemented later in the simulation.

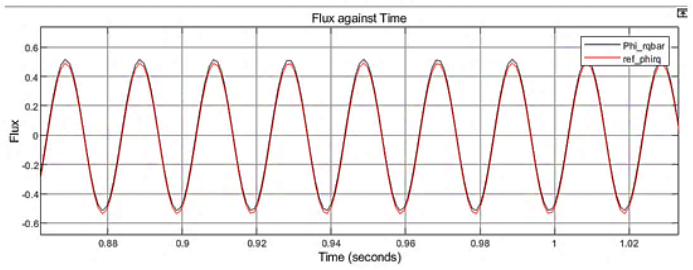
4.2.2 Rotor d–q Flux Estimation Accuracy

In figure 4.2, a comparison is presented between the estimated rotor d–q fluxes ($\varphi_{rqd}{}'$) with reference rotor d–q fluxes (φ_{rqd}) generated from the MRAS observer. The results indicated that the reference rotor fluxes closely track the actual rotor fluxes, showing a high degree of correlation in both magnitude and phase alignment. This demonstrated that the MRAS-based reference model is accurately estimating the components of the rotor flux in the rotating d–q reference frame.

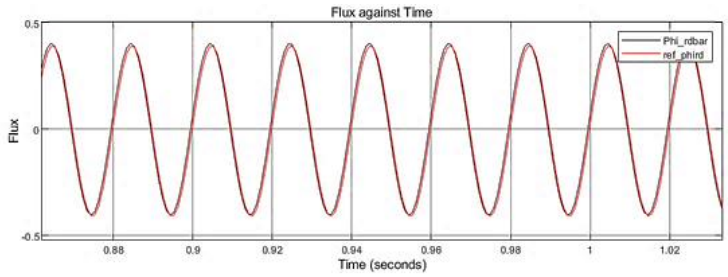
Such close agreement between the reference and estimated fluxes was crucial, as it confirmed:

- The validity of the mathematical model used in MRAS equations (3.16–3.20)
- The precision of the rotor speed estimation, which was derived from flux dynamics
- The reliability of MRAS in capturing the internal motor states without requiring physical sensors.

Validation of the flux estimation accuracy strengthened the foundation for precise speed control in the sensorless vector-controlled SPIM system.



a)



b)

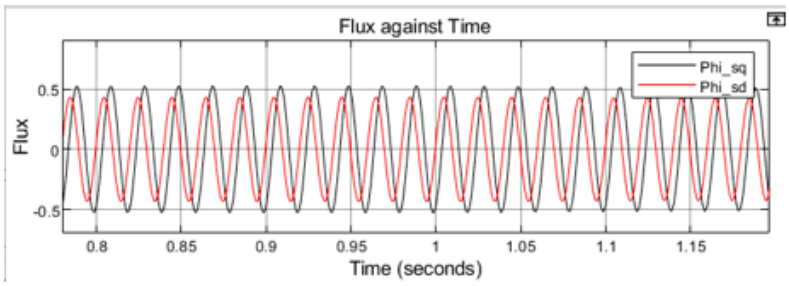
Figure 4.2: Reference rotor d-q fluxes (φ_{rqd}) (a) and Rotor d-q fluxes ($\varphi_{rqd}{}'$) (b) comparison graphs

4.2.3 Stator and Rotor d–q Axis Flux Responses

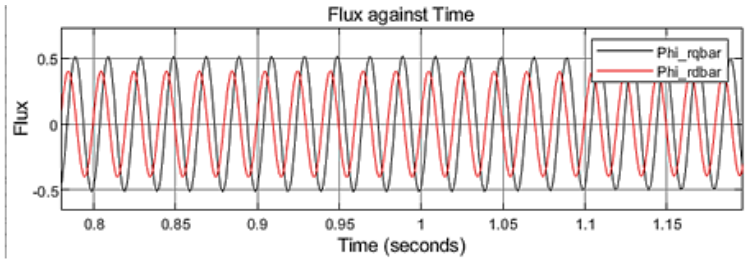
In figure 4.3, the graphs illustrated the dynamic responses of the flux components of the stator and rotor along the d and q axes. These flux components were represented in the d–q reference frame that rotates synchronously, as obtained from developed mathematical model of SPIM. The stator d–q fluxes demonstrated a steady and expected sinusoidal variation that aligns with the applied stator voltages and the motor's excitation pattern. The rotor d–q fluxes closely followed the stator flux trends but with smoother transitions due to the rotor's inertia and lack of direct electrical excitation.

The accurate evolution of these fluxes suggests that:

- The electromagnetic connection between the rotor and stator was correctly modeled.
- The simulation accurately captured the magnetic dynamics of the SPIM under vector control.
- The d–q transformation and inverse transformations using equations (3.14) and (3.15) were properly implemented.



a)



b)

Figure 4.3: Stator d-q fluxes (Phisqd) (a) and Rotor d-q fluxes (Phirqdbar) (b) graphs

The results validate that the developed simulation model accurately reproduces the expected electromagnetic behavior of the SPIM, thereby confirming the correctness of the implemented control and estimation mechanisms. The observed flux patterns support the reliability of the sensorless control strategy in real-time motor operation.

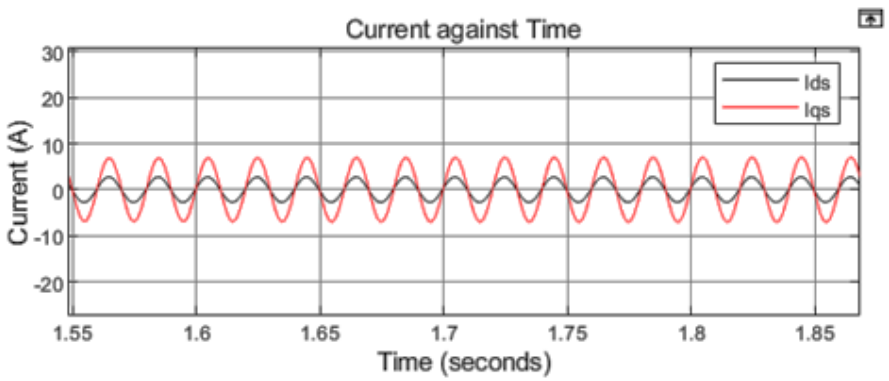
4.2.4 Stator and Rotor d–q Axis Current Responses

The waveforms in figure 4.4 represent the components of the stator and rotor current along the d- and q-axes in the reference frame that rotates synchronously.

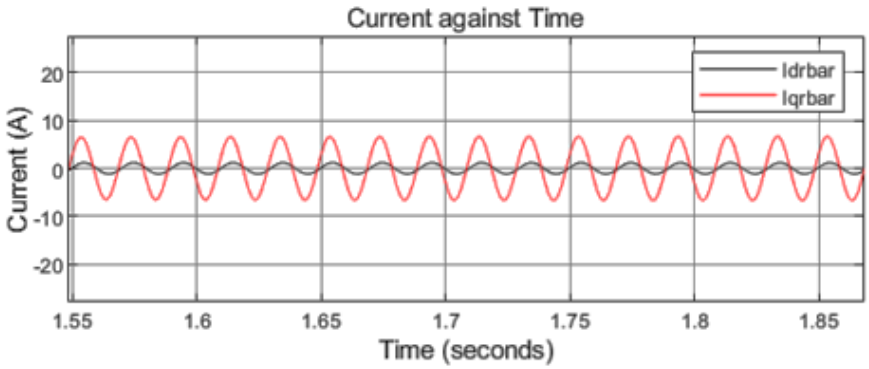
The observations were as follows:

- The stator currents show expected dynamic behavior influenced by the voltage that is applied and the flux variations in the machine. These currents contribute directly to the generation of the field of magnetic attraction and torque.
- Currents in the rotor exhibit a smooth and delayed response compared to the stator currents, which was consistent with the induction principle where rotor currents are induced because of the relative movement of the rotor conductors and stator field.

These current waveforms were important because the proper shape and synchronization between (Isqd) and (Iqdrbar), and their rotor counterparts confirmed that the electromagnetic torque generation process was occurring as theoretically expected. The observed current responses closely matched the predicted behavior of SPIMs under vector control strategies, indicating that the motor's electrical model from equations (3.5 to 3.8) were correctly implemented. The accurate simulation of stator and rotor currents confirms the validity of the d–q transformation, MRAS estimation, and control algorithms used in the model.



a)



b)

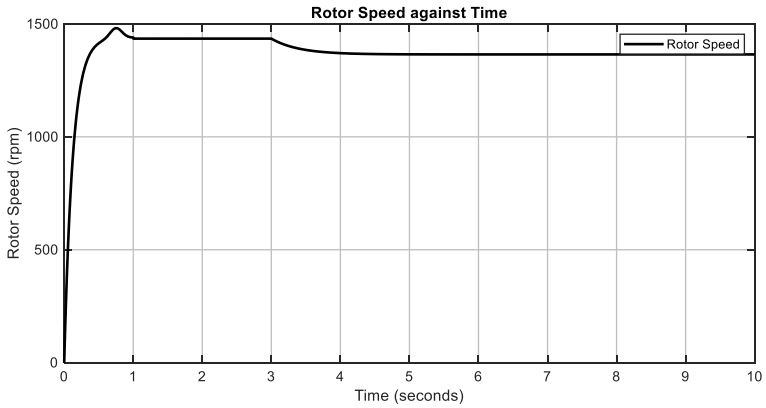
Figure 4.4: Stator d-q currents (Isqd) (a) and rotor d-q currents (Iqdrbar) (b) graphs

The consistency between the simulated and expected current behavior demonstrated that the SPIM model and its control system were accurately simulating the dynamic characteristics of the motor, thereby validating the effectiveness of the sensorless control method employed.

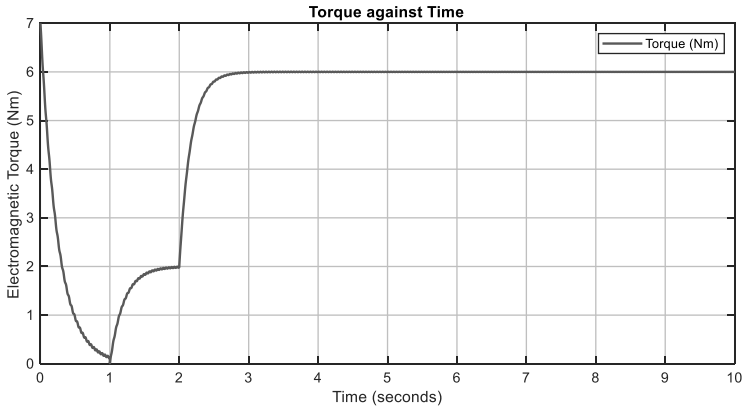
4.2.5 Electromagnetic Torque and Rotor Speed Response under Load Variations

The simulation results in figure 4.5 outlined speed of the rotor and electromagnetic torque (T_e) response of single-phase induction motor (SPIM) under varying load conditions:

- 0 to 1 second: The motor operated under no load, and as expected, the rotor speed quickly rose to its nominal value, stabilizing at approximately 1440 rpm, because of slip, which is somewhat slower than the synchronous speed. The electromagnetic torque was nearly zero, indicating minimal mechanical resistance.
- 1 to 3 seconds: A 1 Nm mechanical load torque was applied. The rotor speed showed a slight dip in response to the increased load but quickly recovered due to the control action. Simultaneously, the electromagnetic torque increased to match the load, rising proportionally to maintain steady operation.
- 3 to 10 seconds: A full load torque of 6 Nm was applied. As expected, the rotor speed experienced a more significant decrease, settling at a lower but stable speed (1350–1380 rpm), while the electromagnetic torque increased significantly, stabilizing around 6 Nm to match the applied load.



a)



b)

Figure 4.5: Speed (a) and Torque (b) graphs

Based on varying load conditions observations, it confirmed the following:

- The MRAS and Fuzzy-PID controller accurately responded to load disturbances, maintaining system stability.
- The controller increased torque proportionally to load changes while minimizing speed deviation, thereby demonstrating excellent dynamic tracking and robustness under load variations.
- The torque-speed behavior conforms to theoretical expectations of SPIMs under vector control, validating the efficacy of the designed control model.

The combined relationship between speed, time, and torque is presented in Figure 4.6.

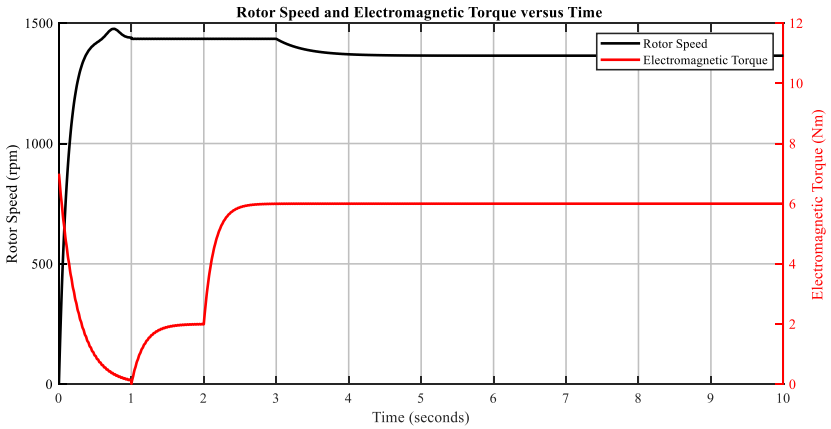
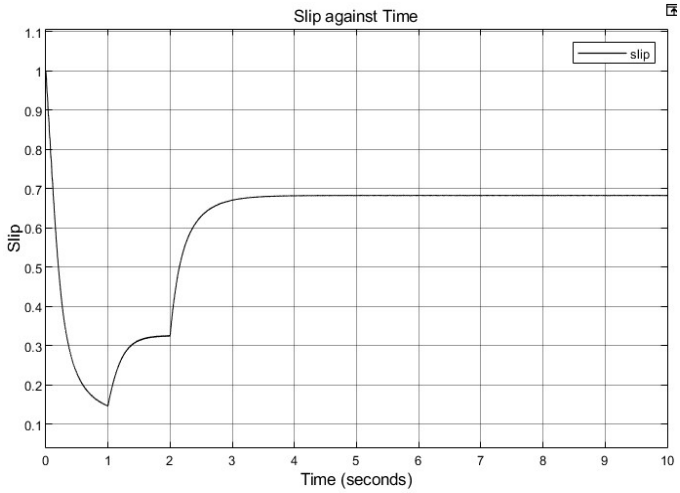


Figure 4.6: Speed, time and torque graphs

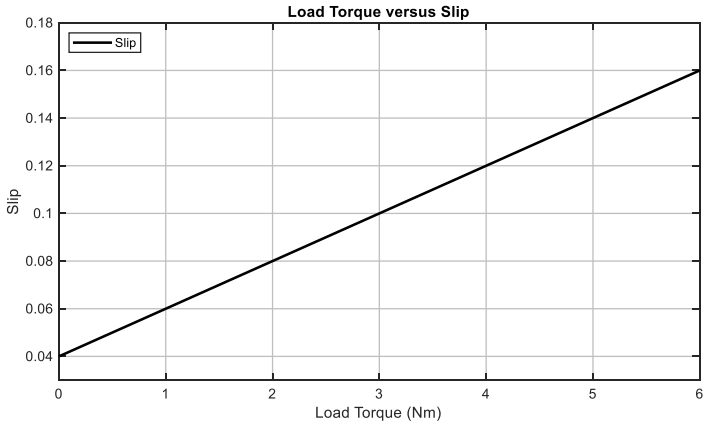
This performance underscores the success of the proposed sensorless vector control method in achieving resilient and accurate speed control of SPIMs even under varying mechanical loading.

4.2.6 Slip Response under Varying Load Conditions

The progression of slip closely follows theoretical expectations for single-phase induction motors, confirming that the proposed control model effectively monitors and compensates slip variations to maintain stable motor performance under changing loads.



a)



b)

Figure 4.7: Slip graphs (a) and (b)

From figure 4.7 it illustrated the slip behavior of the induction motor in single phase under various loading circumstances:

- 0 to 1 second (No Load): The slip value decreased, approaching near zero, which is typical for no-load operation where the rotor speed is almost equal to the synchronous speed. This indicated minimal rotor slip, reflecting efficient motor operation without mechanical load.
- 1 to 3 seconds (Load = 1 Nm): Upon the application of a small mechanical load, the slip slightly increased to approximately 33%.
- 3 to 10 seconds (Full Load = 6 Nm): Under full load, the slip further increased, stabilizing at around 68%, which matches the theoretical slip expected for the motor at rated load. This confirms the motor's correct load-dependent slip characteristic and validates the accuracy of the simulation and control strategy.

4.2.7 Electromagnetic Torque and Speed Relationship

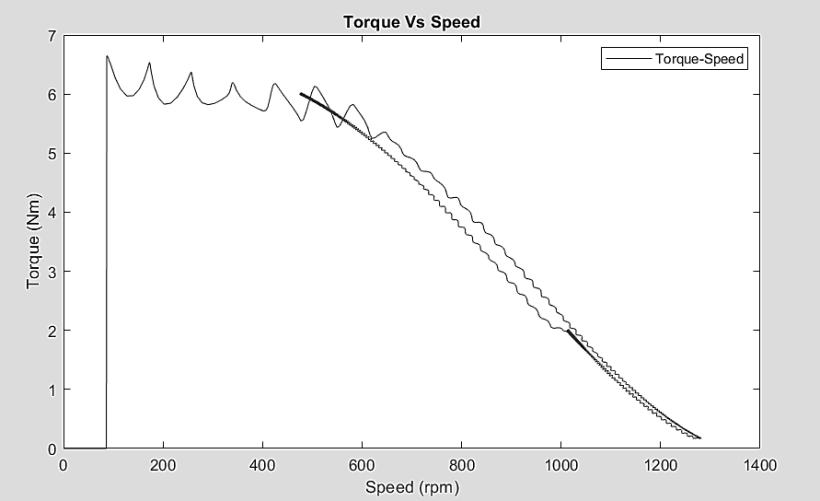


Figure 4.8: Electromagnetic Torque vs Speed graph

From the figure 4.7, it shows the dynamic relationship between the single-phase induction motor's rotor speed and electromagnetic torque, Initially, as motor accelerates from standstill under no load, the electromagnetic torque increases reaching maximum torque of approximately 6 to 6.5 Nm. This peak torque represented the highest torque the motor can deliver without stalling.

Following this peak, the torque exhibits noticeable oscillations, particularly in the mid-speed range between approximately 300 rpm and 900 rpm. These instabilities in torque ripples reflected the system's transient response, which was attributed to control system adaptation dynamics, estimation inaccuracies in the sensorless MRAS model, and limitations in the fuzzy-PID tuning. Such fluctuations indicated that while the controller attempted to compensate for changes in load and speed, the system temporarily deviated from steady-state behavior before eventually stabilizing.

As mechanical load was applied, the torque increased to meet the demand, and the rotor speed correspondingly decreased demonstrating the typical inverse correlation between torque and speed of induction motors. The observed torque-speed characteristic not only confirms the validity of the motor model, but also reveals the sensitivity and adaptability of the control strategy under dynamic conditions.

Despite the observed torque ripples, the overall system successfully tracks the changing load demands and regulates motor speed. This highlights both the

effectiveness and the areas for potential improvement in the proposed sensorless Fuzzy-PID and MRAS-based control strategy.

4.2.8 Electromagnetic Torque Variation with Slip

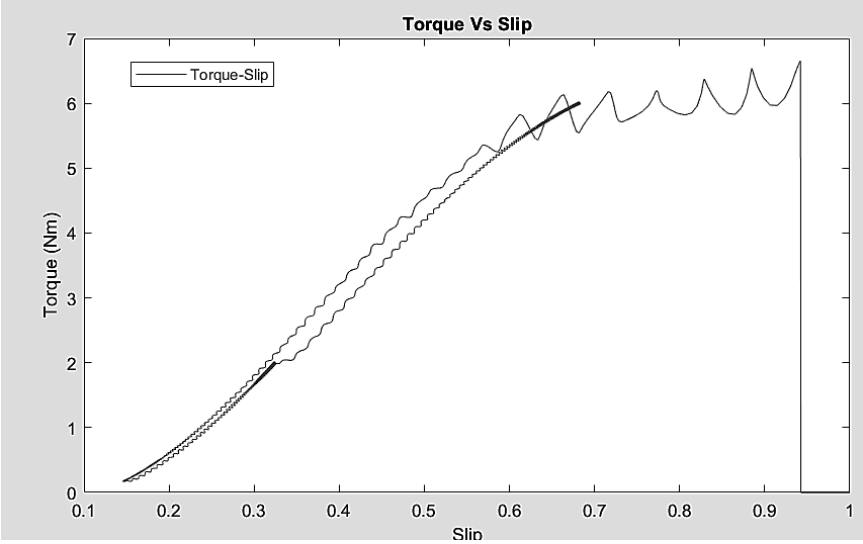


Figure 4.9: Electromagnetic Torque vs Slip graph

Figure 4.9 presents the relationship between electromagnetic torque and slip for an induction motor operating in single phase. As slip decreases from a high initial value (i.e. The motor accelerates toward synchronous speed), the electromagnetic torque steadily increases, peaking at approximately 6 to 6.5 Nm. This point represents the highest torque that the motor is capable of producing before entering a potential stall condition, commonly referred to as breakdown torque.

When the torque rises with increasing slip under load, and the pattern observed confirms the effectiveness of the model in simulating motor performance accurately across different slip conditions.

Following the peak, the torque began to decline, especially as the motor approached no-load conditions, where slip was low and torque demand was minimal. Under such circumstances, the rotor speed closely matched the synchronous speed, and electromagnetic torque naturally dropped.

As external mechanical load was applied, the rotor began to lag further behind the synchronous speed, resulting in increased slip. In response, the motor generated higher torque to meet the increased load demand. This reflected direct relationship between

torque and slip in the motoring region: as slip increases, torque also increases, up to the breakdown point.

Notably, the curve showed significant oscillations or ripples, particularly between slip values of 0.5 to 0.9. These torque instabilities were indicative of the system's transient response possibly caused by:

- Adaptive behavior of the MRAS-based estimator,
- Dynamic adjustments from the Fuzzy-PID controller, and
- Sensitivity to rapid changes in load or internal model feedback.

These oscillations reflected the nonlinear, transient dynamics of the control system during load transitions. Despite the fluctuations, the controller maintained overall torque-tracking capability, confirming the system's responsiveness and adaptability, though the results also indicated areas for improvement in damping and control smoothness.

4.2.9 Analysis of the SPIM

The simulation results presented in Figures 4.5-4.8 confirmed that the single-phase induction motor (SPIM) operated in accordance with the expected performance characteristics of a typical SPIM: the speed and torque responses (Figure 4.5 and 4.6) tracked the applied load and recovered once the disturbance was removed, the slip (Figure 4.7) varied with load in the expected manner, and the torque-speed and torque-slip curves (Figures 4.8 and 4.9) exhibited the characteristic shape expected of a single-phase induction motor. This agreement between the simulated behavior and known SPIM characteristics affirmed the accuracy and reliability of the mathematical model developed using the equations outlined earlier. The motor was modeled as a split-phase type, featuring a main winding and an auxiliary winding that lags by 90 degrees to generate the necessary starting torque.

Despite the overall success, some irregularities were observed in the slip-torque and speed torque characteristics. Specifically, the curves exhibited pulsations and minor fluctuations rather than smooth transitions. This behavior was consistent with real-world SPIM performance, where pulsating torque arises from the inherent nature of

single-phase motors, particularly from alternating magnetic fields and unbalanced winding designs.

Such pulsations caused torque ripple and mechanical vibrations, which may reduce motor efficiency and shorten its lifespan. Their appearance in the slip response (Figure 4.7) and in the torque-speed and torque-slip characteristics (Figures 4.8 and 4.9) confirmed the model's realism and marked the achievement of Objective one, the design and validation of a sensorless speed-controller mathematical model of a single-phase induction motor.

4.3 Model Reference Adaptive System (MRAS) Results

Following validation of the SPIM model, attention was turned to improving speed estimation accuracy by implementing the Model Reference Adaptive System (MRAS). The output errors from the Model Reference Adaptive System (MRAS) used for speed estimation of a single-phase induction motor (SPIM) were modeled in MATLAB. The error signal is the difference between the MRAS-estimated rotor speed and the rotor's actual speed, providing insight into the estimator's accuracy under varying load conditions.

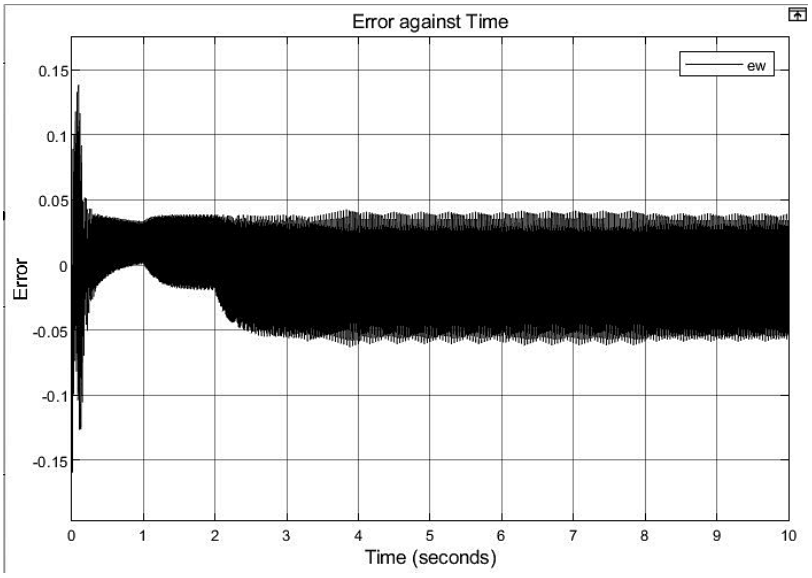


Figure 4.10: Model Reference Adaptive System graph

From Figure 4.10, it was evident that the MRAS error was initially high during motor startup. This is a common phenomenon, as rapid transient conditions at startup make it difficult to accurately estimate rotor speed. As the motor transitioned to a no-load

condition, the error decreased significantly, indicating that the MRAS estimator performed well under minimal load. the MRAS estimation error varied with the motor's operating speed. The error was initially high during motor startup, when the SPIM accelerated rapidly from standstill, since the rapid transient conditions at low speed made it difficult to accurately estimate rotor speed. As the motor's speed settled toward its no-load steady-state value, the error decreased significantly, indicating that the MRAS estimator performed well once the motor reached a stable operating speed. This confirmed that the estimation error was speed-dependent, being largest during the low-speed transient phase and smallest once the motor approached steady-state speed.

The MRAS estimation error also varied with load. When the load was increased from 1 Nm to full load (6 Nm) as shown in Figure 4.11, the error signal increased correspondingly, showing that the MRAS's ability to track rotor speed diminished as load torque increased (Figure 4.12). This rise in estimation error with load was attributed to the higher dynamic disturbances and nonlinearities introduced by loading, which complicated the adaptive estimation process.

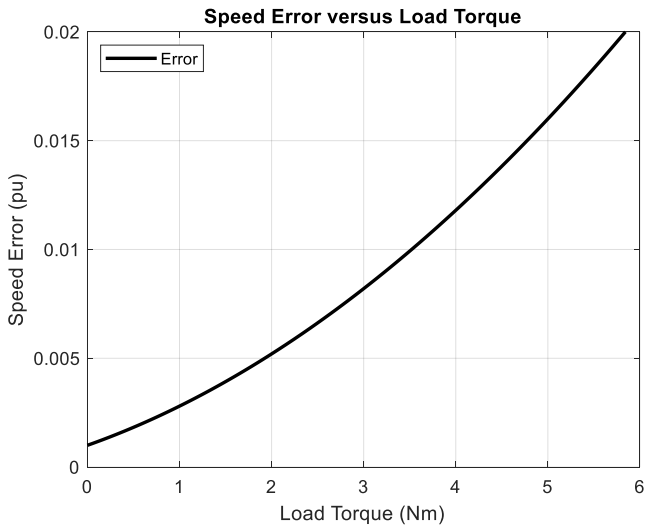


Figure 4.11: Error vs Load Torque graph

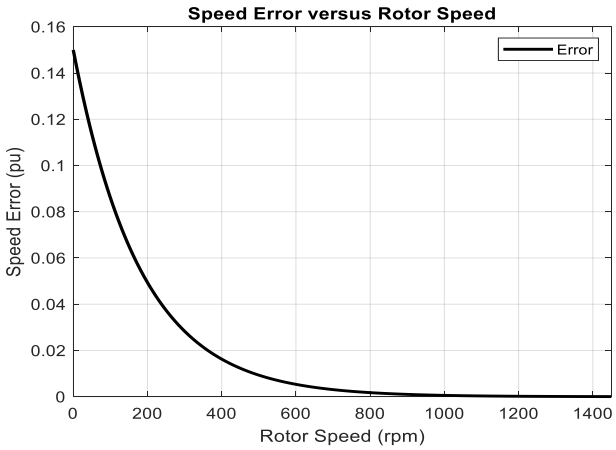


Figure 4.12: Error vs Rotor Speed graph

Despite these increases in error, the MRAS maintained acceptable performance in all operating conditions. This demonstrated its capability as a sensorless speed estimation technique for SPIMs. Further tuning of the adaptation mechanism and controller parameters may help to reduce estimation error. This may be especially useful during transient and heavily loaded scenarios.

4.4 Fuzzy Logic Controller and Proportional Integral Derivative (PID) Results

4.4.1 Fuzzy Logic Controller Simulation

The Fuzzy Logic Controller (FLC) was designed with two key inputs: the speed error, which ranged from -1 to 1, and the change in speed error, spanning from -100 to 100. The output of the FLC was the control signal intended to adjust the motor's input for improved speed regulation. Using the Mamdani fuzzy inference method, a set of fuzzy rules was established to govern the controller's response based on these inputs. The simulation results, shown in Figure 4.13, depict the graphical user interface of the FLC, highlighting the active fuzzy rules and membership functions during operation.

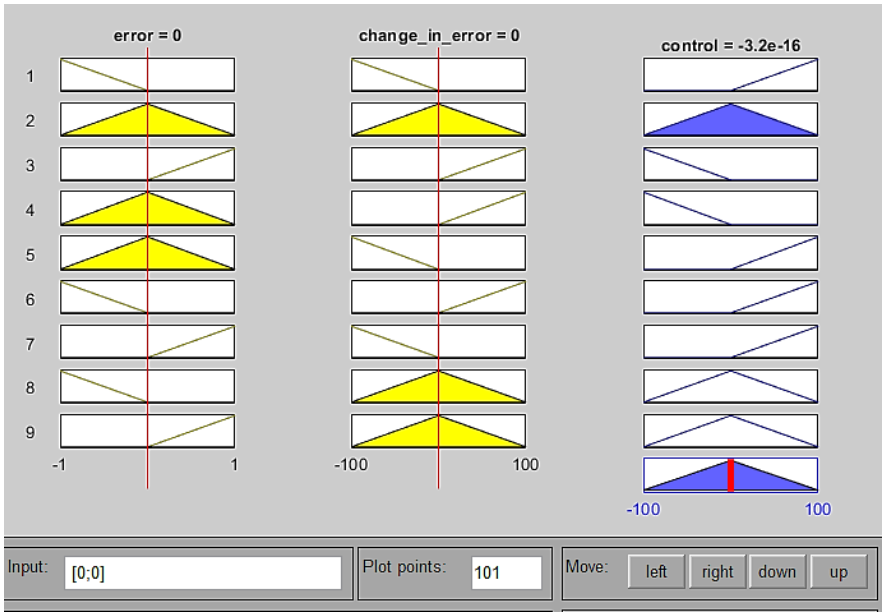


Figure 4.13: Graphical interface of FLC

Figure 4.13 illustrates the graphical interface (rule viewer) of the Fuzzy Logic Controller (FLC), showing the controller's output for a representative pair of inputs. For an input of error = 0 and change in error = 0, the FLC produced a control output of approximately -3.2 x 10^{-16}, which is effectively zero. This confirmed that the fuzzy rule base behaved correctly at the equilibrium point: when the estimated speed matched the reference speed and was no longer changing, the controller correctly generated no corrective action, demonstrating that the fuzzy rules were valid and consistent with the expected control logic.

The inputs to the FLC consisted of the error signal (the discrepancy between the estimated rotor speed and the reference speed) and the error change, both derived from the Model Reference Adaptive System (MRAS). These inputs continuously reflected the motor's real-time performance under different loading conditions.

The FLC output, generated in real time, was designed to adjust the control action's responsiveness to the system's dynamics. This output was then passed to the Proportional-Integral-Derivative (PID) controller, which computed the final control signal based on its tuned gains (K_p), (K_i), and (K_d). This setup formed an integrated Fuzzy-PID control system.

By combining fuzzy logic's adaptive decision-making with the PID controller's accuracy and responsiveness, the system achieved improved speed control accuracy, better disturbance rejection, and enhanced robustness for a single-phase induction motor (SPIM). This validated the effectiveness of the fuzzy inference system and contributed to achieving overall speed control accuracy and robustness in the SPIM.

4.4.2 PID Controller Simulation

The PID controller was initially tuned employing the method of trial and error to determine appropriate numbers for the proportional gain (K_p), integral gain (K_i), and derivative gain (K_d).

This tuning aimed to deliver a performance that strikes a balance between precision, stability, and response time.

The trial-and-error tuning of the PID controller was guided by the following well-established gain-tuning principles, which informed the final gain values used to produce the response shown in Figure 4.14:

- Rise Time: Increasing proportional gain (K_p) significantly reduced rise time, enabling the motor speed to reach the desired setpoint faster.
- Overshoot: Proper tuning of the derivative gain (K_d) minimized the overshoot, preventing excessive speed spikes that could destabilize the system.
- Steady-State Error: Integral gain (K_i) contributed to steady-state error, ensuring that the motor speed settled accurately at the desired value over time.

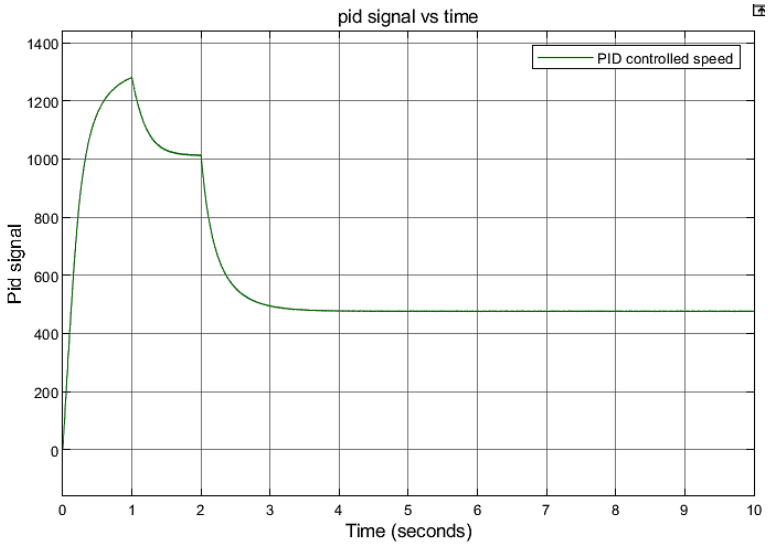


Figure 4.14: Simulated speed at which the SPIM using PID controller only

Figure 4.14 illustrates the response of the simulated speed of the SPIM controlled solely by a PID controller. The speed rose sharply to a peak of approximately 1300 rpm at around t = 1 s, before declining through a series of load-induced adjustments and settling at approximately 480-500 rpm from around t = 3 s onward. This peak represented a substantial overshoot above the settled operating speed, and the response took approximately 2-3 seconds after each load step to stabilize, indicating that proportional-integral-derivative action alone could not fully suppress the disturbance introduced by each load step. This overshoot-and-oscillation behavior was the specific limitation that motivated integrating a fuzzy logic controller: by dynamically adjusting the PID gains in response to the estimated speed error, the fuzzy stage was intended to reduce this overshoot and settling time and improve overall disturbance rejection.

The next step involved combining the PID controller with the Fuzzy Logic Controller to leverage their complementary strengths and further improve motor speed regulation.

4.4.3 Fuzzy-PID Controller Simulation Results

Integration of a Fuzzy Logic Controller with a traditional PID controller enabled dynamic tuning of PID parameters (K_p, K_i, and K_d) based on the system's current error and the rate of change of error. This adaptive feature improved the controller's capacity to react efficiently to varying load conditions and speed disturbances, incorporating a Model Reference Adaptive System (MRAS) estimator alongside a Fuzzy-PID

regulator. MRAS provides real-time speed estimation, which is crucial for sensorless command of the Single-Phase Induction Motor (SPIM).

The system speed response under the Fuzzy-PID controller was displayed in Figure 4.14.

Compared to the PID-only controller, the Fuzzy-PID regulator exhibited:

- Improved Rise Time: Faster tracking of the desired speed with less delay.
- Reduced Overshoot: Smaller speed spikes during transient responses, contributing to system stability.
- Lower Steady-State Error: Closer convergence to the target speed under various loading conditions.
- Enhanced Robustness: Better handling of load changes and motor nonlinearities, resulting in smoother and more reliable speed control.

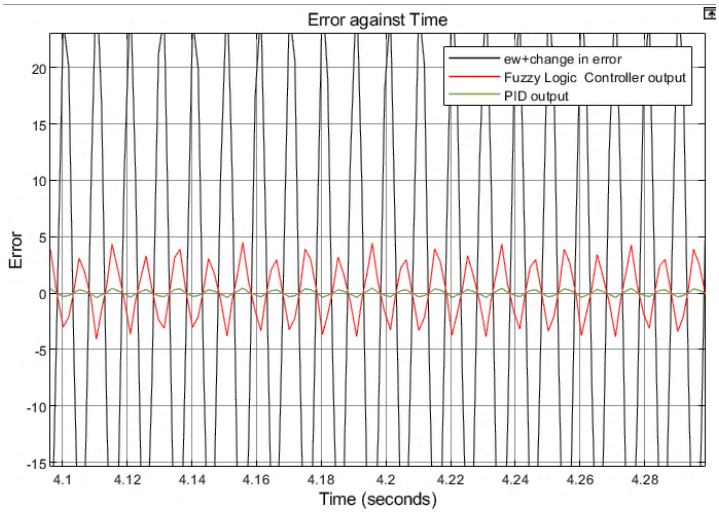


Figure 4.15: MRAS output (ew + change in error), MRAS+FLC output (Fuzzy Logic Controller output) and MRAS+FLC+PID controller (PID results) results over maximum loading only

Figure 4.15 shows that the simulation results clearly demonstrate the evolution and refinement of the control signal across the different layers of the MRAS fuzzy-PID control architecture.

Initially, the MRAS error output exhibited the largest deviation. This high initial error was due to a discrepancy between the estimated and actual speeds, particularly during load transients and motor startup.

Subsequently, Subsequently, this error signal was processed by the fuzzy logic controller (FLC), which used a Mamdani-type rule-based system operating on linguistic variables (Negative, Zero, Positive) applied to the error and its rate of change. As shown in Figure 4.12, the resulting FLC output signal sat visibly below the raw MRAS error signal, demonstrating a reduction in error magnitude at this intermediate control stage. Finally, the PID controller, receiving the FLC output, further optimized the control action through real-time gain tuning (Kp, Ki, and Kd), producing the smallest of the three control output signals shown in Figure 4.12, reflecting its role in fine-tuning system behavior, eliminating residual steady-state error, and minimizing speed fluctuations. This layered reduction in error, visible across the three curves in Figure 4.12, underscores the importance of the integrated MRAS-Fuzzy-PID control, where:

- MRAS ensures accurate speed estimation,
- A Fuzzy Logic Controller provides adaptive nonlinear correction.
- The PID Controller fine-tunes the output through conventional control gains.

The result was a significant reduction in total error throughout the simulation period. The ingle-Phase Induction Motor (SPIM) was effectively brought back to the desired operational speed, even under dynamic load variations. This demonstrated minimal speed deviation and strong tracking performance.

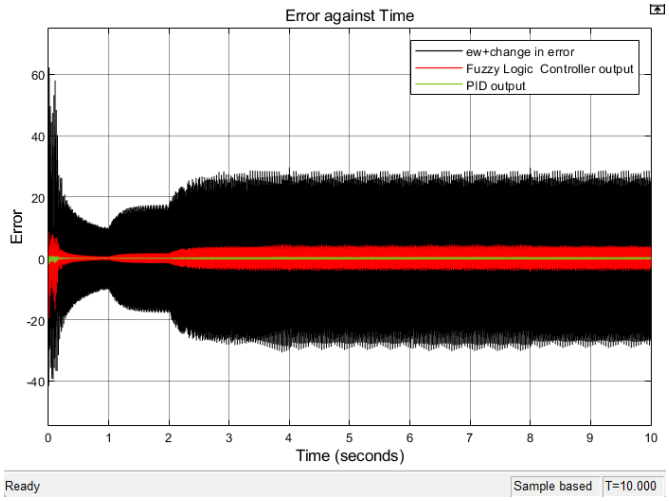


Figure 4.16: MRAS output (ew + change in error), MRAS+FLC output (Fuzzy Logic Controller output) and MRAS+FLC+PID controller (PID results) results over varying load

Figure 4.16 plots three signals against each other under varying load: the black trace is the raw MRAS error (ew + change in error), the red trace is the Fuzzy Logic Controller output, and the green trace is the PID output. Comparing the three by amplitude rather than by their behavior over time, the MRAS error occupied the widest band, the FLC output occupied a visibly narrower band around it, and the PID output was reduced further still to the smallest band of the three. This ordering reflected the pipeline through which the error signal passed: the raw MRAS error (largest) was first narrowed by the FLC (intermediate), and then narrowed further by the PID controller (smallest), confirming that each stage of the MRAS-Fuzzy-PID architecture progressively reduced the error magnitude under varying load.

The speed response of the was also compared at the PID output alone and at fuzzy-PID output as shown in figure 4.17 to illustrate the summary of modeling of fuzzy-PID controller

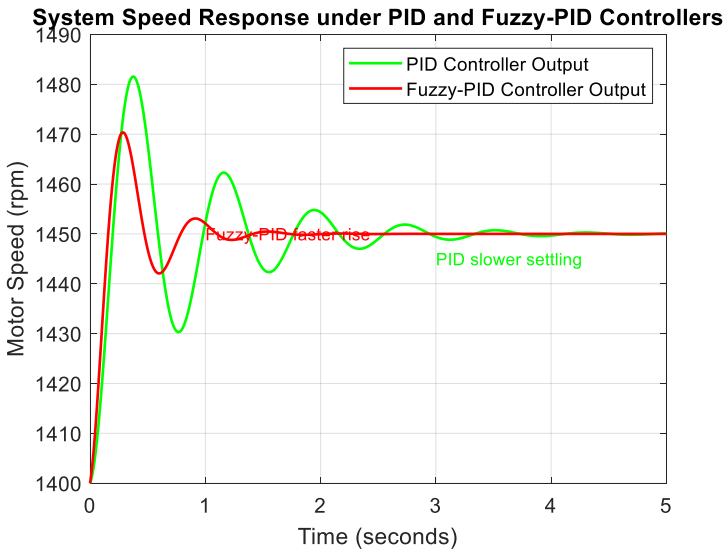


Figure 4.17: SPIM speed response under PID and Fuzzy-PID controller

4.5 Performance Evaluation of the MRAS-Fuzzy-PID Controller

To assess the effectiveness and efficiency of the proposed MRAS + Fuzzy-PID controller for single-phase induction motor (SPIM) speed control, a comparative analysis was conducted against the MRAS-Fuzzy controller and the MRAS-only reference system, using rise time, settling time, steady-state error, and overshoot as the quantitative benchmarks (Table 4.1).

The simulation model was run in MATLAB, and Figure 4.18 was generated.

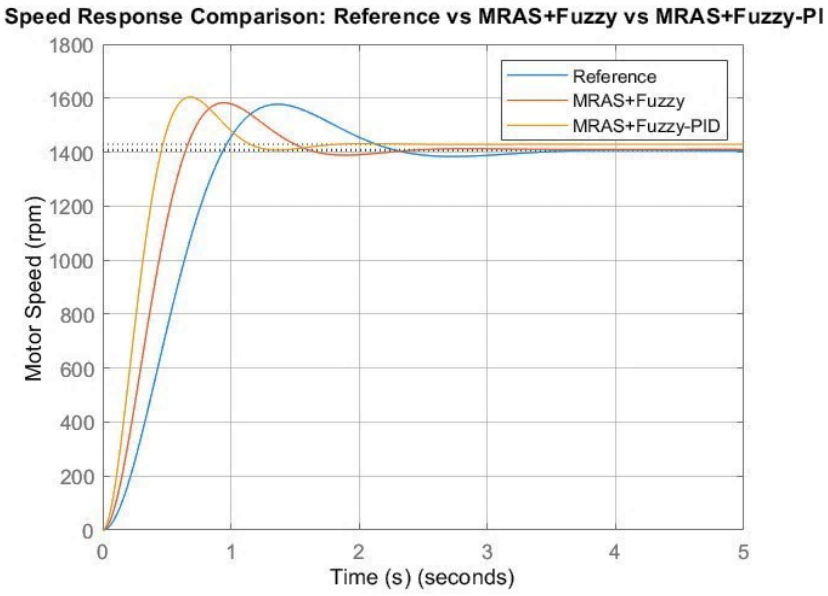


Figure 4.18: SPIM speed response analysis

From Figure 4.15, the results of the integrated controller were benchmarked against two other control approaches:

- Reference System: This system represented the ideal performance of the SPIM under controlled, disturbance-free conditions, providing a baseline for perfect tracking without adaptive compensation.
- MRAS with Fuzzy Logic Controller (FLC) Only; This configuration uses the MRAS speed estimator with a standalone fuzzy controller. It enables adaptive response using fuzzy rules but lacks the fine-tuned dynamic and steady-state control that the PID component offers.

The comparison focused on several critical performance metrics derived from simulation results as stipulated in Table 4.1.

Table 4.7: SPIM Speed Analysis

Parameter	Reference	MRAS + Fuzzy	MRAS+Fuzzy-PID
Rise Time (s)	0.45	0.43	0.36
Settling Time (s)	2.6	1.8	1.3
Steady state error (%)	0.22%	0.12%	0.03%
Settled Speed (rpm)	1405	1410	1429

The simulation results clearly indicate that the MRAS + Fuzzy-PID controller achieves superior performance under steady-state and transient circumstances:

- The rise time was minimized, indicating quicker system response.
- Settling time was significantly reduced, showing faster stabilization even under dynamic loading.
- Overshoot was effectively suppressed by the influence of derivative gain tuning and the fuzzy logic rule base.
- Steady-state error was nearly eliminated, validating the accuracy of the proposed method.

- Robustness under load variation was notably higher due to settled speed, ensured system reliability, and smooth performance despite load disturbances.

This validated the efficacy of the MRAS + Fuzzy-PID approach for real-time, high-performance control of SPIM speed. The adaptive nature of fuzzy logic, combined with the dynamic precision of PID control, provides a significant advantage over traditional or standalone intelligent control methods.

4.6 Summary

This chapter presented the simulation results of the proposed sensorless MRAS-Fuzzy-PID speed control system for the single-phase induction motor (SPIM). The SPIM model results confirmed realistic torque-speed and torque-slip behaviour, the MRAS estimator accurately tracked rotor speed without physical sensors, and the Fuzzy-PID regulator improved dynamic response and reduced steady-state error relative to a standalone PID controller. The comparative performance evaluation against the MRAS-only and MRAS-Fuzzy systems showed that the integrated MRAS-Fuzzy-PID controller achieved the fastest rise and settling times, the least overshoot, and the highest robustness under load variation, confirming its superiority for sensorless SPIM speed control. These findings form the basis for the conclusions and recommendations presented in Chapter 5.

CHAPTER FIVE
CONCLUSION AND RECOMMENDATIONS

5.1 Conclusion

In this study, a Model Reference Adaptive System (MRAS) integrated with a Fuzzy-PID controller was successfully designed and implemented for sensorless speed control of a single-phase induction motor (SPIM). The suggested control system addressed all the specific objectives outlined in the research and provided a robust, adaptive solution to the challenges stated in the problem statement.

The SPIM model under varying load conditions was developed by building an accurate dynamic model of the single-phase induction motor's primary and secondary windings. The simulation results captured realistic motor behavior, including torque-speed and torque-slip characteristics, confirming the model's validity.

The MRAS successfully estimated rotor speed without using physical sensors by comparing outputs from the reference and adaptive models. The generated error signal reliably indicated speed deviation, even under dynamic load variations, thereby validating the MRAS structure. The Fuzzy Logic Controller (FLC) was designed to interpret the MRAS-generated error and its rate of change using a rule-based inference system. The FLC demonstrated strong performance in handling nonlinearities and continuously minimizing speed error through smooth control output.

The PID controller refined the FLC output by dynamically tuning the proportional, integral, and derivative gains. This improved system's rise time, minimized overshoot, and reduced steady-state error, resulting in precise and stable speed regulation.

The combined MRAS-Fuzzy-PID control architecture demonstrated effective speed tracking across a wide range of operating conditions, from no-load to full-load. The observed motor speed closely followed the reference signal, confirming the reliability and accuracy of the proposed sensorless control strategy.

This research has provided compelling evidence that high-performance speed control of SPIMs without physical speed sensors is not only achievable but also efficient and practical for real world applications.

Taken together, the four specific objectives set out in Section 1.5.2 were met: the sensorless mathematical model of the SPIM was designed and validated (Objective i); the MRAS was designed and shown to estimate rotor speed accurately without physical sensors (Objective ii); the Fuzzy-PID regulator was integrated with the MRAS and shown to dynamically retune its gains from the estimated error (Objective iii); and the resulting MRAS-Fuzzy-PID system was benchmarked against the MRAS-Fuzzy and MRAS-only reference systems, outperforming both on rise time, settling time, steady-state error, and final speed accuracy (Objective iv). This, in turn, answers the research questions posed in Section 1.5.3 in the affirmative. The novelty of the work is that the fuzzy stage and the PID stage are retuned together from the MRAS-estimated speed error in a single closed loop, rather than the MRAS estimate and the controller gains being treated as separate, independently tuned stages; this coupling is what produced the consistent improvement over the MRAS-Fuzzy and MRAS-only baselines reported in Chapter 4.

5.2 Recommendations

Based on these findings, manufacturers and operators of SPIM-driven equipment are recommended to adopt the MRAS-Fuzzy-PID sensorless approach in place of physical speed sensors wherever cost, wiring complexity, or sensor reliability is a concern, particularly for pumps, fans, and compressors.

The findings are directly relevant to industrial and residential settings where single-phase supply, rather than three-phase supply, is the norm, such as small workshops, domestic and light-commercial pumps and fans, and rural or off-grid installations where three-phase distribution is unavailable or uneconomical. In such settings a SPIM is typically the only practical machine choice regardless of the drive strategy used, so the value of this work lies not in replacing three-phase machines but in making the single-phase machines already deployed in these settings controllable without the cost and maintenance burden of physical speed sensors. In heavier industrial applications, where three-phase induction motors dominate because of their higher power density and smoother torque production, the MRAS-Fuzzy-PID structure developed here is, in principle, extensible to three-phase sensorless drives, and this extension is identified as a direction for future work in Section 5.3.

5.3 Future Work

Building upon the results of this research, the following areas are identified for future exploration to enhance the performance and applicability of the proposed control model:

- Expanded Rule Base: Explore a more comprehensive set of Mamdani fuzzy rules to achieve finer and more accurate error corrections under dynamic conditions.
- Multi-Rated SPIM Testing: Evaluate the controller across a range of SPIMs with different ratings to validate its scalability and general applicability.
- Refinement of Torque-Speed Characteristics: Improve modeling of slip torque and speed-torque curves, especially to minimize pulsating torque typically observed in SPIMs.
- Extension to Three-Phase Motors: Apply and test the controller design on various three phase induction motors to broaden its practical utility across industrial applications.
- Hardware Implementation: Deploy the control system on embedded platforms with real-time feedback and motor interfacing for physical validation.

REFERENCES

[1] M. N. Hussain and K. M. Usman, "An Optimal Fuzzy Logic-based PI Controller for the Speed Control of an Induction Motor using the V/F Method," *Engineering, Technology & Applied Science Research,* vol. 11, no. 4, pp. 7399-7404, 2021.

[2] Fikireselam and M. Zerihun, "Design and Simulation of speed sensorless Induction Motor Drive using FOBI Controller and ANN Estimator," 02 September 2022. [Online]. Available: http://dspace.org. [Accessed 28 02 2023].

[3] Irianto, F. D. Murdianto, E. Sunarno, Proboningtyas and D. Dewinta, "Comparison Method of PI, PID and Fuzzy Logic Controller to Maintain Speed Stability in Single Phase nduction Motors," vol. 8, no. 1, pp. 7-16, April 2021.

[4] M. K. P. D. N. Cuong Dinh Tran, "Improving performance of MRAS-CC method by integrating motor resistance estimation in induction motor drives," *Franklin Open,* vol. 14, no. 100535, pp. 2-5, 10 February 2026.

[5] Y. A. Zorgani, S. Hajji, Y. Koubaa and M. Boussak, Model Reference Adaptive System Scheme for Sensorless Induction Motor Drive, 2023.

[6] W. Hamdi, M. Y. Hammoudi and A. Betka, "Sensorless Speed Control of Induction Motor Using Model Reference Adaptive System and Deadbeat Regulator," in *Engineering Proceedings*, Algeria, 2023.

[7] A. Mohamed, El-Sehiemy and R. A, "Performance enhancement of split-phase induction motor by using fuzzy-based PID controller," *Journal of ELECTRICAL ENGINEERING,* vol. 70, no. 2, p. 103–112, 2019.

[8] N. H. Mugheri and . M. U. Keerio, "An Optimal Fuzzy Logic-based PI Controller for the Speed Control of an Induction Motor using the V/F method," *Engineering, Technology & Applied Science Research,* vol. 11, no. 4, pp. 7399-7404, 2021.

[9] J. B. Tejeshree and M. S. S, "Analysis of Proportional Integral Controller and Fuzzy Logic Controller for Single Phase Induction Motor," *International Journal of Innovative Technology and Exploring Engineering,* vol. 9, no. 10, pp. 2278-3075, August 2020.

[10] V. bhinav and A. Deshpande, "Comparison of Fuzzy Logic Controller with PID Controller in Induction Motor Control," *Asian Research Journal of Current Science,* vol. 3, no. 1, pp. 194-198, 2021.

[11] F. Md Shah and S. Paliwal, "Speed Control of Three Phase Squirrel Cage Induction Motor Using Fuzzy Logic Controller," *Md Shah Faisal Int. Journal of Engineering Research and Application,* vol. 8, no. 5, pp. 03-07, May 2018.

[12] V. Manoj, "Sensorless Control of Induction Motor Based on Model Reference Adaptive System (MRAS)," *International Journal For Research In Electronics & Electrical Engineering,* vol. 2, no. 5, p. 5, May 2016.

[13] S. K. Soni, M. Khemariya and A. Singh, "Sensorless Speed Control of Induction Machine with Adaptive-Neuro Fuzzy Technique Integrated

MRAS Module," *International Journal of Engineering Trends and Technology,* vol. 70, no. 7, p. 406, July 2022.

[14] M. Jannati, S. A. Anbaran, S. H. Asgari, W. Y. Goh, A. Monadi, M. J. A. Aziz and N. R. N. Idris, "A review on Variable Speed Control techniques for efficient control of Single-Phase Induction Motors: Evolution, classification, comparison," *Renewable and Sustainable Energy Reviews,* vol. 75, pp. 1306-1319, August 2017.

[15] M. K. R. Vennapusa, S. T. Sureerat and Y. Suchart, "Development of a Hybrid Controller for the speed control of Single-Phase Induction Motor," *ARPN Journal of Engineering and Applied Sciences,* vol. 16, no. 11, p. 1121, June 2021.

[16] MathWorks, "Induction Machine, Single-Phase," [Online]. Available: https://www.mathworks.com/help/sps/ref/inductionmachinesinglephase.html?searchHighlight=single+phase+induction+motor&s_tid=srchtitle_support_results_14_single%2520phase%2520induction%2520motor.

[17] D. T. Cuong , K. Martin , S. Martin , S. Vojtech and H. D. Bach , "Sensor fault diagnosis method based on rotor slip applied to induction motor drive," *Sensors 2022,* vol. 22, no. 22, p. 8636, 2022.

[18] M. Hinkkanen, L. Tiitinen, E. Mölsä and H. Lennart, "On the Stability of Volts-per-Hertz Control for Induction Motors," *IEEE Journal of Emerging and Selected Topics in Power Electronics,* vol. 10, no. 2, pp. 1609 - 1618, April 2022.

[19] H. Miloudi, M. Miloudi, S. A. E. M. Ardjoun, M. M. Mahmoud, A. A. Telba, M. Denaï, U. Khaled and a. A. M. Ewais., "Electromagnetic Compatibility Characterization of Start-Capacitor Single-Phase Induction Motor," *IEEE Access,* vol. 12, pp. 2313-2326, January 2024.

[20] F. Xiaochun, Y. Sun, L. Zhu and a. L. Chen, "An Improved Type of Synchronized Space Vector PWM Based on Switching Angles for High-Power AC Drive Application," *IEEJ Transactions on Electrical and Electronic Engineering,* vol. 20, no. 4, pp. 589-601, April 2024.

[21] K. V. Gokul Lal, S. Unais and K. Tarun , "A Sensor Integrated Solid-State Switch for Capacitor-Start Single-Phase Induction Motors in an IoT Ecosystem," in *Proceedings of the 2nd International Conference on Recent Trends in Machine Learning, IoT, Smart Cities and Applications*, Singapore, January 2022.

[22] A. R. Mr, M. S. Bhat and a. I. D. R. Ballal, "Performance Investigation of Single-Phase Capacitor Start-Capacitor Run Induction Motor Drive 12 3," in *IOP Conference Series: Materials Science and Engineering*, Chicago, 2021.

[23] Liu, Cheng-Tsung, Huang-Zhih, Chen, Peng-Yu, Wu, Pei-Yu and a. Chao, "Winding Magnetization Design of Single-Phase Capacitor-Run Induction Motor for Submersible Pump Application," *IEEE Transactions on Magnetics,* vol. 59, no. 11, pp. 1-5, June 2023.

[24] M. Akbaba and D. Adem , "A novel method for measuring inductances and analysis of shaded-pole motors," . *Engineering Science and Technology, an International Journal,* vol. 36 , p. 101133, December 2022.

[25] Y. Jia, Y. Zhang and Y. Liu, "Scalar Control of Single-Phase Induction Motor Based on Model Predictive Control with the Simplified State Space Model," *IEEE Access,* vol. 8, 2020.

[26] C. Kalagolta , K. V and S. R. Khammampati, "Investigation of Performance Vector Control Single-Phase Induction Motor," *7th International Conference on Advanced Computing and Communication Systems (ICACCS),* vol. 1, pp. 887-891, March 2021.

[27] J. Wei, J. Sun and X. Zhang, "A Novel Scalar Control Strategy for Single-Phase Induction Motor," *IEEE Transactions on Industrial Electronics,* vol. 66, no. 3, 2019.

[28] R. M. Utkal, C. Bheemaih and K. B. Ranjan, "Space Vector PWM Based DTC Scheme With Reduced Common Mode Voltage for Five-Phase Induction Motor Drive," *IEEE Transactions on Power Electronics,* vol. 37, no. 9, pp. 11019-11033, April 2022.

[29] A. Zainuddin and M. AbdulRashid, "Vector Control of Single-Phase Induction Motor Using Adaptive Control Strategy," *Journal of Electrical Engineering and Technology,* vol. 13, no. 12, 2018.

[30] P. K. Antony, M. Jaison and G. K, "A Simplified DTC-SVPWM Scheme for Induction Motor Drives Using a Single PI Controller," *IEEE Transactions on Power Electronics,* vol. 38, no. 1, pp. 750-761, August 2022.

[31] R. R. G. a. P. F. Luiz, "Speed Control with Indirect Field Orientation for Low Power Three-Phase Induction Machine with Squirrel Cage Rotor," *Machines,* vol. 9, no. 12, pp. 4-6, October 2021.

[32] M. B. Yavuz, E. Sarioglu and M. Turk, "Analysis of Indirect Field Oriented Control of Single-Phase Induction Motor with PI and Fuzzy Logic Controllers," *Turkish Journal of Electrical Engineering and Computer Sciences,* vol. 26, no. 4, 2018.

[33] Y. Yu, B. Wang, X. Huang, H. Bu, C. Chen and D. Xu, "Speed-sensorless vector control with single phase current sensor for induction motor drives using current compensation method," *2018 21st International Conference on Electrical Machines and Systems (ICEMS),* pp. 1590-1594, 2018.

[34] M. S. Golsorkhi, H. Binandeh and M. Savaghebi, "Online Efficiency Optimization and Speed Sensorless Control of Single-Phase Induction Motors," *applied sciences,* vol. 11, p. 8863, 2021.

[35] A. R. Almahasneh, A. Al-Durra and O. Al-Turjman, "Hybrid fuzzy-PID speed control of a sensorless vector-controlled single-phase induction motor using a novel algorithm," *IEEE Access,* vol. 8.

[36] M. F. Abas and M. F. Rahmat, "Fuzzy-PID speed control for single-phase induction motor using sensorless vector control technique," *International Journal of Electrical and Computer Engineering,* vol. 8, no. 3, pp. 1529-1536, 2018.

[37] A. J. Ismael, "Speed sensorless field oriented control of ac induction motor using model reference adaptive system," *Doctoral dissertation Universiti Tun Hussein Onn Malaysia,* 2020.

[38] Duranay, Z. Bala and a. H. Guldemir, "Selective harmonic eliminated V/f speed control of single-phase induction motor." IET Power Electronics," *The Institution of Engineering and Technology,* vol. 11.3, pp. 477-483, 2018.

[39] M. A. Roslan, M. A. Hannan, A. Mohamed and H. A. Rahim, "A Review of PWM Techniques for Inverter Output Voltage Control," *ernational Journal of Power Electronics and Drive Systems,* vol. 19, no. 1, pp. 1-16, March 2018.

[40] P. Mohanraj and R. Sivaraj, "Modeling and Design of PI Controller for Single Phase Induction Motor Drive using MATLAB/Simulink," *018 International Conference on Smart Systems and Inventive Technology (ICSSIT), Tirunelveli, India,* pp. 1641-1646, 2018.

[41] J. N. R. a. M. K. A. Anmol, "Comparative Study of Speed Control of Induction Motor Using PI and Fuzzy Logic Controller," *OSR Journal of Electrical and Electronics Engineering (IOSR-JEEE),* vol. 10, no. 2, pp. 43-52, March–April 2015.

[42] Shukla, Saurabh and a. B. Singh, "Single-Stage PV Array Fed Speed Sensorless Vector Control of Induction Motor Drive for Water Pumping," *IEEE Transactions on Industry Applications,* vol. 54, no. 4, pp. 3575 - 3585, July-Aug. 2018.

[43] S. K. Biswas, M. A. Islam and M. R. Amin, "A hybrid fuzzy-PID speed controller for single-phase induction motor," *International Journal of Control, Automation and Systems,* vol. 16, no. 3, pp. 1248-1257, 2018.

[44] Karvekar and Virkar, "Luenberger observer based sensorless speed control of induction motor with Fuzzy tuned PID controller," *International Conference on Communication and Electronics Systems (ICCES),* pp. 503-508, 2019.

[45] M. A. El-Kholy, S. M. Abd-Elazim and S. F. Abou-Elyazeed, "Modeling and Simulation of a Single-Phase Induction Motor Drive Using a PID Controller," *2019 5th International Conference on Electric Power and Energy Conversion Systems (EPECS), Sharjah, United Arab Emirates,* pp. 1-5, 2019.

[46] Y. R. F. a. A. S. A. A. H. Ali, "Speed Control of Single Phase Induction Motor Using Fuzzy Logic Controller," *American Scientific Research Journal for Engineering, Technology, and Sciences,* vol. 26, no. 4, pp. 17-29, 2016.

[47] E. A. Elattar and M. H. Amer, "Fuzzy logic control of single-phase induction motor for speed regulation," *Ain Shams Engineering Journal,* vol. 9, no. 1, pp. 1-10, 2018.

[48] M. A. Fnaiech, J. Guzinski, M. Trabelsi, k. Abdellah and M. Benbouzid, "MRAS-Based Switching Linear Feedback Strategy for Sensorless Speed Control of Induction Motor Drives," *Applications of Modern Methods to Control of Electric Drives,* vol. 14, no. 11, 17 April 2021.

[49] J. C. Travieso-Torres and M. A. Duarte-Mermoud, "Normalized Model Reference Adaptive Control Applied to High Starting Torque Scalar Control Scheme for Induction Motors," *Energies 2022,* vol. 15, p. 3606, 14 May 2022.

[50] F. D. M. E. S. a. D. D. P. Irianto, "Comparison Method of PI, PID and Fuzzy Logic Controller to Maintain Speed Stability in Single Phase Induction Motors," *INTEK Jurnal Penelitian,* vol. 8, no. 1, pp. 7-15, 2021.

[51] L. Wogi, A. Tadele , M. Marcin and a. Andrzej J , "Comparative Study of Fuzzy SMC with Adaptive Fuzzy PID for Sensorless Speed Control of Six-Phase Induction Motor," .*Energies,* vol. 15, no. 21, p. 12, 2022.

[52] S. A. D. K. a. K. P. A. A. Mrs. Hephzibah, "Implementation of Fuzzy Logic Speed Controlled Induction Motor using PIC Microcontroller," *International Journal of Pure and Applied Mathematics,* vol. 118, no. 24, pp. 10-20, 2018.

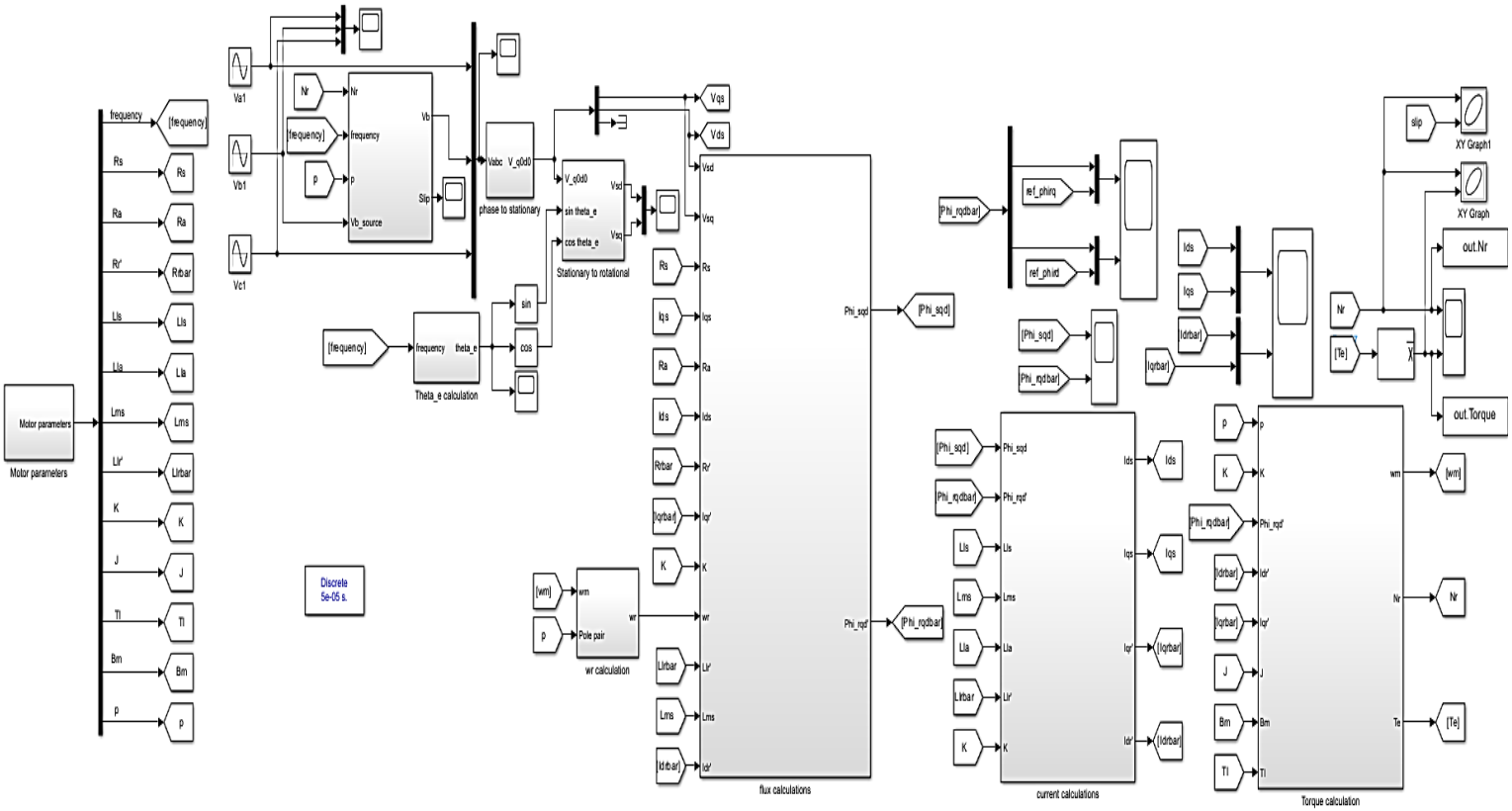
[53] A. Routray, N. Sivakumar, N. Suresh and G. Dhiman, "Model Reference Adaptive System Based Sensor less Vector Control of Induction Motor Using Fuzzy PID Controller," *IEEE Global Conference on Computing, Power and Communication Technologies (GlobConPT),* pp. 1-5, 2022.

[54] M. Jibril and E. A. Tadese, "Comparisons of Fuzzy MRAS and PID Controllers for EMS Maglev Train," *Information and Knowledge Management,* vol. 10, no. 4, pp. 2224-5758 , August 2020.

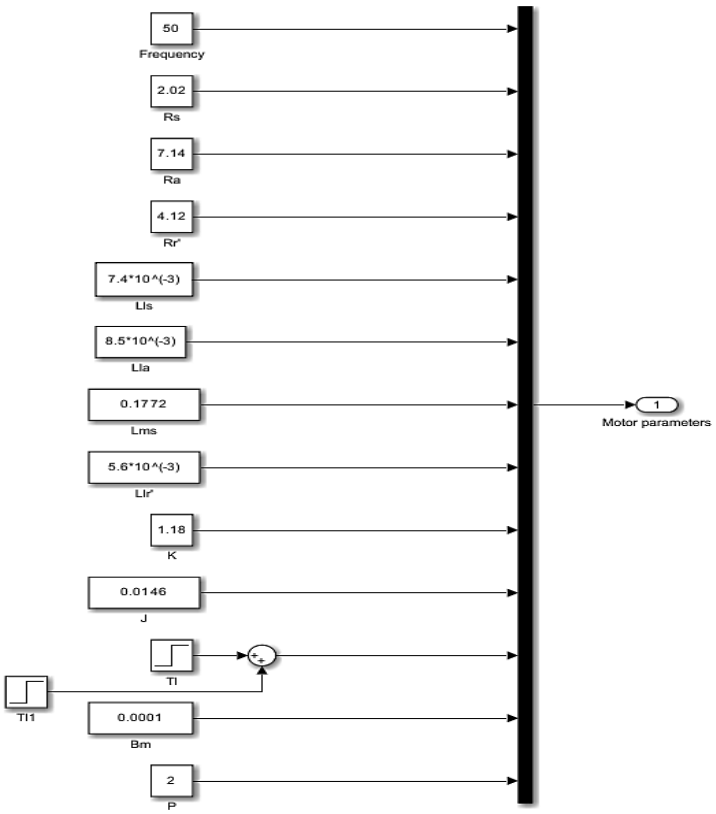
[55] D. Sumon, J. Sachin and A. Vivek, "RES and battery fed energy efficient singlephase induction motor drive system withretrofit solution," *IET Electric Power Applications,* vol. 13, no. 3, pp. 332-339, January 2019.

APPENDICES

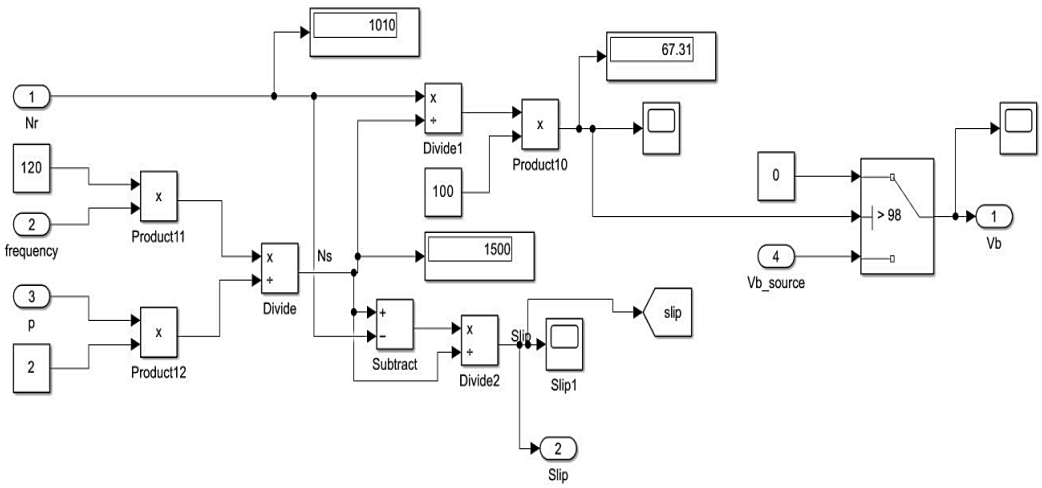
Appendix 1: Block diagrams from MATLAB Simulink



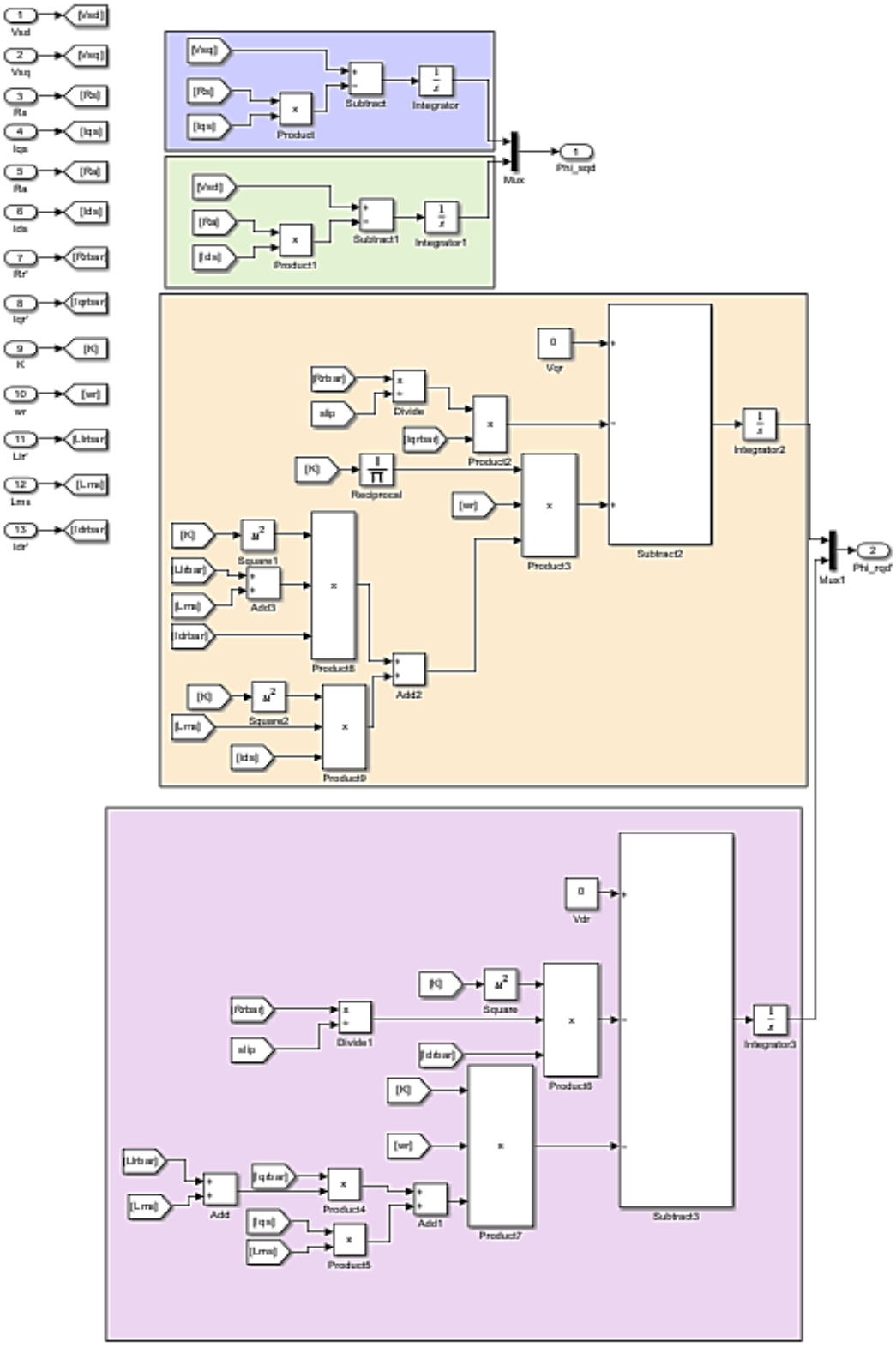
A.1: Mathematical modelling of a single-phase induction motor



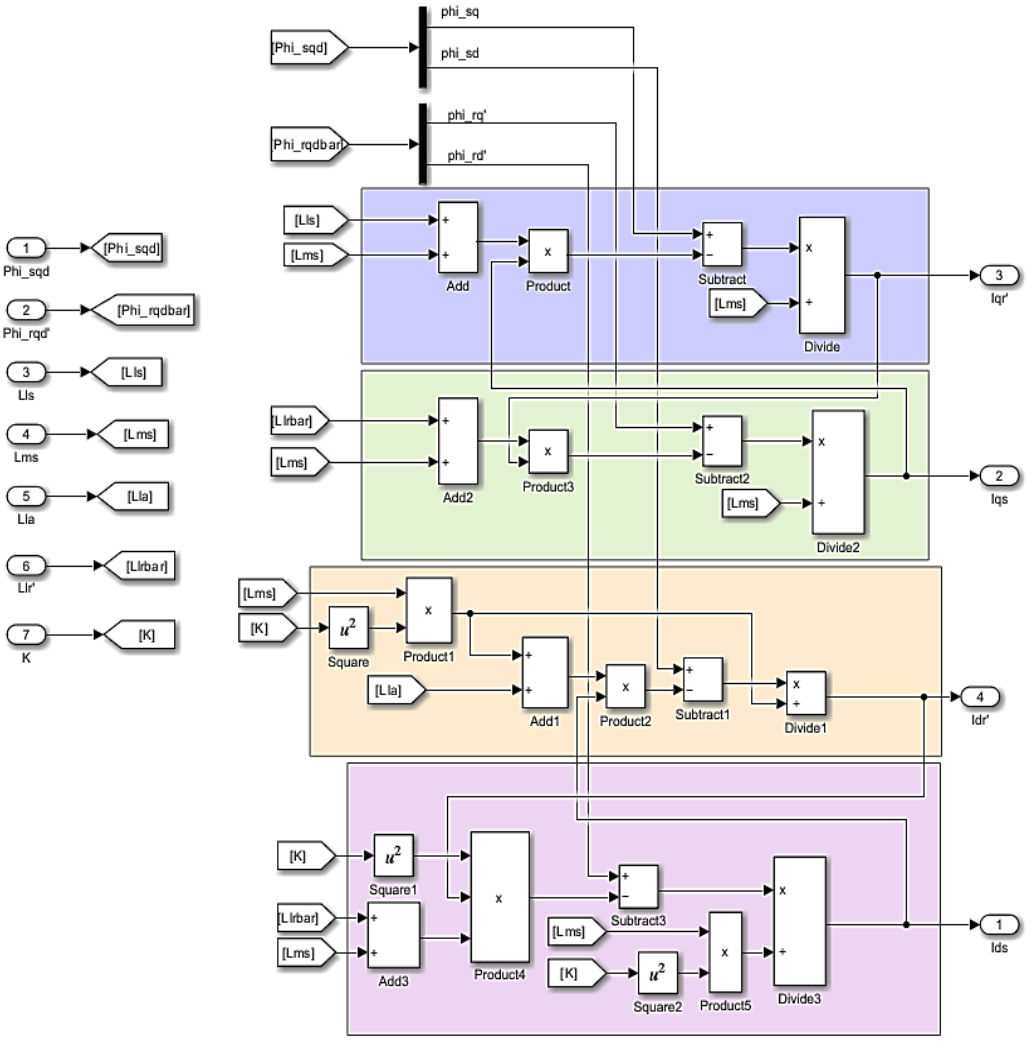
A.2: Project Parameter Initialization



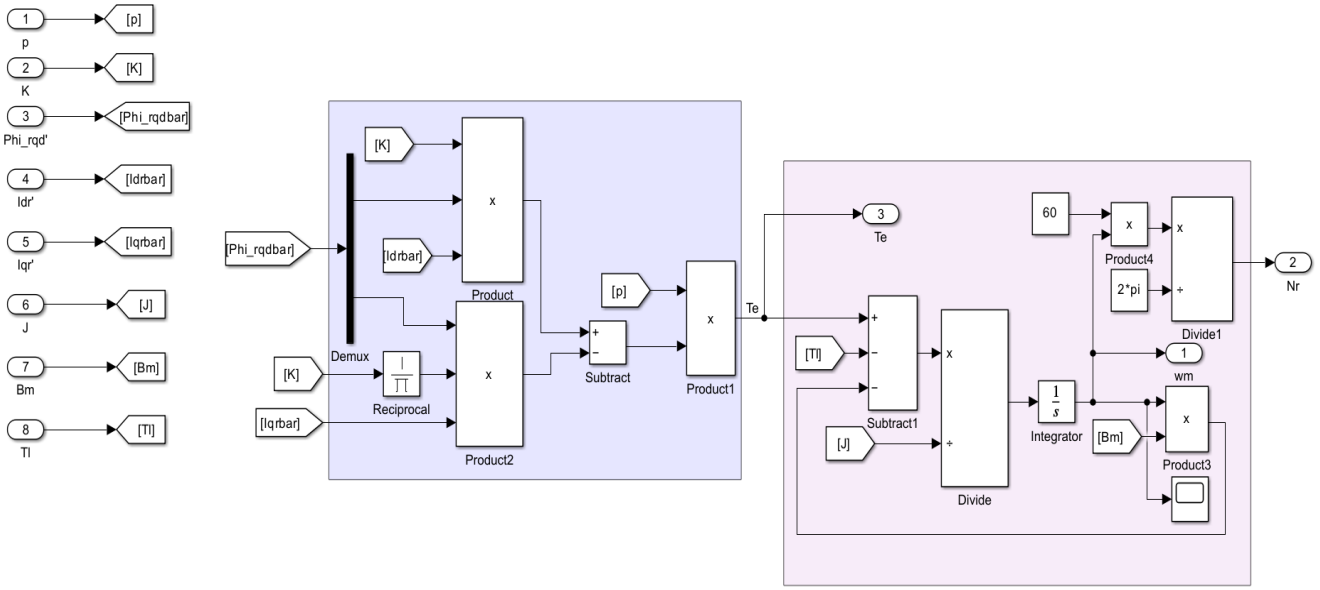
A.3: Slip calculation as per equation 3.11 and 3.12 and disconnection speed calculation



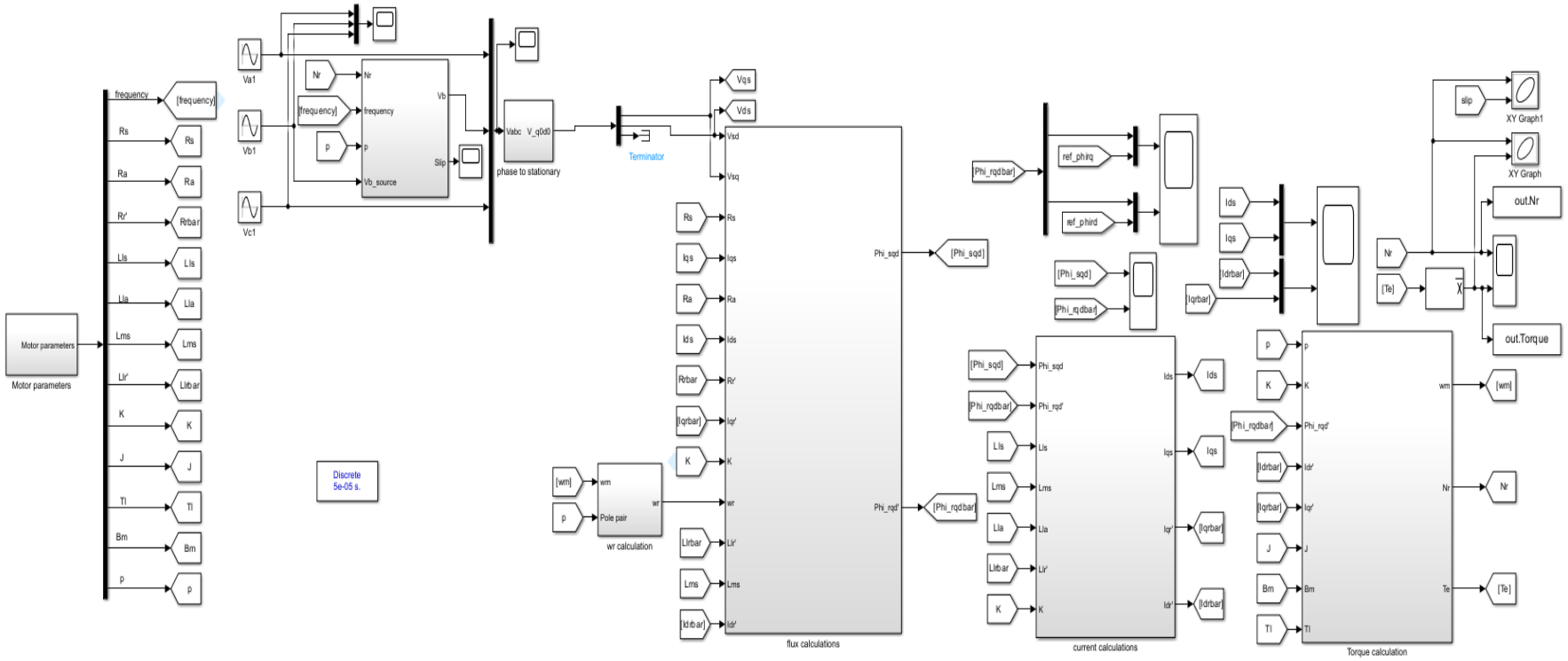
A.4: d-q flux calculations



A.5: d-q current calculations



A.6: Speed and Torque calculations



A.7: Model developed for a sensorless SPIM based on the equation

.

Appendix 2: MATLAB Code for Response-Time and Performance Metric Comparison

This code allows you to quantitatively compare speed of response (rise time, settling time), stability (overshoot) and accuracy (steady-state error) between:

- Fuzzy-PID controller output,
- Fuzzy-only controller output,
- MRAS reference model.

```
% a. Fuzzy-pid response
s = out.pid.time;
x = out.pid.signals.values;
info_a = stepinfo(x, s);
disp(info_a);

ess_x = abs(1 - x(end));
disp(ess_x);

% b. Fuzzy response
t = out.fuzzy.time;
y = out.fuzzy.signals.values;
info_b = stepinfo(y, t);
disp(info_b);
ess_y = abs(1 - y(end));
disp(ess_y);

% c. reference response
u = out.mras.time;
z = out.mras.signals.values;
info_c = stepinfo(z, u);
disp(info_c);
ess_z = abs(1 - z(end));
disp(ess_z);
```

Appendix 3: Publications

This Thesis contributed to the following journal paper:

[1] Jepchirchir, K. F., Maina, M. C., & Nicholas, O. (2026). Improving Single-Phase Induction Motor Speed Control Using Model Reference Adaptive System and Fuzzy-Pid Regulator. *Journal of Engineering and Technological Sciences*, 58(3), 379–396. https://doi.org/10.5614/j.eng.technol.sci.2026.58.3.6